Random Neural Networks and LoRaWAN for Location-based IoT Remote Health Applications in Smart Cities

Winfred Ingabire

July 2023

Dedication

I dedicate this thesis to the almighty God and my loving family.

Declaration

I declare that this thesis is a record of my original contribution and has not been submitted to any institution for any other award. The works of others are well cited in the references.

Acknowledgement

I sincerely appreciate and thank my supervisors, Prof. Hadi Larijani, Dr. Ryan M. Gibson, and Dr. Ayyaz-UI-Haq Qureshi, for the tremendous support, guidance, and encouragement that led to this project become meaningful and successful. I also thank all my friends, colleagues, and GCU staff, especially my research program coordinator, Mr. Ian Dawson MacKay. Last but not least, special thanks to my Ph.D. funders, the Commonwealth Scholarships Commission in the UK, the government of Rwanda, and the University of Rwanda.

Abstract

The concept of the Internet of Things (IoT) has led to the interconnection of a significant number of devices and has impacted several applications in smart cities' development. In the era of digital connectivity, information can be gathered, identified, controlled, and monitored with the help of wireless technologies. IoT has impacted various domains, including localization, healthcare, transportation, agriculture, and many more. In addition, Low-Power, Wide-Area Networks (LPWAN) are potential connectivity enablers within the IoT in smart cities. Long-Range, Wide-Area Network (LoRaWAN) is an open industrial, scientific, and medical radio band specification and an emerging LPWAN connectivity solution for IoT applications with minimum energy consumption. However, LoRaWAN is a relatively recent technology under current research and development.

Localization is a vital IoT application that is being considered in different location-based IoT applications, such as in healthcare for the tracking of patients and the elderly, especially in case there is an emergency or in logistics and transportation for fleet management both in indoor and outdoor environments. Bluetooth, WiFi, and Zigbee wireless technologies have been successfully applied in indoor localization but are only limited to a few meters. Global Positioning Systems (GPS) is a frequently utilized solution for outdoor localization services; however, high-power consumption and hardware cost are significant hindrances to dense wireless sensor networks in large-scale urban areas. Also, GPS does work indoors but is limited due to a lack of direct Line-of-Sight (LOS) satellite signals from the End Device (ED) due to building materials blocking the ultra-high frequency signals.

Various localization methods, including Received Signal Strength Indicator (RSSI) fingerprint localization techniques, are present in the literature, but all with different limitations. Therefore, LoRaWAN is being investigated in different location-based IoT applications due to more advantages with

low-cost, long-range, and low-power characteristics. Furthermore, Random Neural Networks (RNN) has been used to develop different robust models in different IoT applications with significant accuracy, yet RNN applied to localization and heart disease prediction IoT applications is a research topic to be explored.

In this thesis, a novel low-power intelligent localization model using LoRaWAN RSSI values is developed and evaluated using RNN for outdoor and indoor environments primarily to be used in location-based IoT Remote Health Monitoring (RHM) applications in smart cities where patients can be accurately located. Different RNN architectures and learning rates are used to evaluate the performance of the proposed LoRaWAN-RNN-based ED localization model using real-world RSSI LoRaWAN measurements collected in a three-floor building to evaluate the performance of the proposed model in an indoor scenario. Furthermore, real-world data sets collected from an outdoor urban area of Glasgow city and a dense urban area of Antwerp city are used to evaluate the performance of the developed model in an outdoor urban environment. The developed system is trained and used to predict unknown positions. It demonstrates a significantly higher accuracy compared to the results from the related work with a minimum mean localization error of 0.29 m in an outdoor urban environment and 0.12 m in LOS, and 13.94 m in Non-Line of Sight (NLOS) in indoor scenarios, respectively. The proposed localization system demonstrates 95% and 98.5% improvement in average localization error compared to related studies in outdoor and indoor environments, respectively. The obtained results confirm the developed LoRaWAN-RNN-based localization systems suitable for indoor environments in LOS, which can be applied in big sports halls, hospital wards, shopping malls, airports, and many more. Furthermore, the obtained results in NLOS confirm the developed systems appropriate for indoor NLOS applications, which can be applied in managing and controlling vehicles in indoor car parks, industries, or any other fleet in a pre-defined area.

Additional contributions:

- Performance Evaluation of LoRaWAN Propagation Models in an Urban Area.
- LoRaWAN Scalability for Remote Health Monitoring Applications in Dense IoT Networks.

- Heart Disease Prediction Using Random Neural Networks.

List of Publications

Journal Articles

Ingabire, W.; Larijani, H.; Gibson, R.M.; Qureshi, A.-U.-H. LoRaWAN Based Indoor Localization Using Random Neural Networks. Information 2022, 13, 303. https://doi.org/10.3390/info13060303.

Ingabire, W.; Larijani, H.; Gibson, R.M.; Qureshi, A.-U.-H. Outdoor Node Localization Using Random Neural Networks for Large-Scale Urban IoT LoRa Networks. Algorithms 2021, 14, 307. https://doi.org/10.3390/a14110307.

Conference Proceedings

Ingabire, W., Larijani, H., Gibson, R. M. (2021). LoRa RSSI based outdoor localization in an urban area using random neural networks. In K. Arai (Ed.), Intelligent Computing: Proceedings of the 2021 Computing Conference (Vol. 2, pp. 1032-1043). (Lecture Notes in Networks and Systems; Vol. 284). Springer. https://doi.org/10.1007/978-3-030-80126-7-72.

W. Ingabire, H. Larijani and R. M. Gibson, "Performance Evaluation of Propagation Models for LoRaWAN in an Urban Environment," 2020 International Conference on Electrical, Communication, and Computer Engineering (ICECCE), 2020, pp. 1-6, doi: 10.1109/ICECCE49384.2020.9179234.

Contents

List of Figures

List of Tables

Chapter 1

Introduction

IoT originates from two different words: the "Internet" and the "Things." Whereby 'Internet' refers to a global network composed of millions of networks form various organizations that can be academic, government, business, public, or private networks; however, a 'thing' is an entity or physical object having an embedded system, a distinctive identification, and the capacity to send data via a network. These may include but not limited to electronic things like gadgets and equipment [1], [2]. Due to IoT's ability to track things, industries have managed to be more efficient with minimum errors and can produce much better with limited resources in less time. Remote healthcare is one of the promising IoT smart applications in developing smart cities [3].

The connected IoT-enabled devices are expected to increase to 75.44 billion devices by 2025 [4]. LoRaWAN, is a long-range LPWAN technology for IoT applications and has been recently used in various IoT smart applications [5] though LoRaWAN propagation models, and LoRaWAN scalability for IoT RHM applications needs further investigation. Furthermore, RNN has recently been used to create several resilient models such as intrusion detection systems with significant results [6]. Nevertheless, RNN applied to end device localization and Heart Disease Prediction (HDP) is a research topic to be further studied.

Therefore, this thesis evaluates the performance of LoRaWAN and RNN for location-based IoT remote health applications in smart cities. Initially, this study analyses the performance of LoRaWAN propagation models in an urban environment. Secondly, LoRaWAN scalability is analysed for RHM IoT applications in a dense urban environment. Then, RNN is used to de-

velop and evaluate End Device (ED) localization models for indoor and outdoor environments. This is crucial for location-based IoT applications such as RHM in case a patient is in a critical condition or unconscious and needs to be accurately located for quick intervention. Hence, a patient or an elderly individual can be located based on the RSSI values of their body vital signs such as blood pressure or heart rate, which are normally sent for health monitoring on a real-time basis. Furthermore, RNN is used to develop Heart Disease Prediction (HDP) model, and the obtained results are significant.

In this chapter; thesis aims, motivation, and research contributions are given, and it is concluded by the organization of the rest of this thesis.

1.1 Research Aim and Objectives

The overall aim of this research project is to evaluate the performance of LoRaWAN and RNN to provide indoor and outdoor localization-based remote health monitoring services.
The main objectives of this thesis are as follows:

1. Performance evaluation of LoRaWAN propagation models in an urban area using four popular propagation models.

2. LoRaWAN scalability analysis for IoT RHM applications in an urban area.

3. Development and evaluation of an energy efficient localization model using LoRaWAN RSSI values and RNN to predict unknown positions in small scale urban area.

4. Development and evaluation of a low-power, large-scale localization model using LoRaWAN RSSI values and RNN to predict unknown positions in a dense urban area.

5. Development and evaluation of an energy efficient localization model using LoRaWAN RSSI values and RNN to predict unknown positions in an indoor environment.

6. Development and evaluation of a heart disease prediction model using RNN.

1.2 Motivation

The main motivation of this study is the importance of accurate and energy efficient localization models which are very crucial in IoT remote health applications. Furthermore, another motivation of this study is to exploit the advantages of LoRaWAN such as low power, long range and is within the license-free spectrum. Moreover, RNN has more advantages compared to other algorithms; among others RNN can be easily implemented on hardware, and has a stronger generalisation capacity for predicting patterns not covered in the training phase. Furthermore, this is an exploratory research worth doing since no one has reported to have used RNN in localization in the literature. Finally, this study is an important contribution especially in countries with less economies where power and internet infrastructures are still limited.

1.3 Thesis Contribution

The first contribution of this study is to evaluate the performance of LoRaWAN propagation models in the urban area of Glasgow city. To achieve this, ICS Telecom is used to investigate LoRaWAN radio network coverage at 868 MHz using the Okumura-Hata, COST-231 Hata, Extended Hata, and ITU-R 1225 propagation models. The simulation results are compared with real test data collected in the urban environment of Glasgow city to evaluate the performance of the used four propagation models. Our results and analysis give essential insights into the performance, evaluation, and comparison of existing propagation models for IoT connectivity with LoRaWAN technology within an urban environment, and accurate evaluation of LoRaWAN network radio coverage is crucial before any LoRaWAN network implementation for current and future IoT applications. Subsequently, propagation models are used to characterize the propagation of signals in different scenarios and are the tool to achieve the best coverage prediction [7].

In addition, reliable LoRaWAN scalability with interference analysis is a fundamental research topic yet to be thoroughly investigated. As the next contribution, this thesis analyses and discusses LoRaWAN scalability for IoT RHM applications using the ICS Telecom simulator. A network model was developed for fixed and mobile ED using health traffic requirements for blood pressure. Results of Reception Threshold Degradation (TD) [8] of three Lo-

RaWAN gateways due to uplink interference of an increasing number of ED is recorded and analysed for the urban area of 0.75 km^2 in Glasgow city. The obtained TD results give important insights to be considered when deploying scalable LoRaWAN dense networks, particularly for remote health IoT applications in an urban scenario. Hence, sufficient links' fade margin values will be planned to keep the gateway TD values within the recommended range, and evade network outage.

Furthermore, in this thesis we develop and evaluate the performance of the following IoT applications using RNN:

- A novel energy-efficient LoRaWAN-based localization model is developed and its performance evaluated in indoor and outdoor environments using RNN. Localization is vital in location-aware IoT applications whereby a sensor node needs to be accurately located for emergency or maintenance services. WiFi [9], Bluetooth [10], and Zigbee [11] are primarily applied in localization systems for indoor environments but only limited to a few meters. GPS is frequently used as a potential solution for outdoor localization applications, but limited in indoor environments and uses high power consumption [12]. RSSI fingerprint localization methods involve mapping RSSI values to corresponding X,Y position coordinates [13]. Moreover, RSSI fingerprint localization approaches have been proposed for accurate localization models in the literature using Bluetooth [10], WiFi [9], and Zigbee [11] wireless technologies and successfully implemented but all with significant drawbacks and limitations.

- Finally, RNN is used to predict and diagnose heart disease using accuracy, precision, specificity, sensitivity, and recall as performance metrics on open-access online repository Cleveland dataset. Heart diseases lead to heart failures and are life-threatening diseases causing deaths globally [14]. Early and correct prediction and diagnosis of heart diseases is essential for treatment and saving lives from heart diseases. Many researchers have recently been using different machine learning approaches to developing models to detect heart diseases in the literature. However, research using data analytics is still under exploration.

1.4 Thesis Organization

The organization of this thesis is as follows:

- Chapter 2 describes the background of wireless technologies for IoT applications, LoRaWAN propagation models, LoRaWAN scalability, RHM, RNN, GD, end device localization, and heart disease prediction.
- In chapter 3, the literature survey carried out on LoRaWAN propagation models, LoRaWAN in RHM, and LoRaWAN scalability is presented. Then, the existing systems that applied RNN are reviewed. ED localization approaches and heart disease prediction approaches are also reviewed.
- In chapter 4, the performance of LoRaWAN propagation models is evaluated in an urban area.
- In chapter 5, LoRaWAN scalability is analysed for IoT RHM applications in a dense urban area.
- In chapter 6, different IoT applications are developed and evaluated using RNN; LoRaWAN-based IoT localization systems are developed and evaluated in indoor and outdoor scenarios.
- Finally an IoT heart disease prediction model is developed and evaluated. Finally, thesis conclusions, limitations, and open research challenges are summarised in Chapter 7.

Figure 1.1 shows a summary of chapters and published and unpublished work.

Chapters	Publications

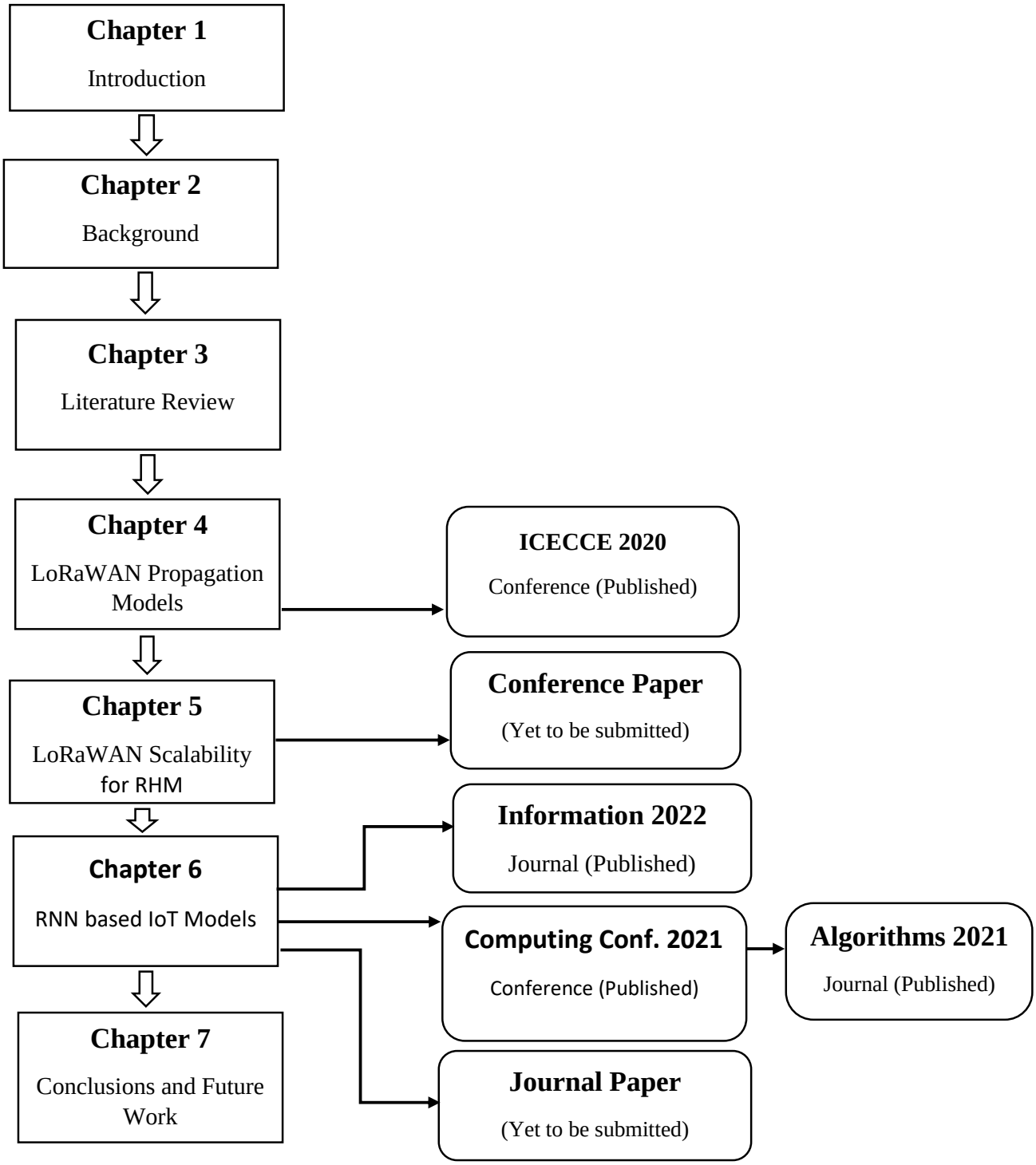

Figure 1.1: A summary of chapters and published and unpublished work

Chapter 2

Background

This chapter is arranged as follows; initially it gives an overview of wireless technologies for IoT applications, LPWAN technologies with emphasis on LoRa and LoRaWAN. Then, four LoRaWAN propagation models considered for this study are described in details. Then, it presents an overview of LoRaWAN scalability, RHM, RNN, Gradient Descent Algorithm (GD), ED Localization, and Heart Disease Prediction (HDP).

2.1 Wireless technologies for IoT Applications

Bluetooth wireless technology, LoRa, and NB-IoT LPWAN technologies are commonly used wireless candidate technologies for IoT applications. The main features and properties of these wireless technologies are discussed in the following section.

2.1.1 Bluetooth

Bluetooth is a low-cost low- power wireless technology used to create Personal Area Networks (PAN) within a short range of less than 10 m with no infrastructure required [15]. It allows several devices to transfer data to other devices in ad hoc networks while overcoming synchronization problems. Bluetooth is managed and supported by Bluetooth Special Interest Group (SIG), and a summary of its main features from IEEE 802.15.1 specifications is presented in Table 2.1, with Frequency Hopping Spread Spectrum (FHSS) among the presented specifications.

Table 2.1: Bluetooth main features

Connection	FHSS
Bandwidth	2.4 GHz
Supported Data Rate	0.723-1 Mbps
MAC Scheduling	FH-CDMA
Transmission Range	1-10 m
Maximum number of cell nodes	8
Transmission Power	>20 dBm
Voice Channels	3
Data Security-Encryption key	8-128 bits (configurable)
Data Security-Authentication key	128 bits key

2.1.2 Protocol Stack

Bluetooth protocol stack standard that defines how devices should communicate with each other using Bluetooth technology is presented in Fig 2.1 [16]. The links set up by devices in communication are managed by the link manager layer using 34 link manager protocols to negotiate and maintain connections between user devices. Link manager layer operates above the baseband and physical layer. The Logical Link Communication and Adaptation Protocol (L2CAP) formats the data to be transmitted into small packets.

2.1.3 Physical Layer

Bluetooth radio network technology uses the Industrial, Scientific, and Medical (ISM) 2.4 GHz frequency band and uses frequency hopping spread spectrum modulation scheme with 79 channels of 1MHz bandwidth each [17]. Bluetooth supports three power classes, as shown in Table 2.2, whereby a class with the highest power has the most extended transmission range, and the lowest power class has the shortest transmission range.

Table 2.2: Bluetooth power classes

Class	Signal strength	Transmission Range
1	1 mw (0 dBm)	Short range <= 10 cm
2	25 mw (4 dBm)	Range <= 10 m
3	100 mw (20dBm)	Long Range <= 100 m

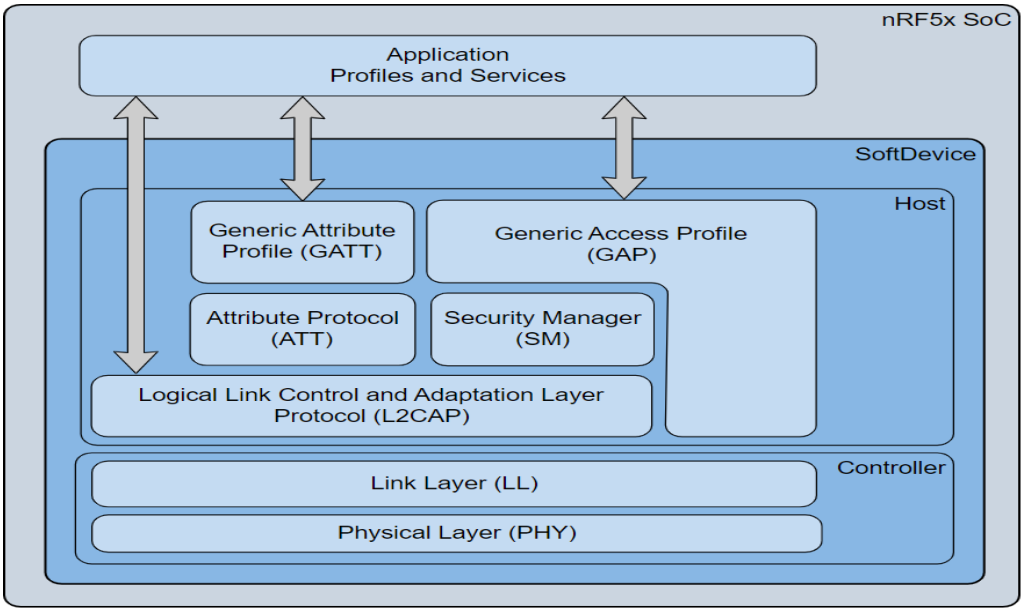

Figure 2.1: Bluetooth protocol stack [16]

The Bluetooth basic unit of network is known as a piconet. It is made up of one master node and a maximum of seven slave nodes connected as in Fig 2.2. Two or more connecting piconets as shown in Fig 2.3., form a scatternet which supports more than 8 nodes to connect. However, less implementations of scatternets are currently in existence.

Bluetooth allow Point-to-Point and Point-to-Multipoint connections. Master nodes allow slave nodes to be served using time division duplex mechanism.

2.2 LPWAN Technologies

Wireless technologies play an essential role in enabling connectivity among IoT devices and objects. Among others, we have dominant cellular networks such as 4G widely known for reliable long-range connectivity for mobile communications (GSM). However, cellular technologies are not energy efficient, hence not a right choice for IoT connectivity solutions in large scale networks. Furthermore, Wi-Fi technology, in addition to its high energy consumption, it has a short range of operation.

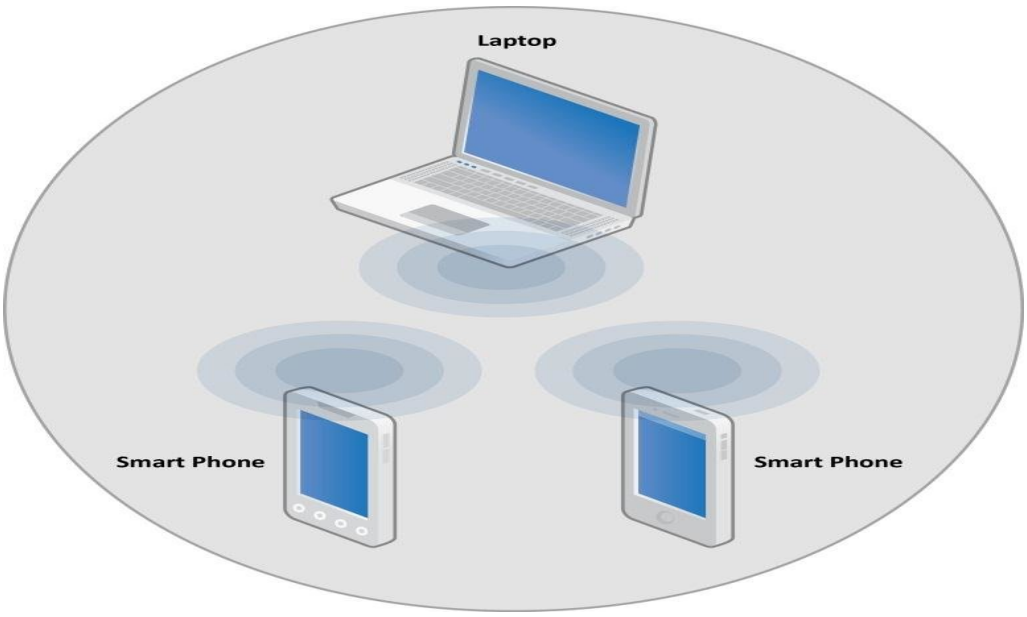

Figure 2.2: A piconet [16]

The invention of LPWAN technologies such as Long Range (LoRa), Sigfox, and other emerging technologies for the Internet of Things (IoT) in smart applications, came as a perfect solution to energy efficiency [18]. Apart from LoRa, which is covered in more detail in the following sections, this chapter briefly introduces the most well-known and advanced LPWAN technologies. LPWAN technologies such as LoRaWAN are license-free and offer low-power, long-range, and wide area networks [21]. However, diverse LPWAN technologies are best suitable for different specific smart city applications depending on the required connectivity features or characteristics. LoRaWAN protocol uses lower power consumption levels than other LPWAN technologies based on LoRaWAN architecture to provide reliable communication for mobile devices [22].

2.2.1 NB-IoT

NB-IoT is also an emerging LPWAN licensed technology by 3GPP. It is a new air interface integrated into LTE standard [23].

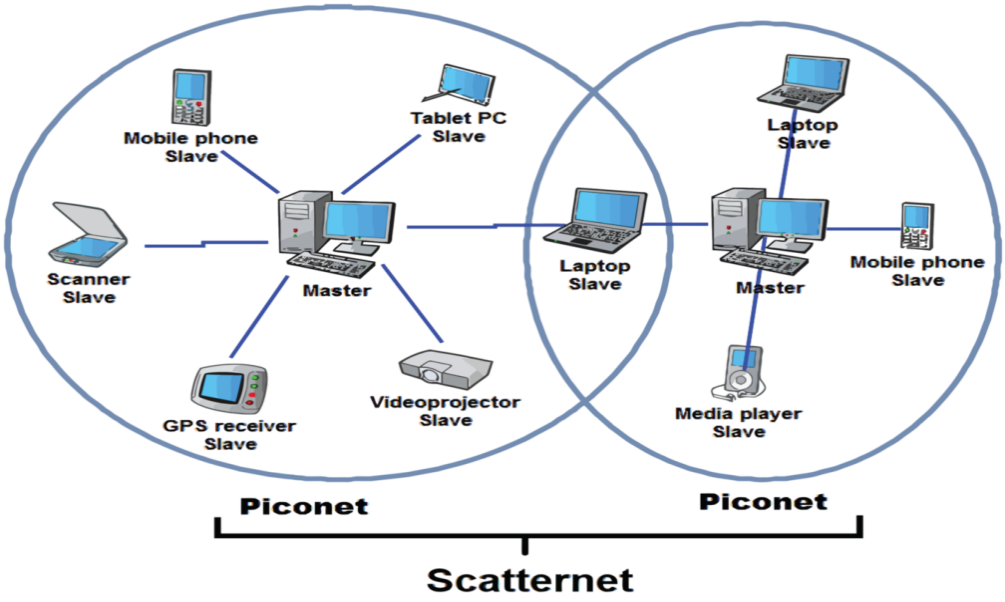

Figure 2.3: A scatternet [16]

It is a simpler LTE version without handover, channel quality monitoring measurements, dual connectivity and carrier aggregation for minimal device power consumption, and reduced costs. It uses LTE frequency numbers with QPSK modulation technique, and some of its main features are presented in Table 2.3.

NB-IoT operates in standalone, guard-band, and in-band modes as shown in Fig 2.5, whereby 12 subcarriers of 15 kHz using OFDM are in the downlink and 3.75/ 15 kHz using SC-FDMA are in the uplink [24].

MAC Protocols

NB-IoT uses enhanced LTE general fundamental protocol stack reduced to a minimum for re-using. Control and User planes are the two planes of NB-IoT protocol structure. Non-Access Stratum (NAS) of the NB-IoT protocol stack manages mobility, controls security, and performs authentication between the core network and end user.

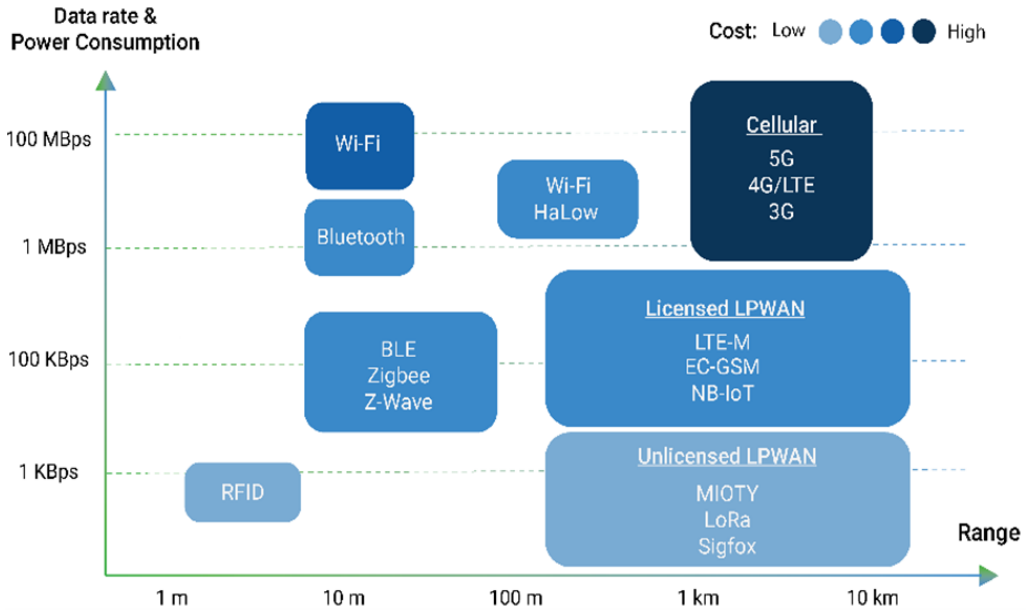

Figure 2.4: Different wireless IoT-enabling technologies (Adapted from: IoT for all)

NAS is encrypted by layer 2 (L2) with 1600 bytes. Access Stratum (AS) layer manages NB-IoT radio resources between the radio network and end-user. The radio resource control (RRC) layer minimize signaling by suspending or resuming the operation of the user plane. The random-access channel (RACH) procedure is always contention-based and begins with the transmission of a preamble [23].

NB-IoT and LoRaWAN key features are different as seen in this section. Therefore, each technology should be considered for any specific application depending on its properties [24].

2.2.2 SIGFOX

The first LPWAN technology to hit the market SIGFOX was developed by a French business established in 2009 [25]. In order to transmit data utilising ultra-narrow (UNB) technology, a cellular-style system, and binary phase-shift keying (BPSK) modulation are used. The 868 MHz, ISM frequency range, split into channels of 100 Hz width, is used for data transmission. In rural areas, messages are claimed to reach up to 50 Km and 10 km in cities.

Table 2.3: NB-IoT main properties

Parameters	NB-IoT
Spectrum	Licensed LTE bandwidth
Modulation	QPSK
Bandwidth	180 kHz
Peak data rate	DL:234.7,UL:204.8 kbps
Link budget	150 dB
Max number message/day	Unlimited
Duplex operation	Half duplex
Voice Channels	3
Power efficiency	Medium high
Energy efficiency	>10 years battery life of devices

SIGFOX constrains both the number of messages per day and the payload data size. This entails a daily limit of 140 messages with a payload size of no more than 12 bytes for uplink transfers. 8 bytes is the maximum size and number of bytes allowed for downlink communications [26]. Each gateway, according to SIGFOX, can manage one million connected devices. The lack of publicly accessible documentation for SIGFOX's internal workings is because its network layer is not open to the public.

2.2.3 WEIGHTLESS

The nonprofit Weightless Special Interest Group (SIG) developed three open wireless technology standards known as Weightless. Each of the weightless protocols has unique properties and operates in sub-GHz frequency ranges. While Weightless-W runs in the (TV whitespace) frequencies between 470 MHz and 790 MHz that were originally designated for analog TV broadcasts, Weightless-N and Weightless-P operate in license-free ISM bands [27]. There can be licensing requirements for using these frequencies. For Weightless-P and Weightless-W, the packet size is configurable and has a minimum of 10 bytes but no set maximum. The maximum Weightless-N packet size is 20 bytes. The channel width and communication range in urban areas are 2 km for -P and 5 km for -W, respectively [27].

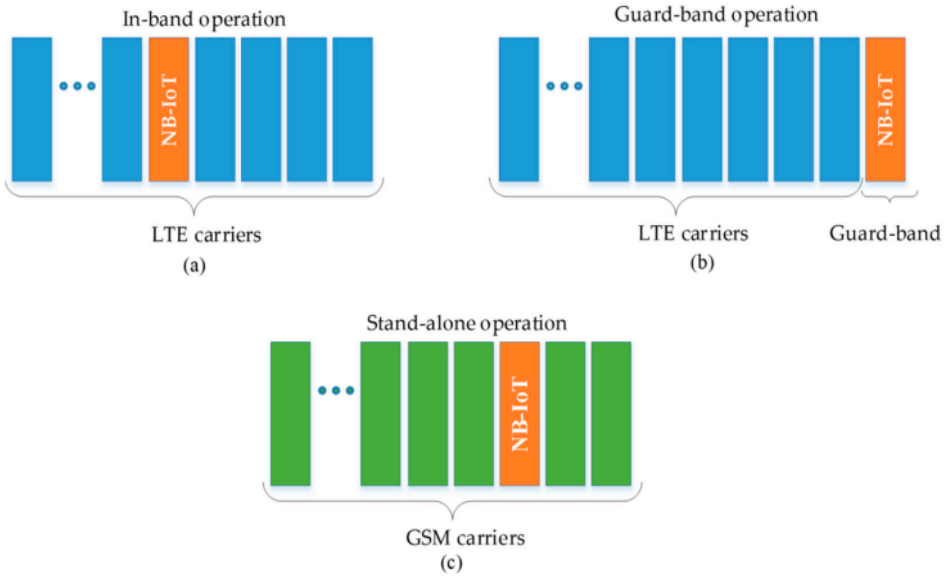

Figure 2.5: NB-IoT operation mode deployment [23]

2.2.4 INGENU

Ingenu, originally On-Ramp Wireless, was established in 2008. The company developed and patents its Random Phase Multiple Access (RPMA) technology, which it utilizes in uplink communication. Additionally supported are downlink communications [28]. However, these use standard Code Division Multiple Access (CDMA) modulation. The RPMA uses 1 MHz wide channels in the unlicensed 2.4 GHz spectrum. In the case of an open line of sight, messages can travel over 500 km and include data ranging from 6 bytes to 10 Kilobytes [28].

2.2.5 LoRa Technology

LoRa is a physical layer with Chirp Spread Spectrum (CSS) modulation technique operated by Semetch [29]. LoRa is usable within the license-free spectrum from 863 MHz to 870 MHz in Europe and from 902 MHz to 928 MHz in the USA.

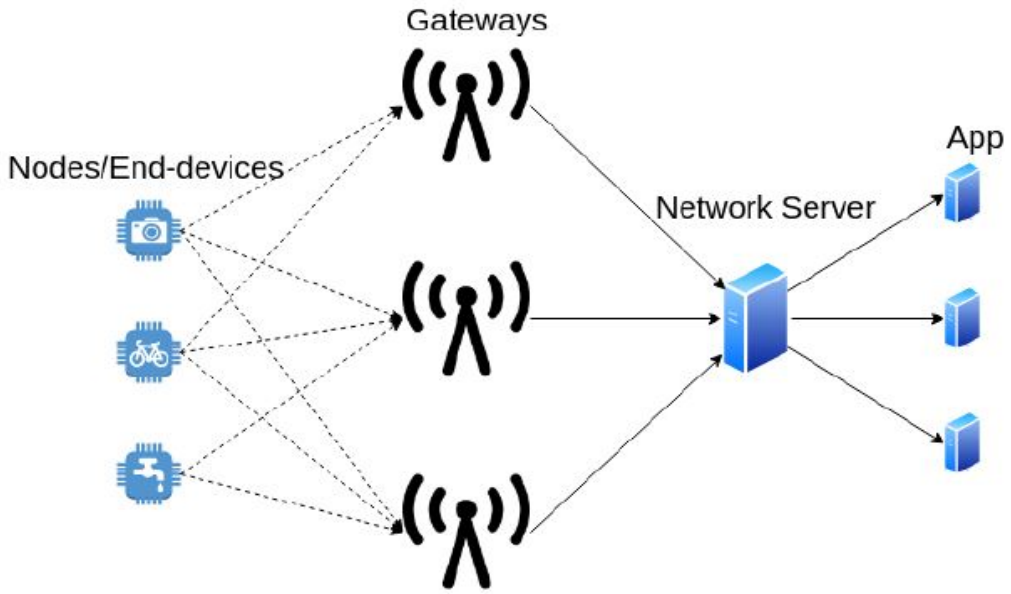

Figure 2.6: LoRa network topology

LoRa reliable radio network coverage is characterized by various combinations of the following parameters: Transmission Power (TP), Bandwidth (BW), Carrier Frequency (CF), Spreading Factor (SF), and Coding Rate (CR) [30]. The connection of the wide area network of LoRa is called LoRaWAN. It is a network protocol stack and offers the architecture of LoRa technology on the MAC layer. A LoRaWAN network is made up of LoRa end devices connected in a star topology that send information to a LoRaWAN gateway, which in turn sends it to a network server, as shown in Fig 2.6.

LoRaWAN network architecture to enable low cost, long-range transmissions at low power consumption as evaluated and confirmed by authors in [31]. The level of power consumption of LoRaWAN sensors determines their battery lifetime and the lifetime of the whole network. There is also a guarantee about LoRaWAN scalability and range of coverage, as reported by authors in [32].

According to their results, only three gateways are enough for reliable radio network coverage of a dense urban city within a radius of 15 km, whereby each gateway can support up to 10^5 end devices. Moreover, in [33], the authors explore and confirm security robustness for LoRaWAN technology. Regarding energy consumption and cheap implementation and deployment costs, LP-

WAN technologies are designed to provide a wide range of features that can sometimes outperform and complement traditional cellular and short-range wireless technologies [19]. This is also demonstrated in Figure 2.4, which compares several wireless communication systems in terms of their range, bandwidth, energy use, and implementation costs. There have been many implementations of LPWAN technologies over the past few years due to the characteristics of these technologies and their anticipated contribution to the growth of IoT communication. The following are the traits that all of these technologies share:

- Long range: End nodes can be more than 10 kilometers apart from gateways.
- Minimal energy usage: sufficient for five to ten years.
- Using sub-GHz frequency bands with less interference to lessen attenuation caused by barriers.
- Low data rate: 20–256 bytes each message, or less than 5.000 bits per second [20].

Spread Spectrum Modulation

Based on Chip Spread Spectrum (CSS) modulation, LoRa is a spread spectrum modulation technique [18]. Because of its broad communication range and robustness to interference, the chirp spread spectrum has been deployed for military and space communication since the 1940s. The sent signal in a spread spectrum system is dispersed over a large frequency band significantly broader than the minimum bandwidth needed to deliver the data. Due to the signal's wide distribution throughout a vast bandwidth, this modulation type is resistant to both narrowband and wideband disruptions [34]. Other advantages of CSS include the ability to demodulate the spread, resistance to Doppler shift, multi-path fading, and low transmission power required to transmit over a specific distance and spread signal's capacity to be demodulated from below the noise floor.
The LoRa modulation technology itself can be applied to a variety of network designs. In LoRa modulation, the signal is distributed across the spectrum by developing chirp signals, which are signals in which the frequency linearly rises (up-chirp) or falls (down-chirp) over time. The spreading factor (SF),

also called the chip data rate, measures how quickly each chirp changes in frequency. These chirp symbols have a capacity equivalent to the signal's spectral range. Each chirp symbol has between 6 and 12 SF-encoded bits. The transmission time, also known as the time on air, is influenced by the SF, which impacts energy consumption. Thus, it establishes the quantity of redundant data dispersed throughout the transmission. A large spreading factor results in the transmission of more redundant data, extending the range but reducing the data rate [35]. Multiple spread signals can be delivered simultaneously and on the same channel using LoRa because it uses orthogonal spreading factors, which prevents signal degradation.

ISM Frequency Band

LoRa utilizes the sub-1 GHz ISM bands 433 and 868 MHz (EU) and 169, 433, and 915 MHz license-free (USA) [29]. The spread of these license-free frequency bands and their rules vary by region. As a result, regional variations in LoRa usage criteria may occur. These specs are only currently available in Europe and North America. The use of LoRa in Europe, where it may operates in 868 MHz frequency band, is considered in this thesis. The European Telecommunications Standard Institute (ETSI) is responsible for defining radio spectrum allocation and ISM band standards for Europe [36]. ETSI refers to the SRD860 band, which has a frequency range of 863-870 MHz, as band G. In general, the maximum transmission power (14 dBm) and duty cycle (0.1%) are constrained by laws while using this spectrum. When an end device uses Listen Before Talk (LBT) and Adaptive Frequency Agility (AFA), which allows it to recognise an open sub-band or other open frequency, less stringent duty cycle requirements are applicable. The device can dynamically switch the temporarily functioning channel if another transmission is detected and can detect an open sub-band or channel before sending. A LoRa end device is not permitted to have an adequate isotropic radiated power (EIRP) greater than 25 mW, except while operating in the G3 band (14 dBm). This indicates that when a theoretically ideal isotropic antenna is utilised, an end device shouldn't emit more energy than 25 mW. A device is not permitted to exceed a cumulative transmission time on one carrier frequency relative to an hour, according to the duty cycle limitations that ETSI has established for each band. Therefore, when the maximum duty cycle is 1%, this restriction results in a total transmission time of 36 seconds per hour. Several sources claim that the maximum continuous trans-

mission time is significantly less than the maximal transmission time within one hour. An end device cannot, for instance, communicate for 36 seconds before going silent for an hour. There are numerous ways to implement these transmission rules, the communication system, and the network architecture. The market adoption of the technology would be aided by the creation of interoperability between LoRa-enabled systems if such design decisions were to be codified into a standard.

2.3 LoRaWAN Propagation Models

Propagation models are used to characterize the propagation of signals in different scenarios and are the tool to achieve the best coverage prediction [52]. Thus, there is a strong need to analyse which of the existing propagation models efficiently models LoRaWAN radio network coverage in specific geographical locations. In this work, four of the most common propagation models that are used in LoRaWAN, and are chosen to be used in this research study: The Okumura-Hata Model, COST-231 Hata Model, Extended-Hata, and ITU R 1225 are considered in this study by analysing the Path Loss (PL) of each propagation model in an urban area.

2.4 LoRaWAN Scalability

In a LoRaWAN network, end devices can use different Spreading Factors (SF) to avoid interfering with each other [29] with increasing number of end devices in a scalable network. Nevertheless, since there is a limited number of SF, the risk of interference between end devices of the same network is essential to evaluate. A gateway can receive signals simultaneously from two end devices using the same frequency, the same SF, and close received signal power. A network system interference increases with an increasing number of radio links resulting in Threshold Degradation (TD) of gateway receivers. Moreover, radio channels reused at the same position leads to TD above recommended values. According to ECC report [8], the maximal TD for one transmitter is 1 dB and 3 dB for the aggregate interference for all transmitters. However, for dense network deployment higher TD values are allowed if the network performance and connectivity targets can still be met. In this regard, average gateway receiver input signal values are set above enough the

corresponding TD values (fade margins) for better network performance and availability contrary to outage time when the average receiver signal values are under the corresponding TD values. Hence, transmission links planned with large fade margin values can withstand large TD without increasing outage time [37].

Henceforth, this study investigates the uplink interference with TD limitations of Scalable LoRaWAN technology, particularly for future remote patient monitoring applications in an urban environment. Furthermore, the used ICS Telecom simulator [38] enables modelling ED with RHM traffic requirements for fixed and mobile ED, and the tool's ability to incorporate most of the terrain details of a relevant specific area is crucial in qualifying the predicted simulation results.

2.5 Remote Health Monitoring

Hospitals or health centers are essential for any existing nation. Patients go to health centers mainly in case their health conditions are abnormal, and a constant monitoring routine is largely possible once a patient is admitted. Physiological monitoring is essential in caring and managing patients dealing with their health deterioration. Health personnel monitor and record vital signs of each of the registered patients on a frequent routine depending on their health condition status. A minimum of five basic vital signs should be considered for any initial physiological monitoring, according to the authors in [39]. These include but not limited to Blood pressure, Heart rate, Respiratory rate, Oxygen saturation, and Body temperature.

Physiological monitoring enables identifying changes in vital health signs of each patient, which helps in determining if there is any health improvement or not or identify any health deterioration and provide appropriate treatment. The frequency of patient monitoring may be increased if patients' health is deteriorating or reduced if there is an improvement; a doctor or a nurse may decide this. Furthermore, elderly and patients with chronic diseases require real-time physiological monitoring but do not need to be admitted. Hence, wireless RHM is a solution for remote physiological monitoring of patients and the elderly wherever they are, whether inside or outside hospitals/health centers. Moreover, RHM is one of the promising smart applications of LoRaWAN [3]. However, LoRaWAN reliable scalability is a fundamental research subject that is still under investigation.

2.6 Random Neural Networks

RNN was first initiated by Erol Gelenbe [40] and has been considered by different researchers as a classification algorithm in various fields. In RNN, layers exchange spiking signal information between interconnected neurons as impulses, and a neuron is either in an excited state with a positive potential of (+1) or an inhibited state with a negative potential of (-1) when it receives a signal. The potential of any neuron i is represented by a non-negative integer $K_i(t)$ at time t. The neuron i is in the idle state when $K_i(t) = 0$, and $K_i(t) > 0$ represents the potential of the neuron i in the excited state. In RNN, the neuron i transmits to the next neuron j at a rate of r_i with a probability of $p^+(i,j)$ when excited or $p^-(i,j)$ when inhibited. Furthermore, the signal transmitted can leave the network with a probability defined as follows:

$$c(i) + \sum_{j=1}^{N} p^+(i,j) + p^-(i,j) = 1, \forall i, \tag{2.1}$$

$$w^+(i,j) = r_i p^+ + (i,j) \geq 0, \tag{2.2}$$

Similarly

$$w^-(i,j) = r_i p^- + (i,j) \geq 0. \tag{2.3}$$

Combining equation 2.1, 2.2, and 2.3

$$r(i) = (1 - c(i))^- 1 \sum_{j=1}^{N} [w^+(i,j) + w^-(i,j)] \tag{2.4}$$

Where $r(i) = \sum_{j=1}^{N} [w^+(i,j) + w^-(i,j)]$. Also, "$w$" refers to the matrices of weight updates from the neurons, which is a non-negative value since it is product of transmission rates with probabilities.
A spiking signal reaches neuron (i) when excited with a positive potential and a rate of $\Lambda(i)$ or inhibited with a negative potential at a rate of $\lambda(i)$. Therefore, each node output activation function "i" is defined by:

$$q(i) = \frac{\lambda^+(i)}{r(i) + \lambda^-(i)}, \tag{2.5}$$

where

$$\lambda^{+}(i) = \sum_{j=1}^{n} q(j)r(j)p^{+}(j,i) + \Lambda(i), \tag{2.6}$$

therefore

$$\lambda^{-}(i) = \sum_{j=1}^{n} q(j)r(j)p^{-}(j,i) + \lambda(i). \tag{2.7}$$

A neural network is a type of function that takes in inputs (data) and outputs predictions. The parameters or weights of the neuron serve as the function's variables. To solve a task given to a neural network, it is crucial to modify the weights' and biases' values in a way that approximates or best represents the dataset. A neural network takes in inputs, which are then forwarded to the layer with the weights' neurons. After multiplying the inputs and weights, the result is added together by an adder, and an activation function controls the layer's ultimate output.

A method for measuring the error between the neural network prediction and the actual data sample value is needed to evaluate the performance of neural networks. This computation produces a factor that affects how weights and biases are modified within a neural network. The cost function facilitates the error gap between the value of a data sample and the value predicted by a neural network. The weights and biases used for the final model are influenced by the cost function's partial derivatives. The Gradient Descent Algorithm (GDA) makes it easier to find biases and weights that reduce the cost function in order to reach a local minimum or optical precision.

According to Cerkez et al. [41] and Abdelbaki et al. [42] results, simple encounters can represent neurons in RNN and hence easy hardware implementation. In addition, RNN accurately predicted unseen patterns not included in the training data when compared with the conventional ANN performance [43]. Furthermore, RNN outperformed ANN during run-time though at the expense of a greater training time [44], and the authors also reported that RNN had a stronger generalisation capacity for the training phase uncovered patterns.

Using the RNN approach consists of directed multiple layers of connected nodes in a network. This network is used to develop a model that accurately maps the input to the output using historical data, and the model can then be used to output any desired unknown output on the network grid as seen in Fig 2.7.

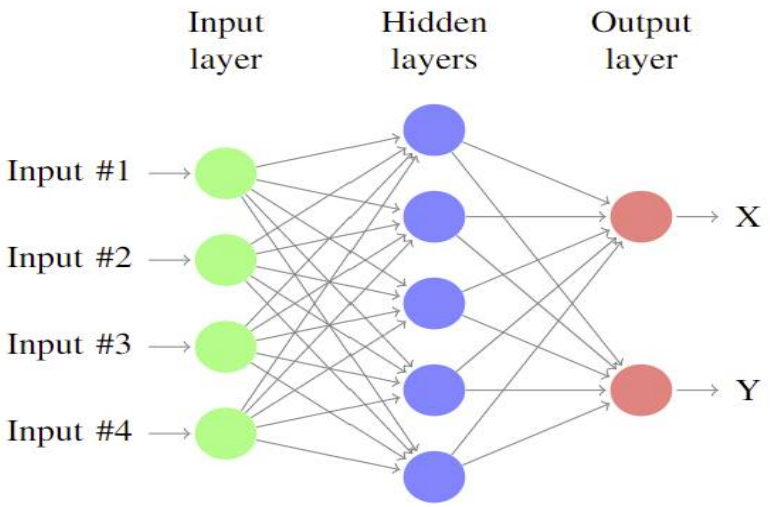

Figure 2.7: A typical neural network architecture [163]

2.7 Gradient Descent Algorithm

Gradient Descent (GD) is a first-order iterative optimization algorithm widely used for training prediction models by different researchers. It is used to minimize the cost function whereby the error cost function is given by:

$$E_p = \frac{1}{2}\sum_{i=1}^{n} \gamma_i (q_j^p - y_j^p)^2, \gamma_i \geq 0 \tag{2.8}$$

whereby $\gamma \in (0, 1)$ presents the state of output neuron i, likewise q_j^p is a real differential function whereas q_j^p is the predicted output value. As, per Equation 2.8, to find the local minima and reduce the error value of the error cost function, the relation between neurons y and z is considered, whereby weights $w^+(y, z)$ and $w^-(y, z)$ are updated by:

$$w_{y,z}^{+t} = w_{y,z}^{+(t-1)} - \eta \sum_{i=1}^{n} \gamma_i (q_j^p - y_j^p)[\partial q_i \partial w_{y,z}^+]^{t-1}, \tag{2.9}$$

also:

$$w_{y,z}^{-t} = w_{y,z}^{-(t-1)} - \eta \sum_{i=1}^{n} \gamma_i (q_j^p - y_j^p)[\partial q_i \partial w_{y,z}^{-}]^{t-1}. \tag{2.10}$$

The proposed RNN-LoRa RSSI based localization model was trained using GD, where the calculated weights and biases are updated to the neurons as the algorithm computes the error. Gradient descent algorithm is used as the optimization algorithm to train the random neural network. More details about Gradient descent and RNN are presented in [45].

2.8 End Device Localization

Localization is vital in developing smart cities applications with the IoT, where ED can be monitored or tracked in both outdoor and indoor environments. GPS are broadly considered for outdoor localization applications [46]. Nonetheless, GPS is not suitable for indoor localization services due to solid and thick obstacles found in buildings, and a higher power consumption [12]. Furthermore, different wireless technologies such as Bluetooth [10], WiFi [9], and Zigbee [11] have been used to develop indoor localization systems but are only limited to the range of 30 to 100 meters. Furthermore, technologies based on satellites are the pioneers in the accurate localization systems for outdoor applications, with errors less than 4 m for Galileo's Open Service and 10 m using GPS [46]. Satellite-based technologies provide continuous global coverage and play significant roles in a wide range of applications. However, Global Navigation Satellite System (GNSS) modules consume high energy, which rules them out for many low-power IoT end devices. Additionally, incorporating many stand-alone sensor nodes in dense sensor network applications with GPS modules would not be efficient due to high hardware cost, high power consumption, and failures due to non-line of sight communications [12]. Time-of-Arrival (ToA), RSSI ranging, and Time-Difference-of-Arrival (TDoA) algorithms are among the most researched range-based localization techniques in IoT and Wireless Sensor Networks (WSN). Trilateration or Triangulation approaches are used to calculate the location coordinates of the end device using multiple anchor end nodes with known location coordinates [47], whereby LoRaWAN gateways may be referred to as anchor points. A propagation model and the RSSI are used to compute the distance between

receiver and transmitter in RSSI ranging. However, multipath and shadow fading lead to the loss profile with indoor RSSI ranging.

A scheduling algorithm with accurate end devices' time synchronization is required for ToA, whereas accurate gateways time stamps for at least three distant gateways are only required for TDoA and make it more suitable for IoT end devices. The calculation of an end device location is made when at least three distant gateways received the same transmission signal from the same end device as ideally, the signal trajectories to the gateways intersect at the location of the end device. However, any slight scheduling error may lead to inaccurate location predictions. The traditional LoRa based localization systems use TDoA [48] and fingerprint algorithms [13], all with limitations in dense large urban areas and still under investigation. TDoA performance is poor in dense urban areas though it performs well in open areas [49] . Fingerprinting localization uses end devices' RSSI fingerprint values received by gateways to localize any end device in the network accurately. A fingerprint-based approach consists of an offline training phase and an online phase [50]. Data samples are collected from a considered service area where localization is to be predicted and used to train a fingerprint algorithm. Therefore, the location of any end device can then be predicted using the trained algorithm in an online phase based on end-device RSSI characteristics. However, all existing fingerprint algorithms also have various challenge.

The following challenges are among the issues limiting the performance of existing RSSI fingerprint techniques for effective ED localization:

- Fingerprint data maps are affected by changing environments.
- Strong fingerprint databases are needed.
- Manpower is needed for creating fingerprint databases.
- Non-linearity challenge between end nodes and target gateways.
- High power-consumption and cost.
- Complicated infrastructure layout.

Studies using LPWAN for sensor node localization are present in literature, however, frequently limited to specific settings such as a small area or fixed end nodes. A typical outdoor localization method in Long Range (LoRa) networks is the Time Difference of Arrival (TDoA) technique [48].

However, this method performs well in open environments and poorly in harsh urban areas.

Thus this study uses RNN in developing a long-range power efficient localization system applying LoRaWAN signal strength values to determine unknown X and Y position coordinates both indoor and outdoor environments. The proposed system achieves higher accuracy than conventional localization systems in current related studies.

2.9 Heart Disease Prediction

According to the World Health Organization (WHO) recent report [14], heart diseases, also known as cardiovascular diseases (CVD), contribute to 17.9 million deaths each year, which is 32% of all deaths occurring worldwide. Moreover, heart attacks and strokes cause 85% of all CVD deaths, and 75% of CVD deaths are in developing countries. CVD comprise various heart conditions such as hypertension, coronary heart and artery diseases, stroke, rheumatic heart disease, and others that lead to the heart failing to supply enough blood to other body parts for normal functioning. CVD's timely accurate prediction and diagnosis are vital for early treatment and minimize the CVD death rate.

Different researchers have used machine learning algorithms on available clinical heart data in repositories to predict and diagnose heart disease with significant outcomes [126]. Furthermore, RNN has been used to develop different models for various applications such as image recognition, intrusion detection with significant results. However, RNN used for heart disease data analysis and prediction is yet to be investigated.

This thesis therefore uses RNN to develop and train a heart disease prediction model to predict and diagnose heart disease using the Cleveland Clinical Foundation dataset, an open-access online repository of the University of California, Irvine (UCI) [51] and the prosed model outperforms traditional machine learning algorithms existing in the literature.

Chapter 3

Literature Review

This section covers studies found in literature related to this research study. Literature has been reviewed for LoRaWAN propagation models, LoRaWAN in RHM, and LoRaWAN scalability. Furthermore, the existing systems that used RNN are reviewed. ED localization approaches and heart disease prediction approaches are also reviewed in this chapter.

3.1 LoRaWAN Propagation Models

Propagation models are required for the accurate Path-Loss (PL) modelling to predict network coverage performance optimization as confirmed in [52]. Research studies about LoRaWAN radio coverage using propagation models are present in literature as presented in [53]-[56]. Moreover, LoRaWAN path loss models were developed and compared to commonly used empirical models as seen in [53]. Using extensive real test measurements taken in urban and open rural areas in outdoor and indoor environments; the authors confirmed their proposed path loss models to be accurate and simple for LoRaWAN technology deployments in Lebanon and other same environments, with coverage of 8 km in urban and 45 km in open rural areas using free-space PL model, log-distance PL model, and multi-wall-and floor model. However, while the Okumura-Hata, COST 231 Hata, Extended Hata, and ITU R 1225 propagation models are primarily used in urban, suburban, and rural settings, we have done a comparative LoRaWAN performance analysis of these models in an urban environment as part of our research study.

Another comparison of the received signal strength real measured values with the radio frequency planning tool has calculated values for Okumura-Hata Model, Irregular Terrain Model (ITM) with Irregular Terrain with Obstructions Model (ITWOM) was made by the authors in [54]. The proposed models accurately fit measurements and are simple to be used. LoRaWAN performance was analysed using packet delivery ratio and signal-to-noise ratio, and the results confirm LoRaWAN communications to be reliable for large-scale urban areas. Nevertheless, LoRaWAN is still under investigation, and our study evaluates different propagation models using LoRaWAN RSSI values. LoRaWAN measured data were also compared with Okumura-Hata model results in urban, suburban, and rural areas, and LoRaWAN was proved to be highly adaptable in several IoT applications in smart cities such as fleet management and tracking as reported in [55]. In this analysis, the received signal power was above -130 dBm for the lowest LoRaWAN data rate, with 12 as the spreading factor. Moreover, LoRaWAN covered 7 km in urban and suburban areas, and 19 km in open rural areas.

More to that, LoRaWAN network performance is experimentally analysed using spreading factors, receiver sensitivity, data rate, and frame format by the authors in [57]. The results show that LoRaWAN has resistance to interference due to high sensitivity and offers a reliable coverage of up to 3 km in a dense residential suburban area. A comparative performance analysis of the Okumura-Hata, COST-231 Walfish-Ikegami (COST-WI) and COST-231 Hata propagation models was performed using the NS3 simulator and the measurements in an urban environment by Harinda et al., in [56]. According to the obtained results, the Okumura-Hata model had a higher accuracy while COST-WI showed lower accuracy. While, the authors in [58] observed a steady difference of 27 dB received signal strength between the Okumura-Hata and the LoRaWAN real measured data. A multi-wall propagation model which was enhanced, and a neural network propagation model were presented by the authors in [59] and [60] respectively. The reviewed studies are a significant contribution to understand LoRaWAN network coverage performance. However, the simulation tools used did not consider the nature of the terrain such as buildings, water or trees of the relevant geographic area as ICS Telecom does. Moreover, no empirical semi-deterministic propagation models were investigated, which is also considered in our study. Semi-deterministic models have the advantage of allowing the evaluation of all environmental impediments, considering all material properties, and accounting for conductivity and dielectric constant at the frequency range

where the system under analysis operates according to the authors in [165].

3.2 Development of RHM Systems

Different prototypes for RHM systems have been designed using IoT, various wireless technologies, and database servers to improve patient-centric services in monitoring the health status of patients on a real-time basis and save lives on time. Gogate J. Bakar, in [61], J.Ma et al., in [62] and P.M.Reddy N.Ome in [63] proposed health monitoring prototypes using biosensors with a microcontroller attached to a human body to measure different body vital signs and send data to thing speak IoT cloud platform using Wi-Fi. Doctors or caregivers can monitor patients' health status and be alerted on their smartphones in case of emergency. P.Kaviya Antony Seba in [64] have proposed an intelligent health monitoring system for patients admitted to a hospital. They also used biosensors with Arduino for sending patient information status to thing speak by virtuino android applications via Bluetooth, Wi-Fi, or the internet. A buzzer would ring in case of an emergency to notify any staff available, and the message would be sent to a doctor. Furthermore, NB-IoT potentials in remote health monitoring applications were considered by authors in [65], [66], [68],[69], and in [70].

3.2.1 LoRaWAN in Remote Health Monitoring

LoRaWAN has been considered by different studies to enhance the development of IoT RHM systems with minimal effect of limited power and network infrastructures, and a number of studies have confirmed LoRaWAN to be promising in providing practical smart solutions in health and wellness monitoring applications as reported by the authors in [3]. Petäjäjärvi et al. in [71] tested LoRa communication technology and confirmed its reliability for both indoor remote health monitoring applications by real test measurements. They used a LoRaMote attached to one of the researcher's human body to send sensed data to a LoRaWAN gateway, and the transmission was successful at a good percentage. This highlights LoRaWAN suitable to provide IoT networks in RHM systems, although the testing was limited to one patient and one gateway. Our study evaluates LoRaWAN reliable scalability with three gateways in outdoor urban environment using health traffic transmission requirements for blood pressure. Also, J. Kharel et al. in [72] proposed

a system architecture to use LoRaWAN in developing a smart health monitor based on fog computing. Their system is relevant to places where the internet connection is scarce. They proposed patients to be equipped with LoRa sensor motes for monitoring various health conditions such as heart rate, blood pressure or body temperature and forward the sensed data to LoRaWAN gateways, which in turn forward data to the nearby health centers and the patient, is offered with relevant help with no delay. Moreover, the same authors deployed a primary LoRaWAN testbed of their previously proposed architecture in [73]. Their results validated LoRaWAN to be able to play a vital role in offering smart health services to patients in remote areas, although their research is limited to one patient. A. Mdhaffar et al. in [74] used LoRaWAN to monitor patients' body temperature, glucose, and blood pressure in remote rural areas where cellular coverage is limited. Their results confirmed LoRaWAN technology to be able to offer a reliable long-range network with low power consumption levels. Likewise, N. Hayati and M. Suryanegara in [75] used LoRaWAN to monitor a patient with a mental disorder. In their system design, the patient is equipped with a tracking LoRa device that sends position information to a LoRaWAN gateway installed at the hospital, which in turn sends the collected data to a cloud or hospital server. Furthermore, P. A. Catherwood et al. in [76] used LoRaWAN to build a network platform for remote screening of urinary tract infection (UTI). Their measurement results proved that LoRaWAN could offer a reliable network for proper remote diagnosis of (UTI) within a community where there no internet access. However, their research is also limited to the physiological monitoring of one patient. This is a useful contribution towards understanding LoRaWAN reliability in RHM. However, the discussed studies considered monitoring of one patient, and no study considered the impact of TD of LoRaWAN gateways of a scalable network due to an increasing number of ED using health traffic transmission requirements for blood pressure which is the focus of this research study.

3.3 LoRaWAN Scalability

Understanding LoRaWAN network scalability before any ED deployment is vital in handling interference and optimizing the network performance. Studies about LoRaWAN scalability have been published in literature, and have

given useful insights about LoRaWAN scalability. O. Georgiou and U. Raza in [77] provided a stochastic geometry to model the performance of a single LoRa channel by studying its Co-spreading factor interference and Signal-to-Noise Ratio. Their qualitative results showed that coverage probability drops as the number of devices increases due to co-SF unless LoRa is assumed to be impervious to cumulative interference. Their findings were limited to one gateway with a homogeneous deployment of end devices. Ahmad.A.I et al. in [5] investigated LoRaWAN scalability and reliability using different scenarios of IoT networks. They considered throughput performance, SF statistics and success probability performance. Their findings confirmed LoRaWAN to be scalable. However, according to their results; scalability could be inversely proportional to performance with a rising number of end devices not gateways. Equally, the authors in [78] performed various practical experiments to analyse the effect of doppler on LoRa modulation. Their results showed that while using the highest spreading factor 12, a range of 30 km can be obtained considering a packet loss of 60%. Their research was limited to one SF, single bandwidth allocation, and one modulation scheme. The scalability of LoRa technology is also not explored in detail for various real-time environments, for multiple applications, given different traffic setting patterns. J. Haxhibeqiri et al. in [79] evaluated LoRa scalability based on measuring the degree of interference with an increasing number of end devices for a single LoRaWAN gateway via simulations. They used signal-to-noise ratio and Received Signal Strength as their performance metrics and evaluated a maximum number of transmitters a single LoRaWAN gateway deployment can support in different use cases. Their results were validated by real test measurements. Correspondingly, F. Van Den Abeele in [80], using the NS3 simulator, made a scalability analysis of a single channel LoRaWAN multi-gateways. They built a LoRa error model from bit error rate simulations. Their research makes a considerable contribution to confirm that LoRa can scale well, but still, their research is limited to LoRaWAN gateways with only one channel. Also, authors in [81] analysed the scalability of LoRaWAN for a large-scale wireless sensor network via extensive simulations. They considered LoRaWAN protocol and evaluated packet collision rate for a single LoRaWAN gateway with an increasing number of LoRa end nodes. Their research is a substantial contribution to LoRa Scalability performance analysis, although it is also limited to one gateway. Moreover, they suggested various ways of boosting the capacity of the communication channel against a packet collision rate with large scale wireless sensor networks. Furthermore, authors

in [32] characterized LoRaWAN scalability under different traffic and network settings with a simulator built on North American specifications and configured to LoRaWAN specifications. Their results showed that three gateways are enough to cover a dense urban city with an acceptable packet delivery ratio. Still their measurements were under ideal conditions with a homogeneous distribution of transmitters per gateway. Furthermore, N. Varsier and J. Schwoerer in [82] evaluated the scalability capacity of LoRaWAN for smart metering applications via MATLAB simulations. Using the packet delivery ratio, data extraction rate, and network energy consumption as their performance metrics, they evaluated the quality of service of a single gateway with an increasing number of nodes. Their simulation results were used to deploy a LoRaWAN network in Paris and gave a guarantee of 98% quality of service with no other traffic considered in the same band. Besides, the authors in [83] evaluated the scalability of LoRaWAN technology for class B LoRa devices in the NS-3 simulator, whereby their results presented duty cycle regulations as the principal limit for downlink frames in class B mode, hence limiting LoRa scalability. Whereas authors in [84] proposed synchronization and scheduling mechanisms for uplink and downlink transmissions as a reliable solution to LoRa scalability limitations and D. Zorbas et al. in [85] proposed using multiple spreading factors configurations to improve LoRaWAN scalability and LoRa network capacity as a result of multiple orthogonal transmissions by many users. Analysis of the scalability of LoRa technology under imperfect orthogonality was evaluated by A. Mahmood et al. in [86]. While B. Reynders et al. in [87] proposed a two-step lightweight scheduling mechanism as a beneficial way to improve the scalability and reliability of LoRaWAN networks. They validated their proposed mechanism by basic implementation and extensive simulations in the NS-3 simulator. Empirical evaluation of the susceptibility of LoRaWAN networks to internetwork interference and its scalability was done by K. Mikhaylov et al. in [88], and authors in [89] proposed a mechanism of improving LoRaWAN scalability by an efficient selection of spreading factors (SFs) by end devices. Additionally, J. Lee et al. in [90] proposed a scheduling algorithm to improve LoRaWAN scalability. The proposed algorithm supports time-synchronized transmissions by scheduling SFs, frequency channels, and time slots between end-devices and gateways and considers the terrain of the geographical area which other studies did not consider in their simulations.

3.4 Existing Systems Using Random Neural Networks

RNN have been used to create resilient models with significant results. Application in Heating, Ventilation, and Air Conditioning (HVAC) systems by Javed. A et al. in [91], [92], and in [93], energy prediction of non-occupied buildings by Ahmad. J et al. in [45], communication systems, image classification, processing, pattern recognition by Simonyan. K and Zisserman. A. in [94], intrusion detection systems by Ul-Haq Qureshi. A et al. in [6], [95], and in [96]. Moreover, the studies in [97] and in [98] used RNN to develop fall detection systems with significant results. Nonetheless, no one has reported RNN algorithms applied in end device localization and heart disease prediction systems and none of them focused on LoRa localization and RHM. Therefore, basing on past research studies that considered RNN and developed robust models with significant results, we propose and develop an ED LoRaWAN-RNN-based localization systems in indoor and outdoor environments, and a heart disease model with improved results. In addition, the obtained RNN-based localization results are compared to results from other related studies that used different localization algorithms. Figure 3.1 presents some of the localization algorithms present in the literature.

3.5 End Device Localization Approaches

ED localization is vital in different IoT applications such as in RHM in case a real time monitored patient is in a critical condition or unconscious and needs to be located on emergency as confirmed in [99]. In this section, we discuss findings from different localization approaches found in the literature that are compared to RNN-LoRaWAN- based localization models that are developed and evaluated in this study.

3.5.1 Localization with Global Navigation Satellite System (GNSS)

Technologies based on satellites are the pioneers in accurate localization for outdoor applications, with errors less than 4 m for Galileo's Open Service and 10 m using GPS as presented in [46].

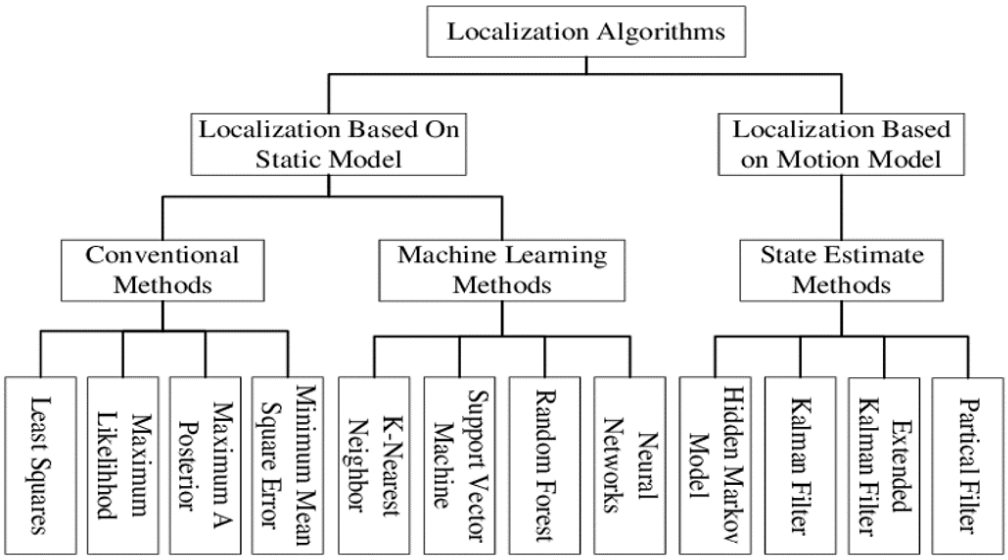

Figure 3.1: Localization algorithms [164]

Satellite based technologies provide a global continuous coverage and play big roles in a wide range of applications. However, GNSS modules consume high energy which rules them out for many IoT end devices.

3.5.2 Localization based on Range

Time-of-Arrival (ToA), RSSI ranging and Time-Difference-of-Arrival (TDoA) algorithms are among the most researched range-based localization techniques in IoT and Wireless Sensor Networks (WSN). Trilateration or Triangulation approaches are used to calculate the location coordinates of the end device using multiple anchor end nodes with known location coordinates according to the authors in [100] whereby LoRaWAN gateways may be referred to as anchor points. A propagation model and the received signal strength are used to calculate the distance between receiver and transmitter in RSSI ranging. However, multipath and shadow fading lead to the loss profile with indoor RSSI ranging. A scheduling algorithm with accurate end devices' time synchronization is required for ToA whereas accurate gateways time stamps for at least three distant gateways are only required for TDoA and makes it more suitable to the IoT end devices. The calculation of an

end device location is made when at least three distant gateways received the same transmission signal from the same end device as ideally the signal trajectories to the gateways intersect at the location of the end device. However, any slight scheduling error may lead to inaccurate location predictions. Several case studies are available in the literature whereby TDoA was used in LoRaWAN IoT networks such as in [101], and in [102]. An acceptable accuracy of less than 100 m in most of the published work was got considering fixed nodes and gateways as anchor points on a small area. However, the performance degraded significantly when mobile nodes or large areas were considered. Fargas et al. in [103] used an iterative TDoA based algorithm to locate static nodes and got a good accuracy with an error of around 100 m. A median error of 200 m was reported by Podevijn et al in [48] by using a TDoA based algorithm that considered map details such as roads. Aernouts.M et al in [104] via extensive simulations used two gateways with combined TDoA and Angle of Arrival (AoA) using probabilistic algorithms. Their simulation results reported a mean error of 548 m with TDoA and managed to reduce the mean error to 399 m by combining TDoA estimate with a single AoA estimate. Furthermore, range-based algorithms do not work in indoor scenarios due to multipath as a result of complicated radio environments. Hence, RSSI fingerprinting localization techniques also explored and proved to be potential candidates for harsh environments both indoor and outdoor dense urban areas.

3.5.3 Localization based on ANN

ED localization using ANN approach consists of directed multiple layers of connected nodes in a network. This network is used to develop a model that accurately maps the input to the output using historical data, and the model can then be used to output any desired unknown output. Different research studies in literature have evaluated ANN methods for sensor localization and confirmed it to be effective as seen in [105]. Besides, localization models using ANN for LPWAN were investigated by the authors in [105], and they confirmed ANN an accurate approach mostly for dense IoT networks. Furthermore, various studies are present in the literature on using ANN to develop LoRa based localization models with high accuracy in [13], [100], and in [106].

3.5.4 Localization based on ML

Different RSSI fingerprint LPWAN based approaches using machine learning algorithms particularly LoRaWAN are also present in [107]. Janssen. T et al. in [108] did a comparative performance analysis of various machine learning algorithms for RSS-LPWAN based localization models. Random forest regression method had the highest accuracy with a mean estimation error of 340 m with k-Nearest Neighbour (kNN) method having a similar accuracy with the least computational performance. An error lower than 20 m was reported by Sallouha.H et al. in [109] while analysing localization in ultra-narrow band IoT networks. Furthermore, RSSI fingerprint localization methods based on deep learning algorithms have also been published in [110], [111], [68], and in [112].

3.5.5 Localization based on RSSI Fingerprinting

Fingerprinting localization uses end devices' RSSI fingerprint values received by gateways to accurately localize any end device in the network. A fingerprinting based approach consists of an offline training phase and an online phase as seen in [50]. Data samples are collected from a considered service area where localization is to be predicted and used to train a fingerprint algorithm. Therefore, the location of any end device can then be predicted using the trained algorithm in an online phase based on end device RSSI and other signal characteristics. Different algorithms using RSSI fingerprinting localization exist in literature using various wireless technologies. However, most of the existing studies investigated indoor environments due to a lot of data required for the training phase. Hence hard work involved in collecting data for a large area. Wi-Fi has been used widely in fingerprint localization by the authors in [113], [114], [115], and in [116] whereby a smart phone can be used to record its RSSI and estimate its own location using a web. A comparative performance analysis different wireless technologies based on RSSI localization is made by the authors in [117]. Research studies using LoRaWAN in fingerprint localization are also available in [118], [119], [120], and in [121]. Gu. C et al. in [105] presented a review of challenges and opportunities of LoRa-based localization approaches. Whereas, Choi. W et al in [50] used LoRa for positioning using three fingerprint algorithms and confirmed LoRa to be effective with the average accuracy of 28.8 m for the three algorithms. Fingerprint localization data sets for LoRaWAN and Sig-

fox in large urban and rural areas are presented by Aernouts. M et al in [122] with a mean estimation error of 398.40 m for the LoRa data set in the urban environment. Similarly, the authors in [123], [17], and in [124] also investigated RRSI LoRa based fingerprint localization algorithms with good accurate estimations.

3.6 Heart Disease Prediction Approaches

A substantial number of researchers has considered different machine learning algorithms for heart disease prediction and got significant results. Moreover, many studies used the same public Cleveland dataset that we also used. Zriqat et al. in [125] did a comparative performance analysis for predicting heart disease using Naïve Bayes, random forest, and support vector machine on two datasets. According to their results, all the investigated algorithms gave significant predictions; however, the decision trees classifier outperformed other classifiers. Fida et al. in [126] used a genetic algorithm to optimize existing heart disease classifiers and significantly improved classification accuracy compared to non-optimized classifiers. Furthermore, Pandey et al. in [127] used J48 decision tree algorithm and developed a prediction model to classify heart disease using fourteen clinical features.The obtained results showed that fasting blood sugar is the most crucial clinical attribute for better classification. However, it does not improve the accuracy. Mohan et al. in [128] developed a linear model using hybrid random forest technique to predict cardiovascular disease and achieved an accuracy of 88.7%. Rindhe et al.in [129] obtained an accuracy 84.0% on their developed heart disease prediction model using support vector classifier. K. Baby and S. Priya in [130] presented significant features for heart disease prediction whereby 86.10% classification accuracy was obtained using Vote classifier.

3.7 Summary

In this chapter various research studies on LoRaWAN propagation models, LoRaWAN in RHM, LoRaWAN Scalability, existing RNN based approaches, end device localization approaches, and heart disease prediction approaches. These are useful contributions towards understanding LoRaWAN capabilities especially for end device localization and RHM, but still more extensive stud-

ies using other techniques such as RNN algorithms and simulation tools are needed to characterise and understand further the performance of LoRaWAN in dense IoT networks. Several studies considered LoRaWAN technologies in RHM prototypes although further study is required to characterize their capabilities and limitations in dense IoT RHM applications. Additionally, research studies about localization approaches that considered ANN, ML and DL and LPWAN for end-device localization models were also reviewed, and the performance of RNN algorithms in end device localization are yet to be investigated. Hence, this project aims at exploring the performance of RNN and LoRaWAN in location based IoT remote health applications in urban areas. Table 3.1 presents some of the results of the benchmark related studies for this research study.

Table 3.1: Results of benchmark related studies for this research study

Research Work	Average error (m)	Approach
Islam et al.[157]	0.71	PR
Sadowski et al.[117]	1.19	Trilateration
Kim et al. [159]	1.6	Trilateration
Anjum et al. [119]	3.06	PL
Henriksson [160]	8	Time of Arrival
Bonafini et al. [147]	6.2	Multilateration
Du et al. [148]	7.57	Hybrid
Shokry et al. [150]	18.8	Deep learning
Anjum et al. [149]	45.75	Linear
Purohit et al. [146]	191.52	ANN-Deep
Janssen et al. [151]	340	kNN
Aernouts et al. [122]	398.4	kNN
Anagnostopoulos et al. [13]	358	ANN
Nguyen [152]	500	ANN

Chapter 4

LoRaWAN Propagation Models

LoRaWAN is a potential technology for the current and future connectivity of the IoT in all environments; however, its network coverage performance is still under exploration. Hence, the core objective of this chapter is to explore the LoRaWAN network performance in an urban environment. In this chapter we developed a simulation model of the radio coverage of LoRaWAN in the urban scenario (Glasgow) with ATDI ICS Telecom using four popular propagation models. Then, a critical analysis of the real-world data collected in Glasgow city was made to evaluate the performance of LoRaWAN in an urban area. Furthermore, a detailed analysis and comparison of four propagation models to the field test measurements was made to analyse the suitability and performance of each of the four propagation models in an urban area of Glasgow city.

This chapter initially describes radio wave propagation and then provides an overview of LoRa and LoRaWAN with CSS modulation. The chapter then details the four propagation models considered for this research study.

4.1 Radio Wave Propagation

According to radio wave propagation fundamentals in [131], the quality and the strength of the received signals depend on the frequency, modulation technique, the distance between the transmitter and receiver, transmission power, and interferences in the environment. Due to the transmission environment, transmitted signals can take different paths to the receiver, called multipath fading. Urban areas are typical examples of the multipath environ-

ment due to tall buildings that cause reflections and scatter the transmitted signals, which affect the strength of the received signals.

4.2 LoRaWAN

LoRa is an emerging open specification managed by Semtech [132]. It enables long-range wireless communications with low power consumption. LoRa modulation is derived from CSS technology whereby chirp pulses are used to encode information with increasing or decreasing frequency over a period. This leads to robust LoRa modulated transmitted signals and can stand interferences and travel long distances. LoRa transmissions depend on three main parameters; the bandwidth, which determines the frequency band, the spreading factor, and the coding rate, which affects the transmission rate, standing to interference, and increases the decoding sensitivity. LoRaWAN specifies the system architecture and defines the protocol stack of LoRa on the media access control layer.

A LoRaWAN network is made up of many end devices connected to one or more gateways in a star topology [29]. The gateways receive information from the end devices and then can forward the received data to the network server. When end devices send information to the gateways, it is called an uplink transmission, and when the gateways send information to the end devices, it is called downlink transmission. There are three classes of end devices in a LoRaWAN network: Class A, B, and C. Class A end devices use ALOHA media access control, and communication is started by an uplink transmission followed by two successive downlink windows. Moreover, end devices save energy if not transmitting by entering a sleep mode. Class B is an extended version of Class A with an added downlink window. In contrast, Class C end devices must constantly listen to the transmission channel.

The most important traits of a typical LoRaWAN compliant end device and its associated theoretical performance are covered in this section. We start by examining the communication traits listed in the proposed LoRaWAN standard, such as the network design, use of the frequency band, and implementation of transmission data rates. Following that, the LoRa packet structure is covered to show the data structure of LoRa and what LoRaWAN adds to it. The Time on Air of a LoRa packet as a result of this packet shape is then explained. This gives an idea of the LoRaWAN transmission times, influencing the end device's maximum transmission interval. Also, the traits

mentioned above are applied to determine various performance traits of an end device running LoRaWAN.

The LoRa Alliance developed a MAC protocol and network architecture for LoRa in an open worldwide standard called LoRaWAN, whereas LoRa is a proprietary modulation scheme for the physical layer implementation. The LoRa Alliance wants to standardise LPWAN technologies and ensure interoperability amongst LoRa devices with the help of this standard. Their goal is to provide consistent battery life, network capacity, and a high level of freedom for users and enterprises to create IoT applications. This thesis adheres to the recommendations made by the LoRa Alliance.

4.2.1 Network Architecture

LPWAN networks often have a star network structure [29]. A central hub or gateway that all devices connect defines the star network design. Unlike a mesh network, each end device passes data to other end devices to extend the communication range. Messages are forwarded by gateways between end devices and a central network server in the star-of-stars topology of the LoRaWAN network architecture. Since nodes do not have to receive and send data from other nodes, a long-range star or star-of-stars network conserves battery life and minimises complexity. According to LoRaWAN specifications, a network's nodes communicate data to all of the network's gateways rather than being connected to only one. Each gateway that receives a message forwards it to a network server over the internet. This server houses the network's intelligence and is in charge of duplicate filtering packets, security checks, and scheduling acknowledgments through the best gateway.

4.2.2 Channels

LoRaWAN solely employs duty cycle limited transmission, which is carried out by implementing a sub-band duty cycle constraint [133]. This indicates that the transmission time, commonly referred to as the Time on Air, is employed to limit transmissions on the same sub-band for a time. During Time off Air, the full sub-band is not available for any transmissions. Therefore the device must use a different sub-band or wait before sending any new messages. As a result, a device that only uses the G1 sub-three band's default channels must wait at least 99 seconds after transmitting a packet with a 1-second Time on Air before it may broadcast another packet on the same

channel. The maximum data rate of the device is then reduced by the duty cycle constraint, in this instance, by a factor of a hundred.

4.2.3 Data Rates

A particular set of Data Rates is defined by LoRaWAN to be used for transmissions [133]. A transmission's bandwidth and spreading factor are both indicated by the LoRaWAN data rate. The number of bits recorded every chirp, the rate at which these chirps are conveyed, and the start and end frequencies of the chirp are all determined by these two variables. It is important to note that data rate 7 employs frequency shift keying rather than LoRa modulation. Additionally, data rates 6 and 7 are not used in the LoRaWAN standard 3-channel implementation, and spreading factor 6 is not used either.

4.2.4 Maximum Payload

The maximum LoRaWAN payload segment length varies by location and depends on the data rate used [134]. This means that for LoRaWAN deployment in Europe, the maximum payload size for each data rate is established. As previously indicated, frequency shift keying modulation is used for data rate 7 instead of LoRa modulation, and data rates 6 and 7 are not used in the basic 3-channel implementation.

4.2.5 Adaptive Data Rate

A network can use an adaptive data rate strategy with LoRaWAN, allowing the network architecture to control end device data rate and transmission power [135]. A downlink message from a gateway providing the data rate and transmission power they should use can be received by end devices supporting adaptive data rate. As a result, the network can improve packet delivery, network capacity, and end device battery life. End nodes adjacent to a gateway may be set to utilise a high data rate and low transmission power, whereas endpoints at the network's edge may be set to use a maximum transmission power and a minimum data rate to optimise their range.

4.2.6 LoRaWAN Classes

LoRaWAN supports three separate device classes to enable optimal implementation for various LoRa-based applications [29]. The timing of the so-called receive windows affects how these classes differ. These windows specify the interval during which the end device starts to watch for downlink messages from the gateway to receive them. LoRaWAN defines these classes:

- Class A: An end device operates in Class A by default, opening two brief receive windows after sending an uplink message. These receive windows enable the network to send and receive downlink messages. The first receive window is established on the same channel and with the same data rate as the initial uplink broadcast. It uses a fixed, adjustable frequency and data rate to make the second window more resilient to channel variations. The second receive window's default data rate and channel frequencies are 0 and 869.525 MHz, respectively. This frequency is a part of the G3 sub-band, which permits transmissions of up to 500 mW with a 10% duty cycle rather than 1%.

- Class B: Class B endpoints have additional receive windows at predetermined periods. These components open their receive windows when a beacon packet from the gateway is detected by listening for it at specific periods. This method ensures the server can synchronise the downlink packet with the end device's receive window. Applications that require data transmission on demand or under remote control can profit from downlink message reception independent of uplink transmission.

- Class C: Only when transmitting themselves Class C end devices close their receive windows. Therefore, Class C end devices consume the most energy due to constant message listening. Preferably, battery power should not be used in devices that implement class C capabilities.

4.2.7 Joining A LoRa Network

Over-The-Air-Activation (OTAA) and Activation by Personalization are ways to connect to a LoRa network (ABP) [132]. The end device does not need to register in networks that support ABP before transmitting. The network security keys required to encrypt the data are predefined in the end device, and it is only possible to identify the end device by its unique device address.

An OTAA-compliant LoRa end device must complete a join setup by sending a join request. The end device obtains a dynamic device address and network session keys during this process.
Over-The-Air-Activation (OTAA) and Activation by Personalization (ABP) are ways to connect to a LoRa network. The end device does not need to register in networks that support ABP before transmitting. The network security keys required to encrypt the data are predefined in the end device, and it is only possible to identify the end device by its unique device address. An OTAA-compliant LoRa end device must complete a join setup by sending a join request. The end device obtains a dynamic device address and network session keys during this process.

4.2.8 Acknowledgements

End devices have the option of sending confirmed or unconfirmed data messages [136]. The network does not recognise unconfirmed messages. Therefore an end device will never be aware of whether the message was successfully received. The application should deliver its data via a confirmed message if it demands that the destination device understand whether the transmission was successful. During one of the receive windows for the end device, the network will respond with an acknowledgment if the data was successfully received. The end device will, if necessary, retransmit the same data if the first transmission or the acknowledgment are both unsuccessful.

4.2.9 LoRa Packet Composition

Three components comprise each LoRa packet: the preamble, an optional header, and the payload [134]. Cyclic redundancy checks can be used to verify the integrity of each packet's header and content (CRC). These CRCs are correspondingly added to the packet's header and payload. A CRC, often known as a checksum, is a widely used error detection method based on a predetermined amount of check bits. CRC identifies small changes in the related data based on the remaining polynomial division of the data's content. When the CRC fails, the packet is deemed tainted and discarded by the recipient. The payload of each LoRa packet is encoded with cyclic error coding to enable forward error correction, increasing the robustness of LoRa packets. The encoding rate can be adjusted to a minimum of 4/5, which means that one bit is added for every four bits of data. The number

of payload bits is doubled at the maximum coding rate of 4/8. The longest possible packet is 256 bytes.

- Preamble: When an end device is going to transmit data, the LoRa preamble alerts a receiver. In order to synchronise with the incoming data, the receiver employs the preamble. If no header is provided, it detects the start of the payload or the start of the header. Between 6 and 65535 (chirp) symbols can be programmed as the preamble's length. This results in a preamble of at least 10.25 symbols long, together with a fixed overhead of 4.25 symbols. The LoRaWAN specification specifies a preamble length of 8 (+4.25) symbols.

- Header: Each packet's configuration is described in the optional header. The payload length in bytes, the forward error correction coding rate, and the presence or absence of the payload CRC at the packet's end are all included in this data. The header is encoded at a maximum coding rate of 4/8. The documentation makes no mention of the header's length. Furthermore, including a header is optional; in the case of not using one, a mode known as implicit header mode is used instead. In this mode, the payload length, coding rate, and CRC presence are fixed and known on both ends of the radio link. The Explicit Header Mode, which requires the header to be present in each packet, is the default mode of operation for LoRaWAN. Implicit Header Mode is only required when SF 6 is utilised.

- Payload: The real data is encoded with the coding rate defined in the header or manually set at the radio link's receiving end in the payload segment. Although it is optional for standard LoRa end devices, the LoRaWAN protocol always uses the 16-bit payload CRC. The PHY-Payload segment in LoRaWAN consists of three fields: a 4-byte message integrity code (MICC), a 1-byte MAC payload (MACPayload), and a 1-byte MAC header (MHDR) (MIC). Only if the frame payload field is empty can the optional actual data (FRMPayload) be omitted from the MACPayload field called a data frame, which is followed by a header (FHDR). The port field's value of 0 indicates that all that is contained in the payload are MAC commands. These commands are designed for managing networks. Four fields make up the frame header: the 4-byte end-device address (DevAddr), a frame control byte (FCtrl), a

2-byte frame counter (FCnt), and a frame options field (FOpts) with a maximum size of 15 bytes for transmitting MAC commands.

4.2.10 Time on Air

The LoRa standard states that the packet's payload, the employed spreading factor, the payload's coding rate, and the channel bandwidth all play a significant role in determining a packet's Timeon Air, or the amount of time it takes to transmit [135]. A LoRa packet's Time on Air is calculated depending on how long each individual chirp symbol lasts. The amount of the time spent on air for both the preamble and the actual packet is known as the total time on air.

4.2.11 Transmission Power

The standard radiated transmit output power for LoRaWAN is 14 dBm [137]. This equates to the 25 mW maximum radiated power for radio devices in Europe as regulated by ETSI. A device's output power can be decreased in 3 dBm steps. Five of the six output power settings that the LoRaWAN specification describes are operable in Europe.

4.3 Propagation Models

Four propagation models that are mostly used in LoRaWAN are discussed in this section. The Okumura-Hata Model, COST-231 Hata Model, Extended-Hata and ITU R 1225 are considered in this study. Simulations of LoRaWAN network coverage in ATDI ICS Telecom are carried out and the received signal strength results from propagation models are compared with the measured data from Glasgow city. Simulations of LoRaWAN network coverage in ATDI ICS Telecom [38] are done, and then the received signal strength results from propagation models are compared with the real-world data from Glasgow city.

1) Okumura-Hata Model: The Hata model is an empirical formulation of the graphical path loss data provided by Okumura and is valid from 150 MHz to 1500 MHz [138]. The median path loss in urban areas (PL_U) measured in (dB) is given by:

$$PL_U = 69.55 + 26.16log(f) - 13.8log(h_1) – a(h_2) + [44.9 - 6.55log(h_1)]log(d_{t_r}) \tag{4.1}$$

With frequency f in MHz, h_1 as the gateway antenna height, and h_2 the ED antenna height in m; d_{t_r} is the distance between the transmitter (gateway) and the receiver (end device) in km, and ah_2 is the correction factor for the end device antenna height and depends on the area of coverage.

Whereby, for a small or medium urban area, the ah_2 is defined as:

$$a(h_2) = (1.1log(f) - 0.7)h_{r_e} - (1.56log(f) - 0.8) \tag{4.2}$$

Whereas for a large urban area, If f $<$ 300, it is defined as:

$$a(h_2) = 8.29(log1.54h_2)^2 - 1.1 \tag{4.3}$$

and if f $>$ 300;

$$a(h_2) = 3.2(log11.75h_2)^2 - 4.97 \tag{4.4}$$

To obtain the path loss in a suburban area (PL_S) the standard Hata formula is modified as follows:

$$PL_S = PL_U - 2[log(f/28)]^2 - 5.4 \tag{4.5}$$

While for rural environments (PL_R), the formula is given by:

$$PL_R = PL_U - 4.78[log(f)]^2 - 18.33log(f) - 40.98 \tag{4.6}$$

2) COST-231 Hata Model: This model was developed as an extension of Okumura Hata for a little bit higher frequencies (500 MHz-2000 MHz), and is mostly used to predict link attenuation in mobile wireless systems. COST-231 Hata is used in urban, suburban and rural areas [138], [52], and is defined in urban areas PL_U by the following formular:

$$PL_U = 46.3 + 33.9log(f) - 13.82log(h_3) – ah_4 + [44.9 - 6.55log(h_3)]log(d_{tr}) + co \tag{4.7}$$

Whereby, the frequency f is in MHz, d_tr is the gateway-end device distance in km, and h_3 is the gateway antenna height in m. The co parameter equals 3 dB for urban areas, and 0 dB for suburban and rural areas. Furthermore,

the ah_4 parameter for urban areas is given by the following formular if f > 400:

$$ah_4 = 3.2[log(11.75h_5)]^2 - 4.97 \tag{4.8}$$

While for suburban and rural areas:

$$ah_4 = (1.1logf - 0.7)h_5 - (1.56logf - 0.8) \tag{4.9}$$

where, h_5 is the mobile antenna height in m above ground level.

3) Extended Hata: This model was also developed from the extension of the Okumura-Hata to determine path losses for higher frequency bands(30MHz – 3000 MH) in urban, suburban and rural areas [52], [139], and is given by the following Path Loss (PL) formular :

$$PL = L_0 + L_1\text{–}H_0\text{–}H_1 \tag{4.10}$$

Where L_0 is the attenuation in the free space given by:

$$L_0 = 92.4 + 20log10(d_{tr}) + 20log10(f) \tag{4.11}$$

L_1 is the path loss given by:

$$L_1 = 20.41 + 9.83log10(d_{tr}) + 7.894log10(f) + 9.56[log10(f)]^2 \tag{4.12}$$

H_0 is the gateway height gain factor defined as:

$$H_0 = log10(h_g/200)(13.958 + 5.8[log10(d_{tr})]^2) \tag{4.13}$$

H_1 is the terminal end device height gain factor for medium urban areas defined as:

$$H_1 = [42.57 + 13.7log10(f)][log10(h_e)0.585] \tag{4.14}$$

Whereby, the frequency f is in GHz, and d_{tr} is the gateway-end device distance in km; h_g is the gateway antenna height and h_e the end device antenna height in meters.

4) ITU-R 1225 Model: This is a radio propagation model defined by International Telecommunication Union radio communication (ITU). It is empirical and semi-deterministic path loss models that can be used in various environments including indoor, outdoor, pedestrian and vehicular in urban or sub-urban areas [140]. semi-deterministic models allow the analysis of all environmental barriers. ITU R 2225 covers the cognitive radio systems that operate above 30 MHz. The ITU-R NLOS loss PL is given by the following formula and defines the worst condition deviation of 10 dB for outdoor users.

$$PL = 40log(d_{tr}) + 30log(f) + 49 \tag{4.15}$$

whereby d_{tr} is the gateway end device distance in km, and the frequency f in MHz with the loss always to be more than the propagation losses of the free space in any circumstances.

4.4 Methodology

This section presents all the details and procedures used in field test real-world measurements, and simulations carried out to evaluate the performance of LoRaWAN propagation models in an urban environment.

4.4.1 Field Test Measurements

Real test measurements were carried out in Glasgow city, which allowed the simulation results to be verified. Data was sent to three LoRa SX1301-capable Kerlink gateways using a MultiTech Systems LoRaWAN mDot mote managed by a Raspberry Pi. One gateway was located 30 meters up on the George More building at Glasgow Caledonian University, another was 27 meters up on the James Weir building at the University of Strathclyde, which is located 1 kilometer away from the first one, and the final gateway was located on 127 metres up on Skypark, which is located 3 kilometers away from the first one. The end device module was used to gather and transmit data to the gateways while moving away from them at a walking speed over various positions. Figure 4.1 displays a map of the examined region with a LoRaWAN gateway and the end device's path for data collection. The

processes and methodology used in our field test measurements are described in detail in [141].

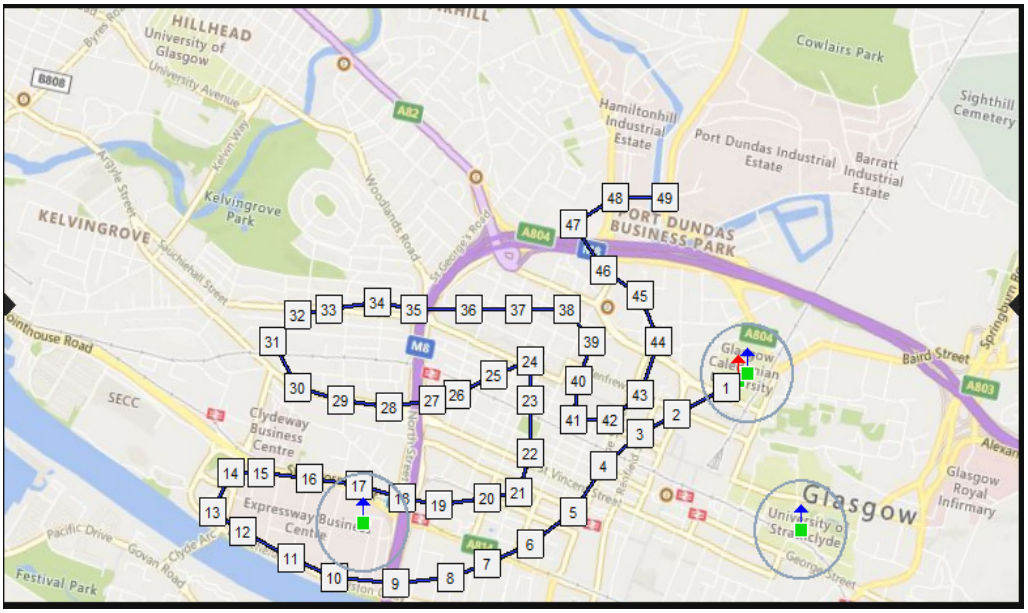

Figure 4.1: Map showing analysed area with a LoRaWAN gateways, LoRa ED positions and the path used for collecting measurements (ATDI ICS Telecom Capture).

4.4.2 Simulation Tools

This section discusses two simulations tools investigated for this research study.

NS3 Simulator

NS3 simulation tool has a LoRa PHY layer that handles LoRa transmissions with LoRaWAN MAC protocol specifications [87]. The extension of LoRaPhy class and LoRaMac class enable the modeling of the features of LoRaWAN end-devices and LoRa gateways in NS3. NS3 simulation tool has the following major classes that manage the performance of LoRa transmissions:

- Node and Application classes for representation and connection management between end devices and the network system for effective simulations.
- NetDevice class for managing connections between channel objects and end nodes
- Channel class for connection management between subnet objects and connecting nodes.
- The Lora Interference Helper class for managing multiple transmitting nodes with the same spreading factors.
- Propagation-Loss Model for predicting received signal strength using propagation models
- Logical loRa Channel Helper for managing MAC layer duty cycle and transmission time

ATDI ICS Telecom

ICS Telecom is commercial software developed by the company ATDI dedicated to planning and analysis of wireless networks, including LoRaWAN and NB-IoT. It supports different types of links (Point-to-point, broadcast network, cellular network, satellite link), various applications (2G,3G and 4G telephony, mobile TV, IoT, WiFi, radar....) and various services (voice, data, VoIP...). ICS Telecom tool is adapted to a varied number of environments (indoor, outdoor, rural, urban...) from the 2D and 3D terrain profile modeling [38]. It offers the essential tools to simulate a digital wireless network:

- Calculation of the link budget according to the parameters of the transceivers and the profile of the ground.
- Analysis of connectivity to a given network
- Determination of the best server
- Traffic Analysis
- Study of intra-system and inter-system interference

- Electromagnetic compatibility
- Radio Frequency Spectrum Management
- Prospective transmitter location research ICS Telecom software integrates many propagation models consider the phenomena of reflection, diffraction by soil and the obstacles of refraction, diffusion attenuation by the atmosphere.

Received power strength for mobile end-nodes on LoRaWAN network varies in time and space. It is characterised by statistic normal laws:lognormal or Rayleigh type that are selected while modeling, and standard deviation of node mobility associated with fading is also indicated.

ATDI ICS Telecom simulator has ability to consider most of the terrain details of a relevant geographical area of coverage. Among others, ATDI ICS Telecom considers digital terrain model data, clutter data, map data, and building data of an area and this is a strong contribution to the accuracy of the predicted simulation results. ATDI ICS Telecom considers most details of the terrain information as consider while analysing a network coverage of a specific area than NS3 simulator. This is very crucial to validate the accuracy of simulation results. Hence, this research study considers ATDI ICS Telecom.

4.4.3 Simulations

The radio planning and spectrum management tool [38] from ICS Telecom is used to analyse the LoRaWAN radio coverage. The quality of the map utilised is a key component when replicating radio environment coverage. The ATDI ICS Telecom software uses five cartographic layers, which must be considered while calculating all of the propagation parameters. Digital elevation models, a clutter layer, map photos, a vector layer, and a colour palette are some of our additional features. Some parameter options used for configuring the end device transmitter and propagation loss models are shown in Table 4.1. During this simulation analysis, only the Glasgow Caledonian University LoRaWAN gateway is taken into account.

Table 4.1: Simulation Parameters

Parameters	Values
Frequency of operation	868 MHz
Bandwidth	125 KHz
Spreading Factor (SF)	12
Number of Gateways	3
Gateway height	50 m
End-node transmit power	14 dBm
End-node antenna height	1.5 m

4.5 Results and Performance Analysis

In this study, ATDI ICS Telecom is used with four current propagation models to analyse the performance of the simulated LoRaWAN coverage. The field test measurements taken in Glasgow city are compared to three empirical models: Okumura-Hata, COST-231 Hata, and Hata Extended, and one empirical semi-deterministic model: ITU R 1225. Figure 4.2 displays a coverage prediction for LoRaWAN modeling using the parameters in Table 4.1.

In this analysis, NLOS scenarios are taken into account. For one LoRaWAN gateway and one LoRa end device located at various locations in Glasgow city center, a function of the distance (m) and received signal power (dBm) is considered. High density and numerous tall buildings in Glasgow city could be assumed to cause packet loss in some spots. Figure 4.3 displays a comparative performance analysis between the simulation results of the propagation models and the real-world measurements.

Figure 4.3 shows that ITU-R 1225 has anticipated signal power values most closely aligned with the measured data, hence the most precise. The Extended Hata model, however, has got signal strength values that are substantially out of alignment with measurements. Consequently, it is also the least accurate of the four examined propagation models.
The following three crucial performance metrics are utilised in our evaluations: Average Error (AE), the mean value of the difference between the real-world received signal strength results x, and the estimated received signal strength simulation results xi.

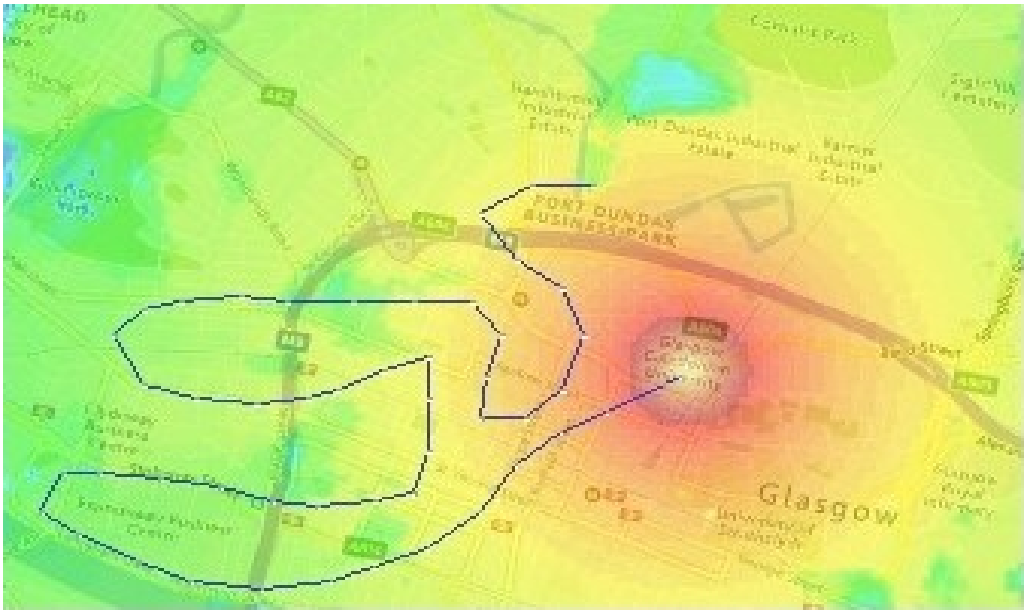

Figure 4.2: Capture of LoRaWAN radio coverage for ITU-R 1225 model

The mean absolute error (MAE), which is the average of all absolute errors between the actual values of the real measured data and the predicted simulation results by the relevant propagation model. The amount of dispersion between the anticipated simulation results of each propagation model and the actual test data were also measured using the standard deviation (S). Furthermore, the performance of each of the examined propagation models is shown in Table 4.2 by comparing the simulation results to real-world measurements of received signal strength for n samples made along the path shown on the map in Figure 4.1. The used performance metrics are defined by the following formulas:

$$AE(X) = 1/n \sum_{i=1}^{n} x_i - x \tag{4.16}$$

$$MAE(X) = 1/n \sum_{i=1}^{n} |x_i - x| \tag{4.17}$$

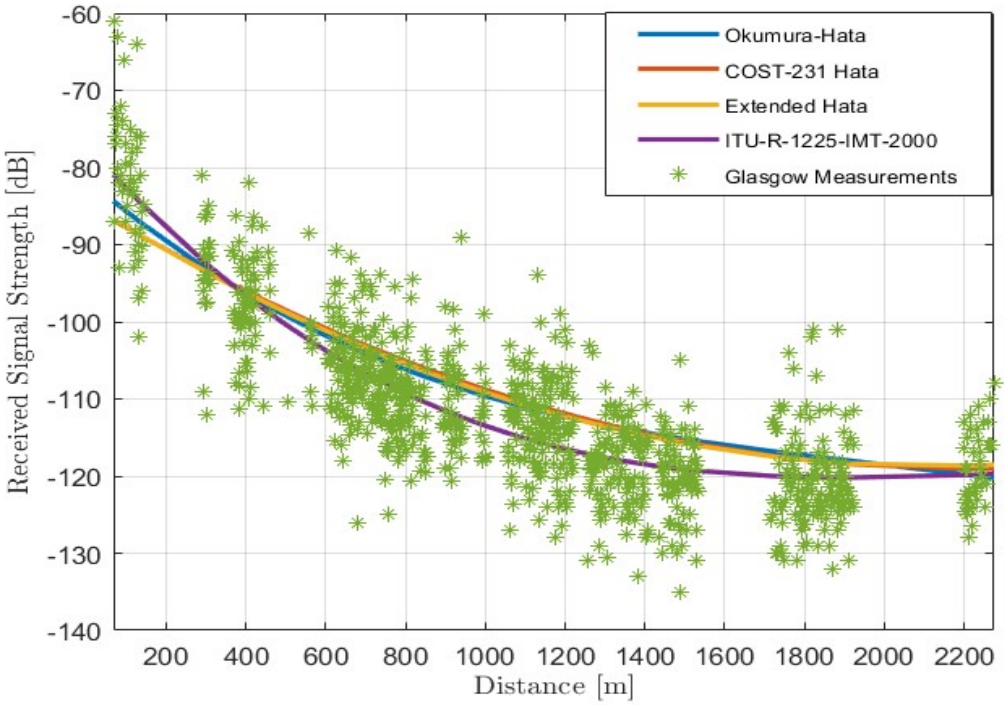

Figure 4.3: Comparative analysis between simulation results of the models and LoRaWAN real test measurement results

$$S = 1/n(\sum(X - x)^2)^{0.5} \tag{4.18}$$

The obtained results show that for the LoRaWAN network in Glasgow city, the received signal strength values for COST-231 Hata and the Okumura-Hata model are underestimated. However, the predictions of the received signal power made by ITU R 1225 and the Extended Hata models overstates the real test measurements. ITU R 1225, on the other hand, exhibits the most remarkable prediction accuracy with the least MAE of 1.13 dBm and a S of 5.49 dBm, which is the lowest deviation from the real measured received signal strength data. With an MAE of 1.82 dBm and a S of 9.19 dBm, the Extended Hata model is the least accurate propagation model and has the most significant deviation from the real test measurements among the four investigated models.

Table 4.2: Performance metrics

Error parameters	AE	MAE	S
Okumura-Hata	-0.91	1.58	8.81
COST-231 Hata	-0.84	1.56	8.56
Extended Hata	0.58	1.82	9.19
ITU R 1225	0.29	1.13	5.49

Furthermore, the performance of the Okumura-Hata and COST-231 Hata models for LoRaWAN networks in Glasgow city appears to be very similar, according to the results. Also, some transmitted signals are lost at some locations and this is thought to have been caused by reflection, diffraction, and scattering where transmitted signals are scattered due to tall buildings in the urban area of Glasgow city.

Chapter 5

LoRaWAN Scalability for RHM

LoRaWAN scalable connectivity capacity is yet to be thoroughly characterized. Henceforth, this chapter investigates the uplink interference with TD limitations of scalable LoRaWAN technology, particularly for future remote patient monitoring applications in an urban environment. Furthermore, the ICS Telecom simulator enables modeling end nodes with remote health traffic requirements in fixed and mobile environments. In this chapter, we develop a detailed simulation model with remote health traffic requirements for Glasgow city using ICS Telecom. Then, we analyse uplink interference for an increasing number of fixed and mobile end devices. Furthermore, LoRaWAN scalability is critically analysed for remote healthcare applications in dense urban IoT networks.

5.1 Wireless Technologies for RHM

The transmission of specific health vital signs requires specific traffic characteristics [142] for successful transmissions in RHM system applications. The required traffic characteristics used in IoT RHM are discussed to determine if the selected wireless technologies can support the required traffic characteristics for RHM applications, as shown in Table 5.1.

Bluetooth, NB-IoT, and LoRaWAN are all potential candidates for RHM applications according to their respective properties or critical features, such as their data traffic rates compared to the required traffic characteristics for the transmission of vital body signs. However, LoRaWAN and NB-IoT use lower power and offer more coverage than Bluetooth.

Nevertheless, LoRaWAN can be easily implemented due to being an open specification.

5.1.1 Sensor for RHM Systems

Many types of sensors are available commercially and can be used to measure heart rate, blood pressure, oxygen saturation, respiratory rate, and body temperature. According to a comprehensive study about remote patient health monitoring systems by Lakmini et al. in [143], the following are the critical vital signs for initial health monitoring with their corresponding measuring sensors/devices. Blood Pressure is among five body vital signs usually considered and can be measured by blood pressure sensors or wrist-worn blood pressure measuring devices. Body temperature is also among the five body vital signs usually considered and can be measured by the resistance thermometer, a thermistor, or a thermocouple. Furthermore, Heart rate is also usually monitored and can be measured by the Electrocardiography (ECG) sensor, pulse oximeter, or heart-rate chest strap. Respiratory rate, which is also vital, can be measured by a wearable pulse oximeter, wearable sensors, a plethysmograph, or a pneumotachograph. Also, Oxygen saturation can be measured pulse oximeter.

Various types of potential sensors to measure vital signs are available. Nevertheless, each type has associated limitations for RHM; for example, ECG requires more hardware unavailable in RHM if a reference signal is used. Also, ECG has an issue with accuracy due to time synchronization in a cardiac cycle between electrical and mechanical activities [143]. Likewise, a heart-rate chest strap can make someone uncomfortable for long monitoring periods.

Table 5.1: Required traffic characteristics for various human body vital signs

Signals	Frequency (Hz)	Accuracy (bits)	Data Rate
Glucose Concentration	40	12	480 bps
Blood Flow	40	12	480 bps
ECG	500	12	6 kbps
Respiratory Rate	20	12	240 bps
Blood pressure	100	12	1.2 kbps
Body Temperature	0.2	12	2.4 bps

In contrast, a pulse rate oximeter that does not require technical skills to place it on a finger can be preferred to be used in RHM due to its flexibility. Wrist-won blood pressure devices are commercially available; they lack communication capabilities for RHM applications. Hence, IBM wireless blood pressure sensors can be used in RHM applications, while wearable respiratory sensors can be a better choice for measuring respiration vitals for RHM. Furthermore, wireless body temperature can be used to measure temperature in RHM. Although some all-in-one vital signs measuring devices can also be considered. However, pulse sensors or smartwatches are the best recommendations for IoT RHM applications due to the capacity of one device to measure all vital signs and the flexibility they offer in mobility [144].

5.1.2 RHM system Architecture

The main components of the considered RHMsystem include:

- Data Acquisition System
- Data Transmission System,
- Control and Data Management system.

In the RHM system architecture, data is acquired by equipping the identified registered individual end-users with various wearables or medical sensors for measuring vital body signs such as blood pressure, body temperature, heart rate, and respiratory rate. End-user devices use LoRa connectivity, whereby the information generated by these end devices is transmitted directly to a LoRaWAN gateway at distant remote health centers or hospitals even without an internet facility, as shown in Figure 5.1. The health information data sent by end-user devices is saved and backed up on database storage servers at the health centers based on the illness or medical condition and interconnected with the desktop computers, smart devices, and laptops of medical personnel for real-time monitoring. The data is analysed for a pattern of change to identify abnormalities, and this can aid in preventing further deterioration of a patient's condition [73]. The transmitted data can also be used for accurate localization of the users. Understanding the right estimation for the maximum number of end devices per gateway before end device deployment is essential for proper network coverage, scalability, and network optimization.

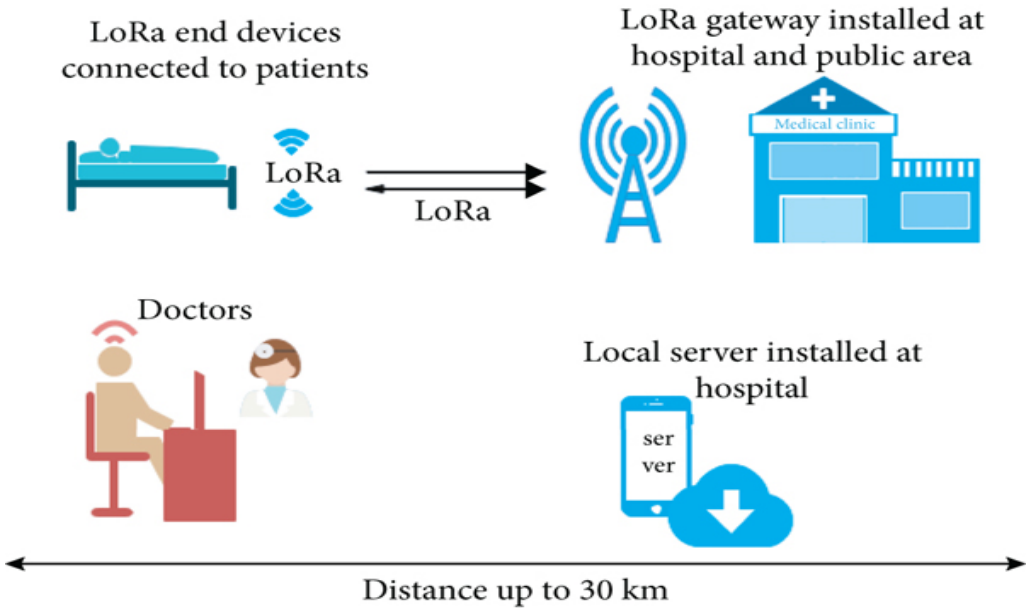

Figure 5.1: RHM system architecture [73]

5.2 Simulations

Scalability analysis of three gateways of a LoRaWAN network is done using the ICS Telecom simulation tool [38]. The same parameter settings are used to model all three gateways, and all end devices were also configured using the same parameters all presented in Table 5.2. Moreover, remote healthcare traffic parameters are considered in modelling the end devices.

5.3 LoRaWAN Interference Modelling

In this analysis, the interference in the uplink direction for many fixed or mobile end devices in ICS Telecom is done by using randomly generating subscribers or end devices, modelling the end devices, and determining the TD of each fixed gateway; equation 5.1 describes TD mathematically.

Table 5.2: Simulation parameters

Parameters	Values
Frequency of operation	868 MHz
Bandwidth	125 KHz
Propagation model	Okumura-Hata
Spreading Factor (SF)	12
Number of Gateways	3
Gateway noise figure	3 dB
Gateway antenna gain	5 dBi
Gateway height	50 m
Gateway activity factor	1
Minimum Threshold required	4 dBu
Minimum C/(N+I) ratio required	0 dB
Maximum gateway total uplink bit rate	50 Kbps
End-node transmit power	14 dBm
End-node antenna height	1.5 m
End-node data rate	1.2 Kbps

The end devices are modelled using traffic requirements for remote health monitoring applications where 1.2 kbps data rate required for transmitting blood pressure in remote health monitoring applications is used in modelling the end devices. The tool then uses TD to analyse the impact of interference on the uplink connectivity. A Bing Map for Glasgow city with three LoRaWAN gateways used in simulations is presented in Figure 5.2.

The end devices are randomly generated on the investigated area of 3.5 km^2 of Glasgow city as presented in Figure 5.3 in the numbers of 500, 1000, 5000, and 10000.

The power received by each gateway from each end node is calculated once the threshold of reception is set. Therefore, the increase of the degradation of the reception threshold is calculated as soon as the end nodes are distributed on the investigated area. If the connection between any end node and any gateway is considered by the tool as the desired link, the contribution of all other end nodes is regarded as interference. Furthermore, to configure this calculation, (N=0-5) interference rejection factors are considered and an activity factor of 1% is used. This factor is an adjustment factor of the transmission power of a gateway.

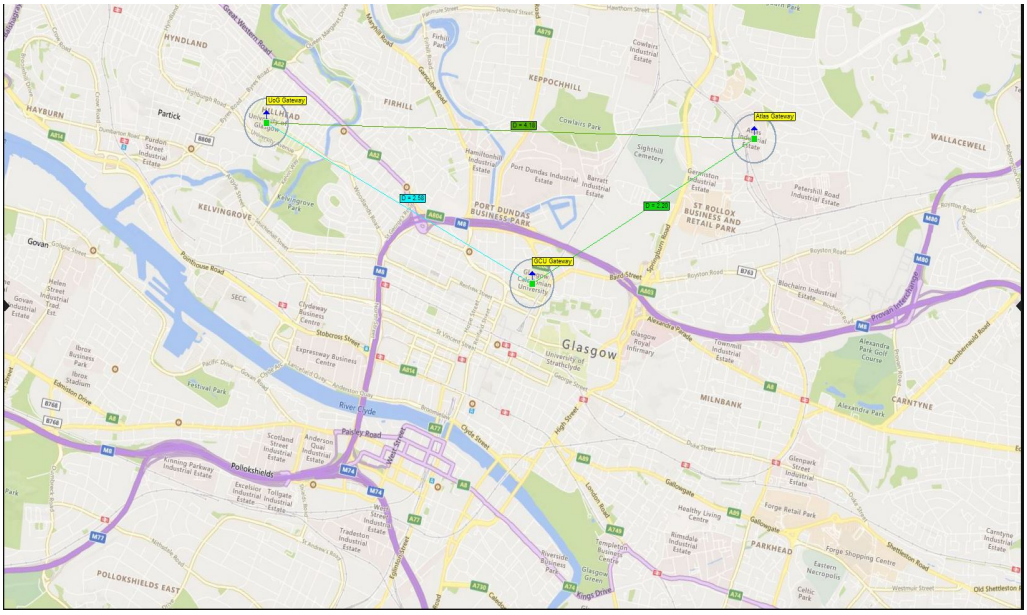

Figure 5.2: Glasgow city map with three LoRaWAN gateways

So, for an end device with a transmit power (Pt), if the activity factor is 100%, the power considered in calculating interference is Pt. If the activity factor is 1%, only 0.01Pt is considered in the interference calculation.

TD which is also referred to as the Noise Increase Level (NIL) of a gateway which is calculated using the following formula:

$$TD = Psum(dBm) - kTBF(dBm) \tag{5.1}$$

Where kTBF is the intrinsic reception threshold only of thermal origin or the physical nature of the individual gateways, without the effect of the interferences, and Psum is the sum of the powers received from all the ED. Furthermore, the reception threshold of fixed gateways increases or degrades in dB as the number of the ED increases.

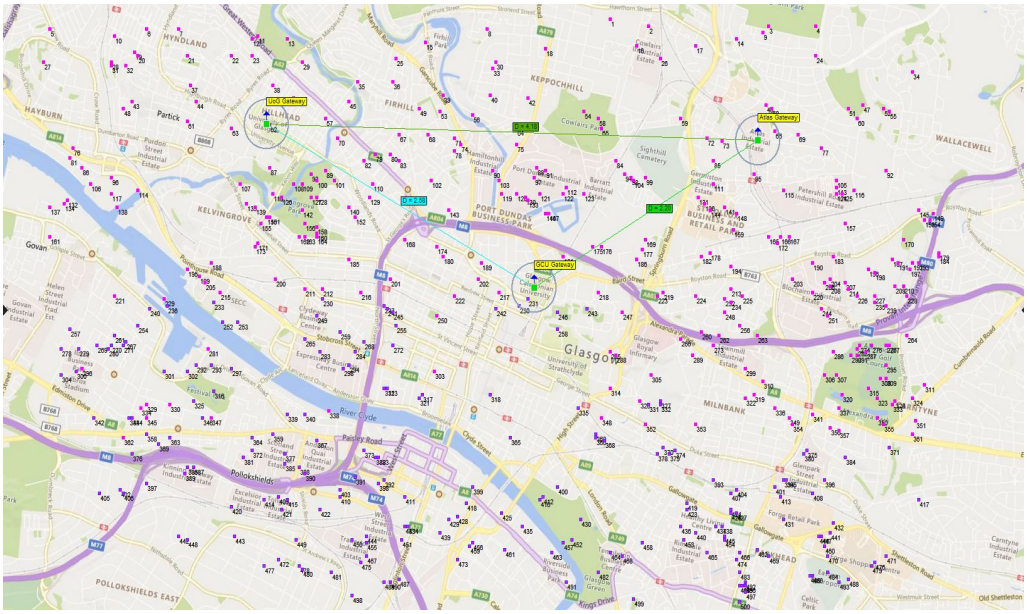

Figure 5.3: 1000 end nodes randomly generated on the investigated service area

5.4 Results and Performance Analysis

The obtained simulation results for the TD of three gateways of a LoRaWAN network with an increasing number of fixed and mobile end nodes are presented in this section. Each ED is identified by its unique serial number.

Table 5.3: Results for gateway 1

Number of ED	500	1000	5000	10 000
TD for Fixed ED	75.03	77.13	87.51	88.15
TD for Mobile ED	91.25	98.42	82.53	105.62

TD increase simulation results for all 3 gateways with an increasing number of fixed (scenario 1 where all ED are fixed) and mobile (scenario 2 where all EDs are mobile) ED are presented in Table 5.3, Table 5.4 and Table 5.5. Furthermore, TD results for mobile ED vary with time.

Table 5.4: Results for gateway 2

Number of ED	500	1000	5000	10 000
TD for Fixed ED	50.59	71.37	86.87	87.55
TD for Mobile ED	93.08	96.78	106.44	103.84

Table 5.5: Results for gateway 3

Number of EDs	500	1000	5000	10 000
TD for Fixed EDs	32.20	54.10	84.21	88.14
TD for Mobile EDs	99.89	96.96	106.54	103.80

5.5 Scalability Analysis

LoRaWAN scalability is analysed using the following three criteria for the end-devices attempt to be able to connect to the best server, and C/N+I (Carrier/Noise+1) bit rate control criteria is considered: An ED connects to the best server gateway if: The C/(N+I) ratio in the uplink is higher than the constraint 0 dB defined in the minimum required field C/I+N, and the received power in uplink is higher than the constraint 4 dBu defined in the Threshold field. Each gateway's total uplink bit rate remains below or equal to 50 kbps, defined as our gateway's data rate. The constraint threshold 4 dBu set in the threshold field of the simulation tool can be updated according to the results of the degradation analysis of the reception threshold. However, this is not considered in this study. The calculation of the interference level is based on the average value of Threshold Degradation (ATD) of the threshold degradation of (n) number of gateways. The average TD (dB) values for three LoRaWAN gateways with an increasing number of fixed and mobile end devices are presented in Figure 5.4.

The results of average degradation of the reception threshold of the three LoRaWAN gateways as 500, 1000, 5000 and 10 000 fixed and mobile end devices are scattered on our investigated area of 3.5 km^2 of Glasgow city are presented in Table 5.6. and the following formula is used to define ATD for n number of gateways with different TD values:

$$ATD = 1/n \sum_{i=1}^{n} TD_i \tag{5.2}$$

Table 5.6: Average TD values (dB) for the three gateways

Number of EDs	500	1000	5000	10 000
ATD for Fixed EDs	52	67	86	87
ATD for Mobile EDs	94	97	98	104

The reception threshold varies according to the number of ED transmitting. It is quite likely that for a moment, no end device will transmit what cancels degradation of the reception threshold. Hence an interference situation is transient, and not permanent.

From Table 5.6, it can be shown that the average TD for the fixed ED ranges from 52 dB to 87 dB while the average TD for the mobile ED ranges from 94 dB to 104 dB for the three fixed gateways.

From Figure 5.4, it can be seen that increasing the number ED increases average TD. The obtained results are crucial for determining the maximum number of ED to be used with three fixed gateways.

Furthermore, in ECC-01-05 proposal [37] which addresses national planning of digital radio connections, recommends an upper limit for threshold degradation of between 0.2 and 1 dB (interference from a single transmitter) and 3 dB (aggregate interference from all transmitters). However, when deploying a dense network, a greater threshold than 3 dB for degradation is permitted as long as performance and availability goals can be achieved. However, no uplink connectivity analysis and network availability performance goals are considered in this study, and this is recommended as a future work.

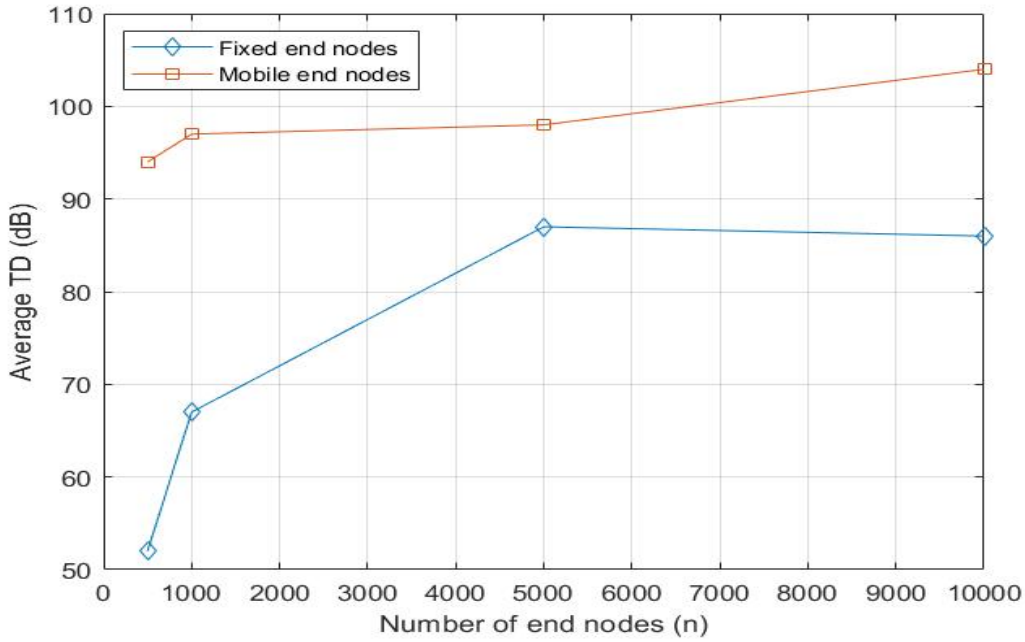

Figure 5.4: Average TD (dB) for three LoRaWAN gateways with an increasing number of fixed and mobile ED

Chapter 6

RNN based IoT Models

In this chapter, we develop different IoT applications using RNN; initially we develop and evaluate an ED LoRaWAN-RNN-based IoT localization system in indoor and outdoor environments. Then an IoT heart disease prediction model is developed and evaluated using RNN, and all the developed IoT models demonstrate improved results.

6.1 RNN-LoRaWAN based IoT Outdoor Localization

Before analysing the performance of LoRaWAN on a large scale dense urban area, a small-scale is first considered to enable us to analyse the performance of LoRaWAN in outdoor small scale urban area. The end-devices are located randomly and transmitted at arbitrary intervals. Furthermore, little study has been done on developing energy-efficient localization systems of wireless sensor nodes, particularly in outdoor urban areas. Thus, a LoRaWAN-based model to locate end devices on a LoRaWAN network grid is developed in this section using RNN. Compared to the existing RSSI fingerprint conventional techniques, the novel RNN-based system increases localization prediction accuracy. The developed localization system is trained and tested using real test datasets gathered in Glasgow city, each with various numbers of hidden neurons. By training and testing several RNN network architectures using various learning rates, the performance of the created RNN-based localization model is evaluated, and better accuracy is attained with a minimum mean localization error of 0.39 m.

6.1.1 Real Test Measurements

Real-world LoRaWAN RSSI datasets are gathered in Glasgow city to develop and test our RNN-based end device localization algorithms. a LoRaWAN mDot end device operated by a Raspberry Pi is used to send the same messages to three LoRa SX1301-capable Kerlink gateways. The three gateways are located at 30 m on the George More building at Glasgow Caledonian University, 27 m on the James Weir building at the University of Strathclyde, and 25 m on top of the Skypark building. The data are gathered and transmitted simultaneously at a walking pace from various locations to the three gateways using the LoRa mote. Figure 4.1 displays a Bing map showing the locations of three LoRaWAN gateways, LoRa end devices, and the path taken for the measurements. Additional information on the method utilised for our measurements is provided in [141].

Data Normalization

The collected dataset has high RSSI values, which caused the network to be unstable due to high weights. Therefore, using the formula shown below, we scale the dataset using the Min-Max Normalization data pre-processing technique in the range of 0 to 1.

$$x_i = \frac{RSSI_i - \min(RSSI)}{\max(RSSI) - \min(RSSI)}, \tag{6.1}$$

where $RSSI = (RSSI_1, ..., RSSI_n)$ is the raw RSSI input values and x_i is the resultant normalized data.

6.1.2 Proposed RNN-LoRaWAN based IoT Localization

We design an RNN-LoRa RSSI-based Localization Model in MATLAB utilising fingerprint data collected from real-world measurements made with three LoRaWAN gateways in Glasgow city. A supervised training RNN learning GD method is considered for this research investigation. The dataset includes the RSSI values at each of the three gateways that receive each message sent by the moving end device and the end device's GPS coordinates for each transmission.

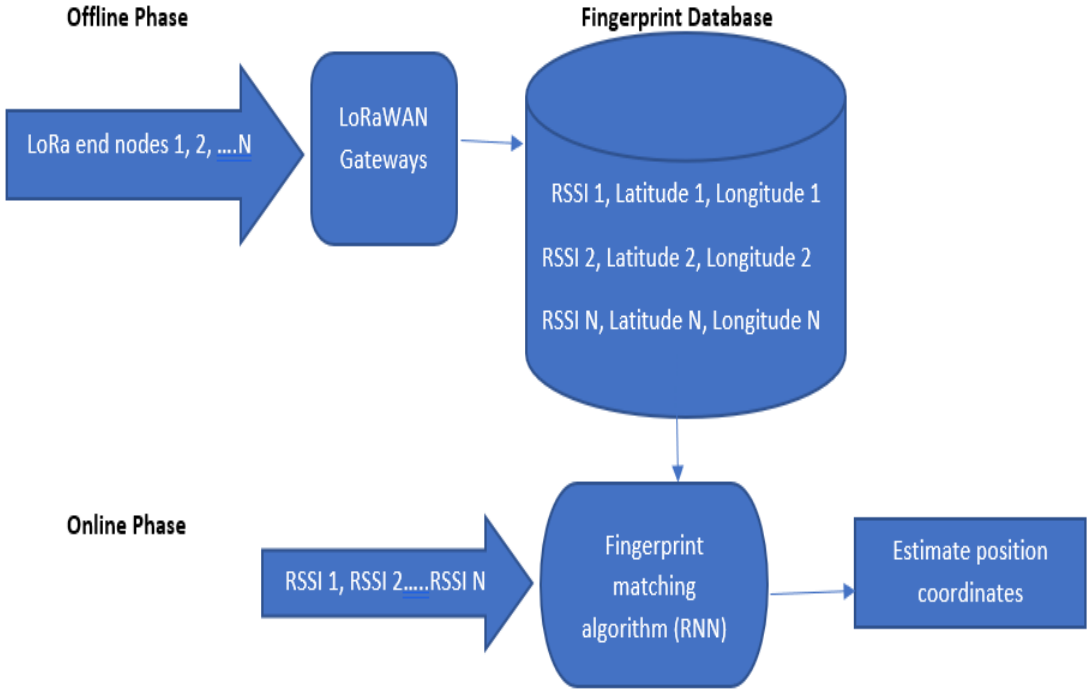

Figure 6.1: RSSI fingerprint localization approach

Furthermore, for each gateway that did not get a specific message, we log -200 dBm as the RSSI number.

6.1.3 Results and Performance Anaysis

In this section, a LoRaWAN based localization model is developed using RNN to predict position coordinates using LoRaWAN RSSI values. Different RNN network architectures of one input layer, one hidden layer and one output layer are used to develop and evaluate different localization models in a small scale urban area of Glasgow city. The approach that is considered in this study is described in Figure 6.1. Multiple RNN designs of 6, 12, and 18 hidden neurons are modeled and analysed using learning rates of 0.01, 0.1, and 0.4. Mean localization error training and test results that correspond are recorded. A sample size of 1931 data points yields a minimal mean

localization error of 0.39 m, with 80% of the dataset used for training and 20% for testing the model. The proposed model runs k-folds with a minimum training mean squared error value of 0.005 m. Using the average localization error (AE), the performance of the developed RNN-based localization model is examined. AE is defined by the following equation 6.2:

$$AE = \sum_{i=1}^{n} ((X_{real} - X_{pred})^2 + (Y_{real} - Y_{pred})^2)^{0.5} \tag{6.2}$$

Where $(Xreal, Yreal)$ represents the actual, real position that was previously recorded using GPS, and $(Xpred, Ypred)$ represents the estimated position of an unknown location predicted by the LoRa RSSI-based localization system that was developed using RNN. In our localization dataset, n represents the total number of samples used. The total number of samples used in our localization dataset is given by n. The obtained findings demonstrate that, for the first system network design (RNN-1) presented in Figure 6.2 with 6 number of hidden layer neurons, where GW1 RSSI, GW2 RSSI, and GW3 RSSI are LoRaWAN RSSI input values from gateway 1, gateway 2, and gateway 3 respectively, while X and Y are output position coordinates. With RNN-1, raising the learning rate from 0.01 to 0.1 enhanced localization performance by reducing the mean localization error. The mean localization error, however, increased when the learning rate was increased to 0.4. Therefore, using a 0.1 learning rate with only six hidden neurons resulted in the best performance.

When the learning rate was raised from 0.01 to 0.1, the performance of the second system architecture (RNN-2) decreased. However, the performance improved when the learning rate was raised to 0.4. The third system architecture (RNN-3), which used 18 hidden neurons, showed that the learning rate increased as the mean localization error decreased.

Table 6.1: Mean localization error (m) of different RNN based localization architectures

Learning rates	RNN-1	RNN-2	RNN-3
0.01	0.76	0.39	0.48
0.1	0.48	0.48	0.45
0.4	0.54	0.41	0.40

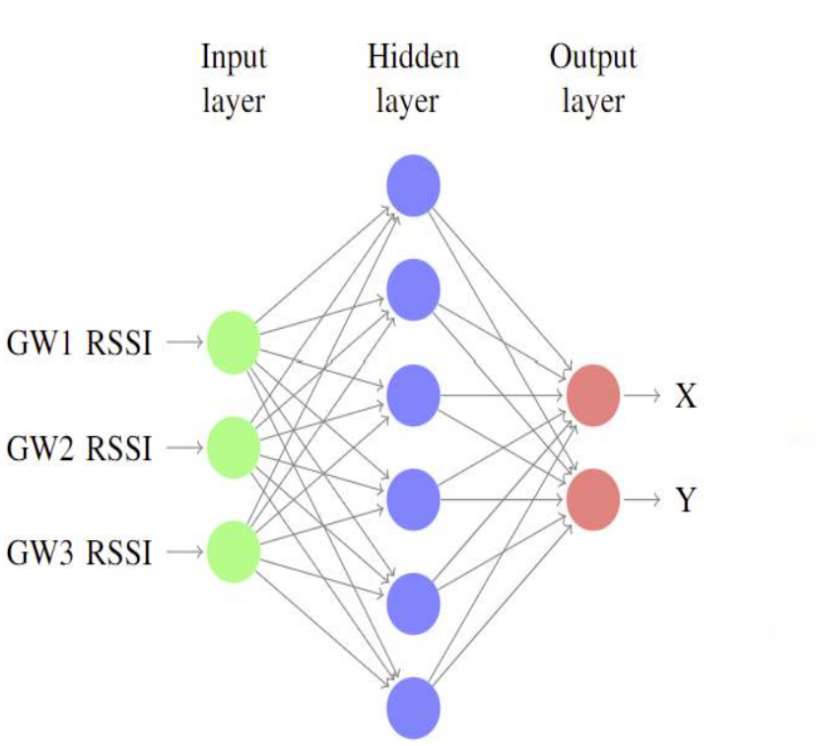

Figure 6.2: Architecture of the proposed RNN-1 localization model

Three input and two output neurons are considered for each of the three RNN localization model architectures in our research. Results for the mean localization error values for the three RNN-LoRa RSSI-based localization system architectures using learning rates of 0.01, 0.1, and 0.4 are shown in Figure 6.3 Our results show that the developed RNN LoRa RSSI-based localization model performed at its optimal when 12 hidden neurons were used, with a learning rate of 0.01. Table 6.1 compares the localization accuracy of all the RNN-based localization architectures that were investigated using different learning rates.

Furthermore, our results confirm that the developed RNN-based localization models are trustworthy and have significantly minimal mean localization errors, and outperform the traditional LoRa localization algorithms published by various researchers in the literature in [13],[145],[122], [146], and in [152] with the highest accuracy for outdoor localization services.

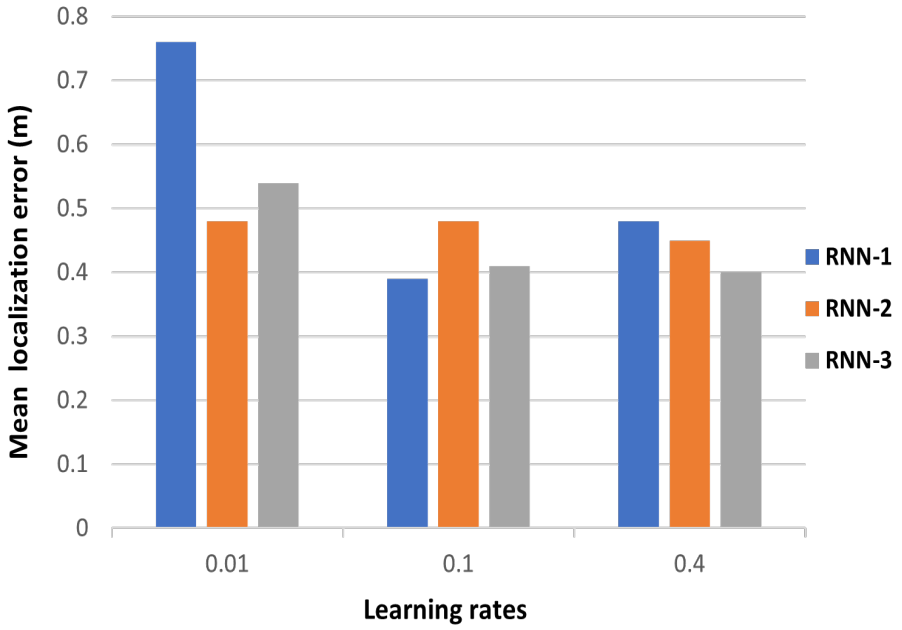

Figure 6.3: Performance analysis between RNN based localization network architectures with different learning rates

6.2 RNN-LoRaWAN based Outdoor Localization for Large Scale IoT Networks

This section presents all the details and procedures used to collect and preprocess the dataset we have used to develop the proposed LoRa-RNN-based localization model for large scale IoT networks in an urban environment. The developed model is mainly to be applied in IoT remote healthcare applications to track or monitor the elderly or patients in indoor or outdoor environments. This is very important especially in cases where a patient or the elderly whose health status is normally monitored on a real time basis falls or is not conscious; these models will assist in locating them quickly for quick intervention. In this study, we develop a RNN-based localization system for a large-scale IoT environment with a significant number of end devices on a large scale in a dense urban area. The environment are regarded as a reference scenario of a smart city because smart cities are an important

use case for LPWAN technology and serve as an excellent illustration of a scenario in which a significant number of IoT devices are located relatively close to one another. These devices' functions and qualities depend on the application for which they are employed. Smart metering and home automation, structural health monitoring, and traffic monitoring, among others, are some examples of IoT concepts for smart cities. Within these categories, various IoT applications with various properties can be used. The end-device transmission interval is the one that matters the most in a dense network. The frequency of an IoT device's transmissions varies depending on the application and can be anywhere between a few minutes (for applications like traffic and air quality sensors) and once per day (e.g., smart lighting). Some event-driven applications do not send data regularly, like wireless (fire) alarms that promote public safety. All communications in smart city scenarios are considered to be periodic.

6.2.1 Dataset

In this investigation, we use the publicly accessible LoRaWAN dataset collected in Antwerp City over a 52 km2 area of Belgium and published by Aernouts et al. in [122]. A total of 130,343 data points have been captured by mounting LoRa modules on postal service vehicles, and over three months, these nodes sent a message to 72 LoRaWAN gateways established by the private company Proximus every minute. Figure 6.4 depicts a map of Antwerp with a random sample of data points uniformly dispersed over the city's streets. The authors noted the X and Y GPS position coordinates of each LoRa node together with the RSSI values it got from 72 different gateways for each data point or message. A score of -200 dBm RSSI value has been noted if any of the gateways missed a particular message. Figure 6.5 shows the RSSI value distribution, which ranges from -122 dBm to -79 dBm.

Our dataset's high absolute RSSI values and the high weights cause an unstable network. As a result, we use the method in equation 6.1 to scale our dataset using the Min-Max Normalization data pre-processing approach to the range of 0 to 1.

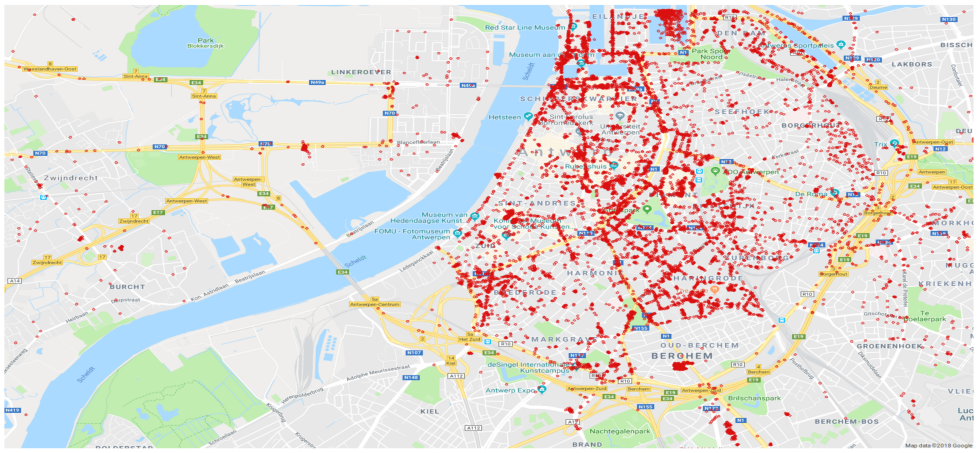

Figure 6.4: A map showing a random sample of used data points [122].

.

6.2.2 Proposed RNN-LoRaWAN based Localization for Large Scale Urban IoT Networks

Using the LoRaWAN Antwerp dataset (RSSI values, Latitude and Longitude coordinates, GPS coordinates), RNN is used in this study to develop our proposed model that accurately maps the input to the output. The developed model outputs any desired unknown X,Y GPS position coordinates. As shown in Figure 6.1, the proposed model is trained using the RNN supervised learning algorithm to locate each end device in the network service area. The trained model is then further extended to predict the position of any additional LoRa sensor nodes on the same network grid based on end-device RSSI values.

To train and test our suggested RNN-LoRa-based localization using a gradient descent algorithm for regression, we use the LoRaWAN Antwerp dataset in [122]. Various experimental designs are created, wherein the first 80% of the 130,343 total data points are used to train the model using the chosen learning rates throughout various epochs, and the second 20% of the dataset is utilised to test the model. The suggested RNN model employed 72 input layer neurons, 72 hidden layer neurons, and two output layer neurons while running k-folds.

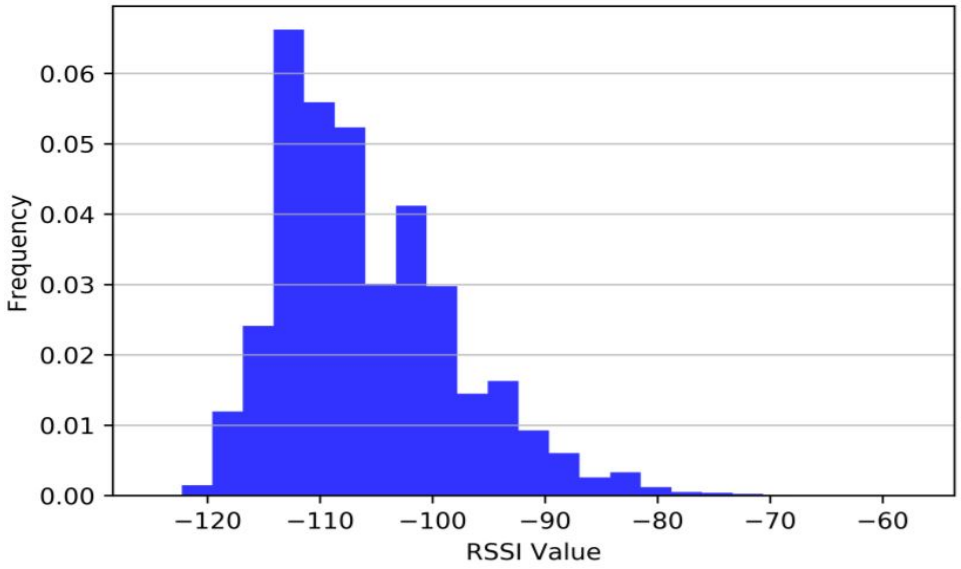

Figure 6.5: The distribution of RSSI Values for Antwerp City.

.

The RNN-based localization algorithm is as follows:

Algorithm RNN Based Localization
Input: RSSIxt,yt in each time slot, M
Output: Regression model based on RNN
1: Use 80% of the collected RSSI values from trajectory where the user moved and consider enough amount of data in this trajectory.
2: Generate the RSSI database in each time slot
3: Initialize the structure of RNN
4: Train RNN and compute the RNN parameters
5: Use 20% of the collected RSSI data for testing, then verify the trained RNN model in step 4
6: Change the RNN parameters and estimate the best parameters for accurate localization using steps 5 and 6.

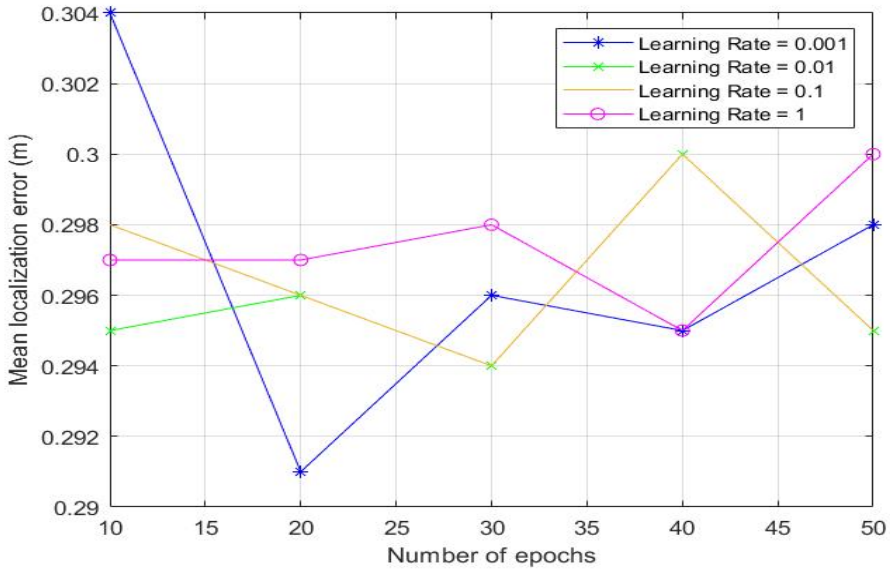

Figure 6.6: Mean localization error for the used learning rates in various number of epochs.

.

6.2.3 Results and Performance Analysis

We use the simulation-controlled environment of MATLAB R2020b to evaluate the performance and localization precision of our proposed RNN model. The average mean localization error values for the system with the used learning rates of 0.001, 0.01, 0.1, and 1 at various epochs are shown in Figure 6.6. The average localization error (AE), as defined by equation 6.2, is used to evaluate the developed RNN-based localization model.

According to Figure 6.7, the proposed model is generally more accurate when learning rates are lower than higher, although this came at the expense of longer training times. The localization system also tends to be less stable throughout training, with larger learning rates. To address these problems, we train our model using several learning rates. The developed system's mean localization error improved by 0.03 m when the learning rate was increased from 0.001 to 0.1, which is not a significant improvement, and may or may not be significant depending on the application. The localization system's accuracy is enhanced by minimizing the mean localization error by 0.02 m

when the learning rate is increased to 1. With a learning rate of 0.001, our system obtained a minimum mean localization error of 0.291 m. Table 6.2 provides more information regarding mean localization error values that are obtained for all of the used learning rates. Additionally, during training our model, a minimum mean square error (MSE) value of 0.09 m is achieved.

Table 6.2: Average mean localization error (m) for used learning rates

Learning rate	AE (m)
0.001	0.291
0.01	0.294
0.1	0.297
1	0.295

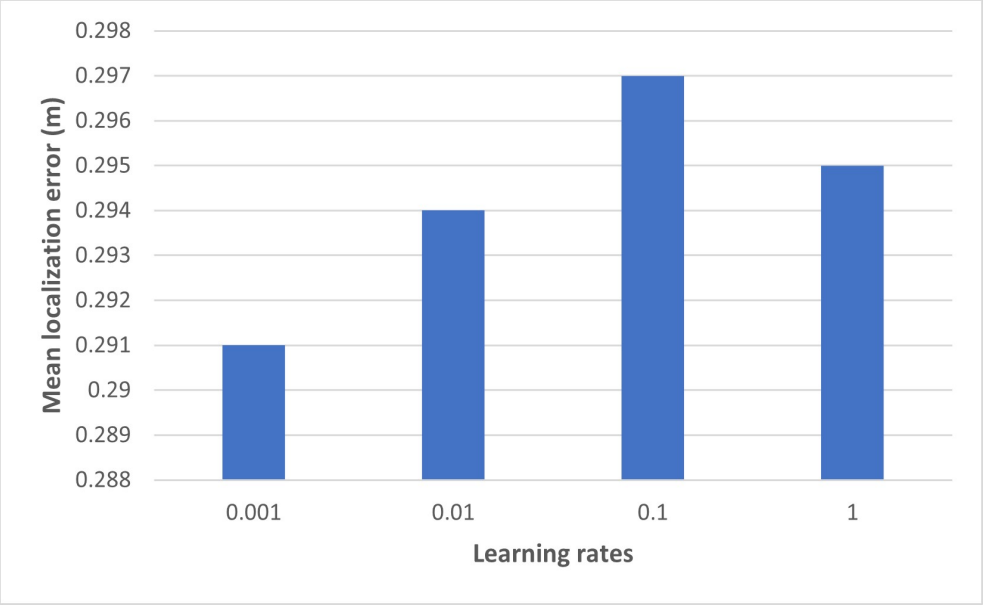

Figure 6.7: Minimum mean localization error values for the used learning rates.

.

We then assess the effects of the various samples because our enormous amount of data required a very long training period depending on the chosen

learning rate. Figure 6.8 illustrates our system's mean localization error values using 1000, 3000, 5000, 10 000, and 15 000 data samples while using the same RNN network architecture with the same learning rates. The system's performance increases as the learning rate increased from 0.0001 to 0.01 for data samples of 1000, 5000, and 10,000, then it drops as the rate increases further to 0.1 and 1. In addition, increasing the learning rate from 0.0001 to 1 decreases the mean localization error for the 3000 and 15 000 data samples, enhancing the system's performance.

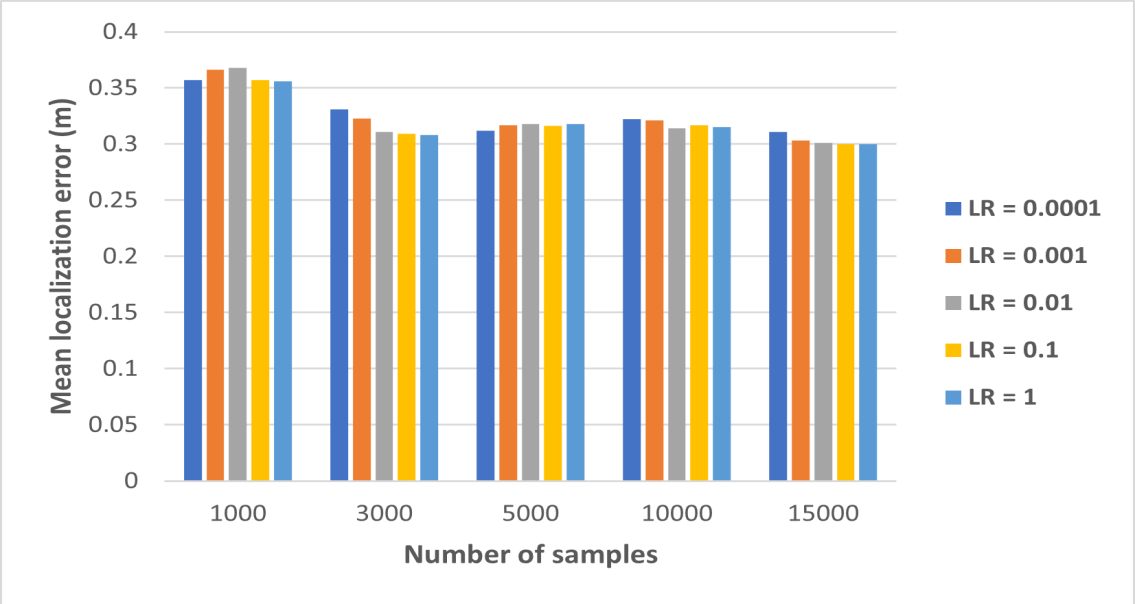

Figure 6.8: Mean localization error for the used samples.

Using learning rates of 0.1 and 1, the minimum mean localization error of 0.3 m is achieved with 15 000 samples. As a result, we look at the overall RNN training time (in seconds) for the variety of samples and learning rates that are used, as given in Table 6.3. Therefore, for the maximum learning rate of one, the quickest training duration of 4970 seconds, and a training error of MSE equal to 0.1 m are used to attain the highest system accuracy. Figure 6.9 presents the mean localization values for all the samples that are used, with Table 6.3 providing extra information. The data sample results demonstrate that increasing data samples from 1000 to 15000 and then to 130,343 samples has no appreciable impact on the system's accuracy because

the difference is only 0.01 m at the cost of longer training sessions.

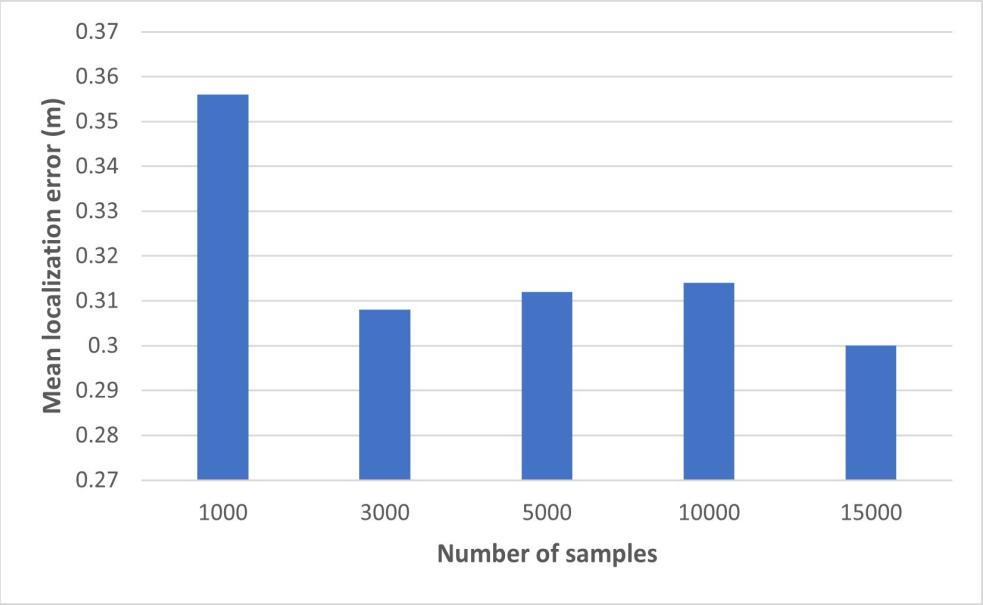

Figure 6.9: Minimum mean localization error values for the used samples.

Table 6.3: Average mean localization error (m) for used samples

Samples	AE (m)
1000	0.356
3000	0.308
5000	0.312
10000	0.314
15000	0.3

6.2.4 Comparative Performance Analysis

Table 6.4 summarises the localization performance of each model and comparative performance analysis of the proposed RNN-based localization approach's localization accuracy to conventional localization methodologies found

in relevant research studies.
Bonafini et al. in [147] used Multilateration algorithm and obtained a minimum localization error of 6.2 m while Du et al. in [148] got a minimum localization error of 7.57 m. Shokry et al. in [150] used deep learning and reported a minimum localization error of 18.8 m, and Anjum et al. in [149] used a linear regression model and reported a localization error of 45.75 m. Purohit et al. in [146] used deep neural networks and got a localization error of 191.52 m, Janssen et al. in [151] also used kNN and obtained a localization error of 340 m. In addition, Aernouts et al. in [122] used kNN method and obtained a localization error of 398.4 m, Anagnostopoulos et al. in [13] also used ANN and got an error of 358 m while Nguyen in [152] used ANN approach and got a localization error of 500 m. From Table 6.4, it is clear that the proposed RNN based localization model outperforms the other RSSI fingerprint LoRaWAN based localization systems from related research with a minimum localization error of 0.29 m.

The proposed RNN method has achieved 95%, 96%, 98.5%, 99.85%, 99.37%, 99.92%, 99.93% and 99.94% improvement in mean localization error compared with the works of Bonafini et al. in [147], Du et al. in [148], Shokry et al.in [150], Anjum et al. in [149], Purohit et al. in [146], Janssen et al. in [151], Aernouts et al. [122], Anagnostopoulos et al.in [13], and Nguyen in [152], respectively.

6.3 RNN-LoRaWAN based IoT Indoor Localization

This section gives the details of the procedures used to collect and pre-process the real-world data, mainly LoRaWAN RSSI values and end device position coordinates that are used to develop the proposed LoRaWAN-based indoor localization system using RNN.

Table 6.4: Accuracy of different LoRaWAN outdoor RSSI fingerprinting approaches from related work

Research Work	AE (m)	Approach
Proposed system	0.29	RNN
Bonafini et al. [147]	6.2	Multilateration
Du et al. [148]	7.57	Hybrid
Shokry et al. [150]	18.8	Deep learning
Anjum et al. [149]	45.75	Linear
Purohit et al. [146]	191.52	ANN-Deep
Janssen et al. [151]	340	kNN
Aernouts et al. [122]	398.4	kNN
Anagnostopoulos et al. [13]	358	ANN
Nguyen [152]	500	ANN

6.3.1 Used Hardware

A LoRa application needs an end device with a LoRa module transceiver and a gateway that can take in LoRa modulated signals. The type of the used end device is discussed first, and then the used gateway and its properties are explained.

The LoRaWAN End-device

End devices are nodes that connect to a network wirelessly. Over wireless networks, end devices can generate, receive, and send data to other end devices or other kinds of network elements. End devices serve IoT applications in LoRaWAN networks that need LPWAN capabilities. Long distances between devices must be traversed by information without using a lot of power. MultiTech mDot Box in [153] is used as the end-device for this study. The mDot Box, consisting of a mDot RF module and a micro developer kit, uses Semtech's LoRa long-range, long-distance RF spread spectrum technology to develop a solution that overcomes the most challenging obstacles in this field of wireless communications, such as distance and obstruction penetration. LoRa offers an incredible asset management range of up to 10 miles (15 km) line of sight and 1-3 miles (2 km) through buildings. Additionally, it uses LoRa's unlicensed ISM band spectrum to deliver low-cost, free bi-directional communications from thousands of mDots to a single conduit. Also, LoRa's

extended Life feature allows battery-powered assets to run for years because of its incredibly low power use. The MultiTech mDot Box LoRa end device set up is shown in Figure 6.10.

Figure 6.10: LoRaWAN ED set up.

.

The LoRaWAN Gateway

A MultiConnect Conduit MTCDT-L4E1-247A—868-EU-GB Gateway in [154] made by MultiTech is the network's receiving node, as seen in Figure 6.11.

All end devices must support the three default channels (0, 1, and 2) implemented in every EU868 MHz end device to comply with the LoRaWAN standards, as the Gateway is designed to listen on the 868 MHz band for incoming messages. These channels are 868.1, 868.3, and 868.5 MHz. There

are no new channels added. The gateway is capable of retrieving a variety of information from each packet received as it serves as the network server when set into server mode, including the node's address or id, the gateway's address, the channel and corresponding frequency at which the packet was transmitted, the used Coding Rate, the Payload the used Data Rate, the Signal-to-Noise Ratio (SNR) of the received packet, the Received Signal Strength Indicator (RSSI) as seen in Figure 6.12.

In order to identify packets, the end-device that transmitted them, as well as the conditions of their transmission (data rate, coding rate, and frequency), as well as to assess how successfully the gateway received the radio signal, the factors mentioned above are necessary (RSSI, SNR). Given the spread spectrum nature of LoRa modulation, it is possible to receive signals below the noise floor. As a result, SNR values that are negative can be expected.

6.3.2 Dataset Collection Setup

MultiTech mDot conduit devices, which are scalable and reconfigurable industrial LoRaWAN gateways [154] were used with a MultiTech mDot Box, a portable device with an operational mobile end device, a radio, and internal sensors for atmospheric pressure, altitude, temperature, light level, and accelerometer [153].
The MultiTech conduit gateway has a server mode feature that allows it to emulate a cloud-based system and function as a stand-alone system acting as a network server. This feature makes it possible to utilise the gateway independently and across a single site without an internet connection. Every conduit gateway was set up first with a static IP address, and a Java-based web-based graphical user interface was used for setting up and logging. We have used a standard straight-through patch lead and immediately connected a Lenovo laptop to the gateway ethernet port so that we can easily access the graphical user interface. Initially, a windows computer configured the device using a static device IP. We also activated Node-RED, a different graphical user interface that could be used simultaneously as a control console on a different web page created by the conduit, to ensure it is appropriately configured, receiving, and processing radio packets.

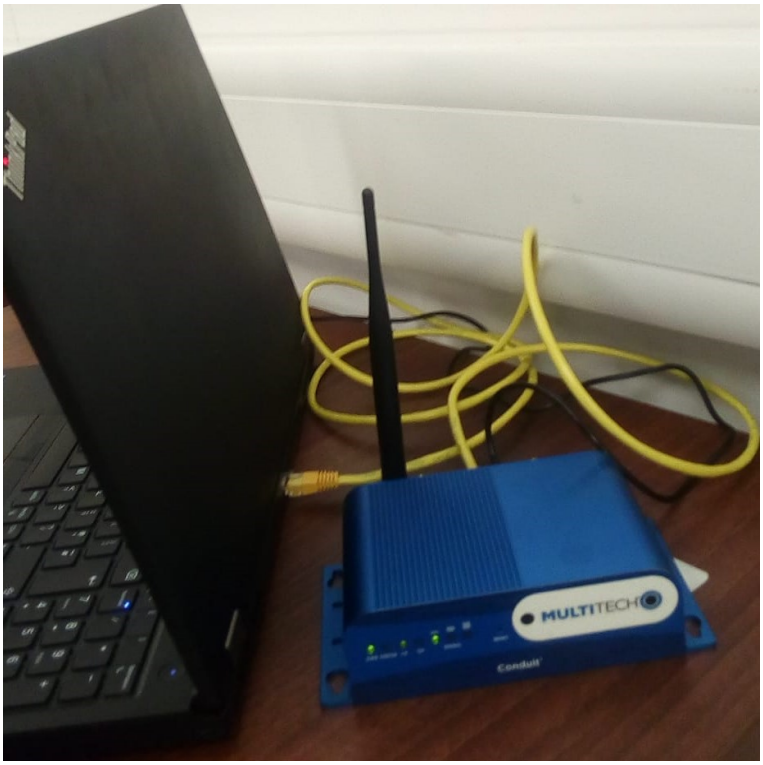

Figure 6.11: LoRaWAN gateway set up..

.

Then, that conduit and end device is configured, among other things, the end device transmits RSSI, atmospheric pressure, altitude, temperature, light level, accelerometer, and signal data to the conduit gateways as metadata message data supplied by the network server in JSON Javascript object notation format. The packet also includes the LoRaWAN frequency (Freq=868 MHz), the spread factor (SF=12), the bandwidth (BW=125KHz), and the applied coding rate (Codr=4/5). Additionally, the captured data is later recovered using a Tera Term software program on a Windows computer and a mDot micro-Development board with an 8-parity programmable connection [155].

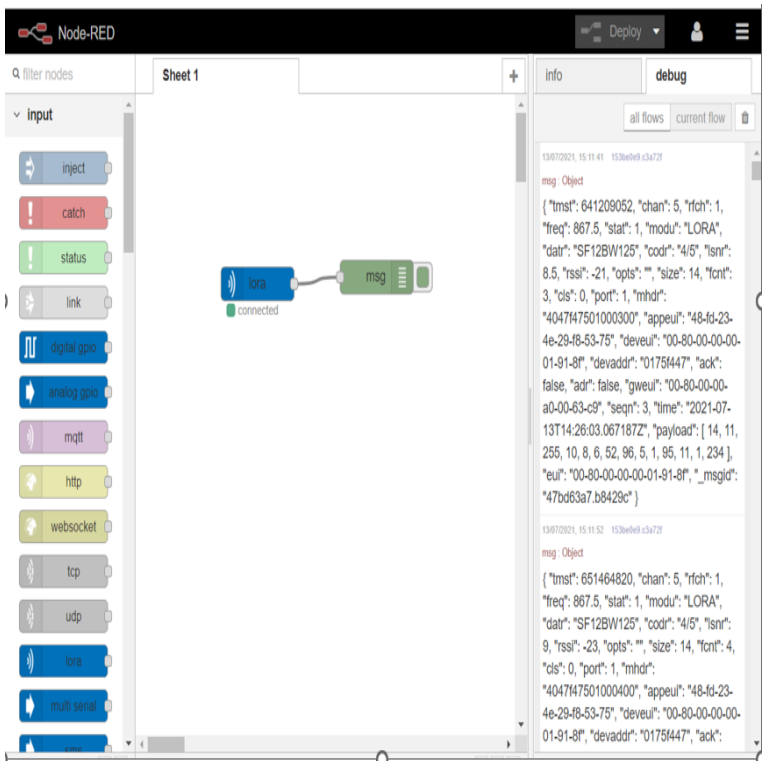

Figure 6.12: A random sample capture of received packets.

6.3.3 Study Environments

In this study, we gather RSSI data at various X, Y ground truth grid points in both LOS and NLOS indoor scenarios in the main building of Destiny College in Glasgow city [156]. The three environments investigated are meeting/lecture rooms that are 8 m $\times$ 22 m, 15 m x 25 m, and 20 m x 25 m, respectively, on the ground floor (floor 0), floor 1, and floor 2, all with different propagation characteristics. One gateway is placed on a table in a corner on floor 0 and another on floor 2. The end device held by a moving user then periodically transmits a beacon message to the reception gateways for two minutes and broadcasts from the three rooms on each of the three floors at various grid position points. Concatenating the data collected from each environment, we have created a dataset with 1205 and 1269 data samples in LOS and NLOS, respectively. Figure 6.13 depicts a representative image of the data location site.

Figure 6.13: A random sample picture of the data collection site.

.

Due to the large weights that result from the large RSSI dataset made the network unstable,then we have scaled our data in the range of 0 to 1 using the Min-Max data Normalization technique. equation 6.1 describes the used formula.

6.3.4 Proposed RNN-LoRaWAN based IoT Indoor localization

Using the collected LoRaWAN RSSI values and corresponding X, Y ground truth coordinates, RNN is used to model the developed system to map the input to the output. As illustrated in Figure 6.1, the developed model predicts any unknown X, Y position coordinates based on end-device RSSI values.

The developed LoRaWAN-based positioning system is tested and trained using RNN as a regression model using the gradient descent algorithm.
In various experiment setups, the model is trained using 80% of the 1205 and 1269 collected data points in LOS and NLOS, respectively, then tested using 20% of the corresponding dataset. The developed RNN model consists of four input neurons, eight, sixteen, twenty hidden neurons, and two output

neurons, using learning rates of 0.0002, 0.002, 0.2, and two in both LOS and NLOS scenarios.

6.3.5 Results and Performance Analysis

The developed RNN-based localization model's accuracy in LOS and NLOS is examined using extensive simulations in MATLAB R2021b. The system's average localization error values are determined with hidden neuron numbers of 8, 16, and 20 and learning rates of 0.0002, 0.002, 0.02, 0.2, and 2. The developed model's accuracy and performance are evaluated using the average localization error formula described in equation 6.2.

6.3.6 Results Analysis in LOS

The accuracy in LOS of the proposed RNN-based indoor localization system increases as the learning rate increases from 0.0002 to 0.2 for all the used network designs, as shown in Figure 6.14. Nevertheless, localization error also increases as the learning rate increases to 2. When 20 hidden neurons are utilised to simulate the developed RNN network architecture with a learning rate of 0.2, the minimum AE attained is 0.1219 m with a 99.52% accuracy. Additionally, a Root Mean Square (RMS) of the training error of 0.06 m is obtained, and the computational training time is 86.45 seconds.
The AE obtained values using the developed RNN network architectures and the used learning rates are shown in Table 6.5.

6.3.7 Results Analysis in NLOS

Table 6.6 shows the average localization error values for the proposed system when 8, 16, and 20 hidden neurons are used, along with learning rates of

Table 6.5: Mean localization error (m) of the used RNN based architectures for the used learning rates in LOS

Learning rates	0.0002	0.002	0.02	0.2	2
8 HN	0.1567	0.1459	0.1258	0.1220	0.1345
16 HN	0.1566	0.1481	0.1373	0.1358	0.136
20 HN	0.1565	0.1504	0.1424	0.1219	0.1412

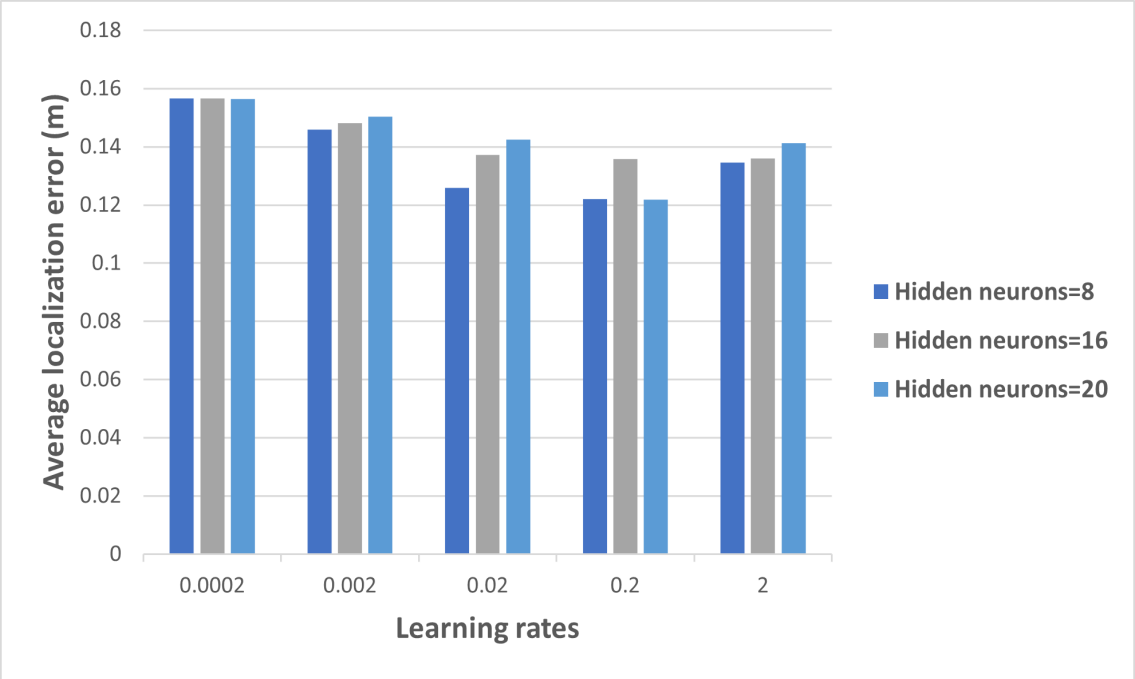

Figure 6.14: Localization accuracy of the used RNN network architectures with the considered learning rates in LOS.

0.0002, 0.002, 0.02, 0.2, and 2. From Figure 6.15, with a learning rate of 0.2 and 20 hidden neurons, the minimum obtained localization error is 13.94 m, with an accuracy of 44.24%.

Table 6.6: Mean localization error (m) of the used RNN based architectures for the used learning rates in NLOS

Learning rates	0.0002	0.002	0.02	0.2	2
8 HN	14.10	13.95	13.97	13.95	13.96
16 HN	14.09	13.97	13.96	14.04	13.98
20 HN	13.97	14.08	14.05	13.94	13.95

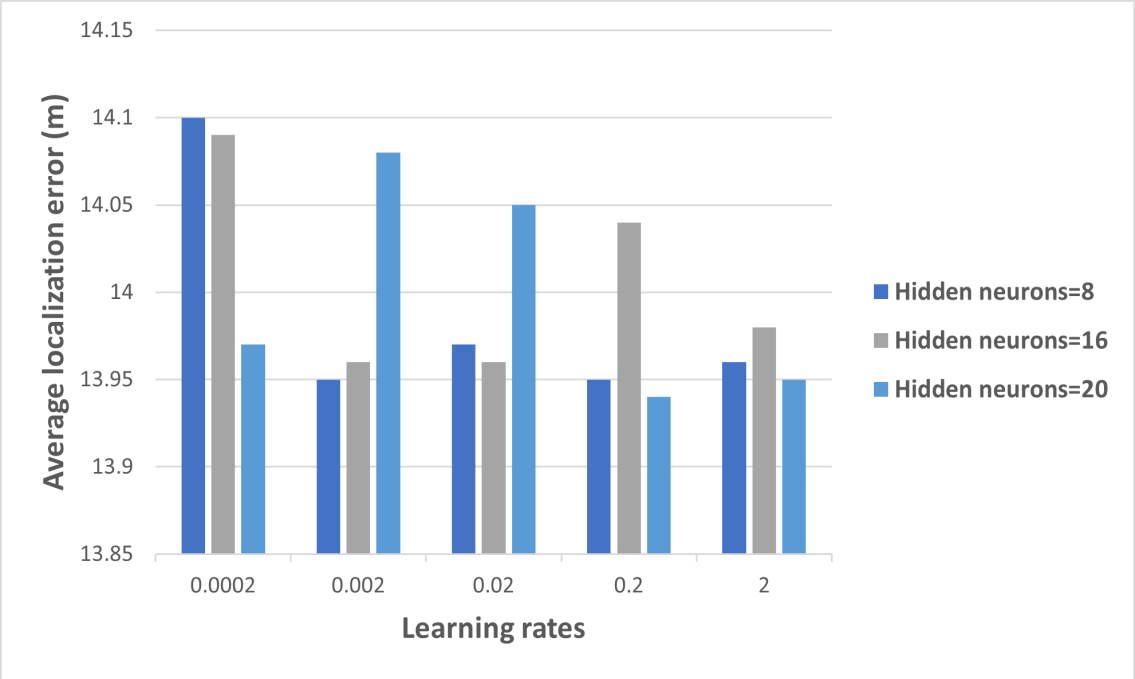

Figure 6.15: Localization accuracy of the used RNN network architectures with the used learning rates in NLOS.

6.3.8 Comparative Performance Analysis

The RNN method is used to map position coordinates to the associated RSSI values to evaluate the performance and position accuracy of LoRaWAN in an indoor environment in both LOS and NLOS scenarios. The localization error is computed by comparing the predicted distances to the ground-truth pre-recorded position coordinates. The results of the proposed localization system in LOS and NLOS scenarios are compared to those of other localization systems that have been previously presented in the literature using Polynomial Regression (PR), Trilateration, Path Loss (PL), Time of Arrival (ToA), and Smoothing Spline (SS) methods.
Table 6.7 shows that the LoRaWAN-RNN location system we developed has the highest accuracy, with an average localization error of 0.12 m in LOS as opposed to the 0.71 m in [157], 1.19 m in [117], 1.6 m in [159], 3.06 m in [119], and 8 m in [160] respectively. Additionally, the developed system demonstrates 83.1%, 89.9%, 92.5%, 96.1%, and 98.5% improvement in av-

erage localization error compared with the results reported by the authors in [157], [117], [159], [119], and [160] respectively. The obtained results provide crucial knowledge for developing LoRaWAN-based indoor localization in LOS using RNN, which can be more effectively used in large indoor sports arenas or fields, large hospital wards, shopping centers, and airports.
Furthermore, the proposed localization system's performance of the minimum average localization error of 13.94 m in NLOS is worse compared to 1.8 m in [158], 3.1 m in [159], 9.38 m in [161] respectively. However, the developed model achieves higher accuracy compared to 20 m obtained by the authors in [162] with a 30.3% improvement in average localization error. This may have resulted from the LoRaWAN signal being lost at various NLOS location points, typically when the ED and the receiving gateways are placed on different floors. One of the suggested explanations for the sub-performance in NLOS is multi-path reflections. The obtained results, however, are suitable for controlling a fleet of vehicles inside a specified area in the NLOS.

Table 6.7: RNN indoor localization results (LOS/NLOS) compared to results from related work

Research Study	AE (m)-LOS	AE (m)-NLOS	Method
Proposed system	0.12	13.94	RNN
Islam et al.[157]	0.71	3.72	PR
Sadowski et al.[117]	1.19	-	Trilateration
Han et al. [158]	-	1.8	KNN
Kim et al. [159]	1.6	3.1	Trilateration
Anjum et al. [119]	3.06	-	PL
Henriksson [160]	8	-	Time of Arrival
Anjum et al. [161]	-	9.38	SS
Manzoni et al. [162]	-	20	Trilateration

6.4 RNN based IoT Heart Disease Prediction Model

This section describes data and presents data pre-processing procedures used on the UCI data set considered in this study to develop a heart disease

Table 6.8: The description of the used clinical features

Feature name	Discription
Age	Age in years
Sex	Gender (Male,Female)
Chest pain type	TA,ATA, N-AP,Asymptomatic
Trestbps(mmHg)	Resting blood pressure
Chol(mg/dl)	Serum cholesterol
Fbs	Fasting blood sugar
Restecg	Resting electrocardiographic results
Thalach	Maximum heart rate achieved
Exang	Exercised induced angina
Oldpeak	ST depresion induced by exercise relative to rest
Slope	The slope of the peak exercise ST segment
Ca	Number of major vessels coloured by flourosopy
Thal	Normal,Fixed defect,reversible defect
Target	Absence or Presence of heart disease

prediction model using RNN that and the evaluations are conducted via extensive simulations in MATLAB.

6.4.1 Dataset Description and Pre-processing

In this study, we used Cleveland Clinic Foundation heart disease prediction dataset from the UCI machine learning repository for the experimentation [51]. In pre-processing, the used dataset comprised of 303 patient records, and the following fourteen clinical features from patients aged 29 to 79. Table 6.8 gives a detailed description of the used clinical features. We only employ binary-class in this investigation where we designate normal records as 0 and abnormal records as 1.

Furthermore, data inputs are normalized using Max-Min normalization procedure in equation 6.1 to train the RNN effectively. This is because data inputs are very large, and this would lead to unstable RNN networks, hence data are normalized in to the range of 0 to 1.

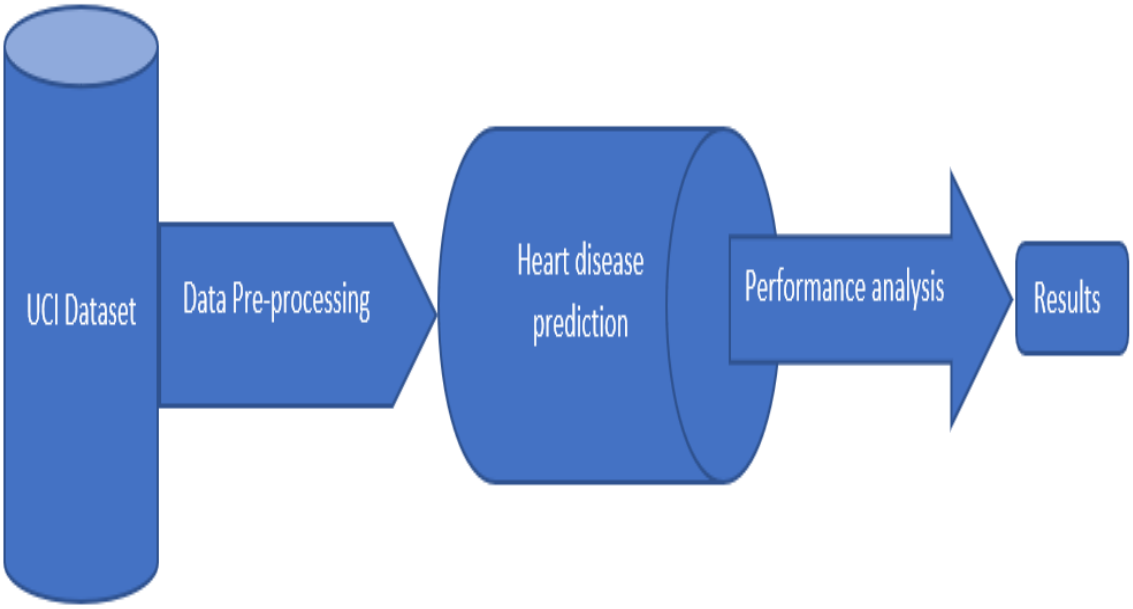

Figure 6.16: Stages of the experimentation.

6.4.2 The proposed RNN-based IoT Heart Disease Prediction Model

In this section, a heart disease prediction model is developed using RNN to predict heart diseases. RNN network architecture of one input layer, one hidden layer and one output layer are used to develop and evaluate the model. Figure 6.16 describes the steps and stages used in this study's experimentation. In this study, RNN is used via extensive simulations in MATLAB to predict heart disease using the UCI dataset, where 80% of the 303 data points is used for training and 20% for testing the developed model. With thirteen clinical features used as input layer neurons, twenty hidden layer neurons are used, and one output layer neuron is used, which predicted whether a patient had heart disease. The developed model runs k-fold and is evaluated using 0.01, 0.1, and 0.4 as learning rates.

6.4.3 Results and Performance Analysis

The performance of the developed RNN model is analysed using the confusion matrix described by the True Positive (TP), True Negative (TN), False Positive (FP), and False Negative (FN). TP presents positive occurrences with correct identification. TN describes negative instances that are correctly identified. FP is the number of positive occurrences with a false prediction. FN is the number of negative cases with a false prediction.

$$Accuracy = \frac{TP + TN}{TP + TN + FP + FN} \tag{6.3}$$

$$Sensitivity = \frac{TP}{TP + FN} \tag{6.4}$$

$$Precision = \frac{TP}{TP + FP} \tag{6.5}$$

$$Specificity = \frac{TN}{TN + FP} \tag{6.6}$$

$$F - measure = \frac{2TP}{2TP + FP + FN} \tag{6.7}$$

The classification accuracy of the used RNN algorithm in heart disease prediction is evaluated using the following commonly used performance measures. The first measure is accuracy which evaluates the performance of the used classification algorithm and is the ratio of true classified samples to the total samples as shown in equation 6.3. The second measure is sensitivity, defined as the ratio of TP samples to the sum of TP and FN, as shown in equation 6.4. The third metric is precision which measures the probability of how correct the positive prediction is made and is defined by equation 6.5. The fourth was specificity which evaluates how well the negative cases are classified and is defined as the ratio of TN samples to the sum of TN and FP, as shown in equation 6.6. F-measure was the fifth performance metric and is a system's Precision and Recall values that are harmonically averaged to provide an F-score, which can be calculated using equation 6.7.

From Figure 6.17, it is shown that the highest accuracy of 98.02% is obtained using 0.01 as the learning rate. More details on the obtained results are shown in Table 6.9.

Table 6.9: Results of the used learning rates

Learning rates	0.01	0.1	0.4
Accuracy (%)	98.02	62.29	96.08
F-measure (%)	94.99	79.00	98.00

Table 6.10: Results of the proposed system compared to results in [128]

Model	Proposed system	HRF with a linear model [128]
Accuracy	98.02%	88.47%
Sensitivity	91.06%	90.8%
Precision	96.03%	87.5%
Specificity	90%	82.6%
F-measure	94.99%	90%

In addition, Table 6.10 presents a comparative performance analysis and the developed RNN-based heart disease prediction model outperform the results obtained by Mohan et al. in [128] that also used the same Cleveland data set.

Table 6.11: Results of the proposed system compared to related work

Model	Accuracy	Method
Proposed system	98.02%	RNN
Mohan et al.[128]	88.47%	Vote
K. Baby and S. Priya [130]	86.1%	HRF with a linear model
Rindhe et al.[129]	84.0%	Support vector classifier

Furthermore, it is evident that the obtained results show a higher level prediction accuracy of 98.02% when compared to recent related work results in [128], [130], and in [129] that used the same Cleveland data set as shown in Table 6.11.

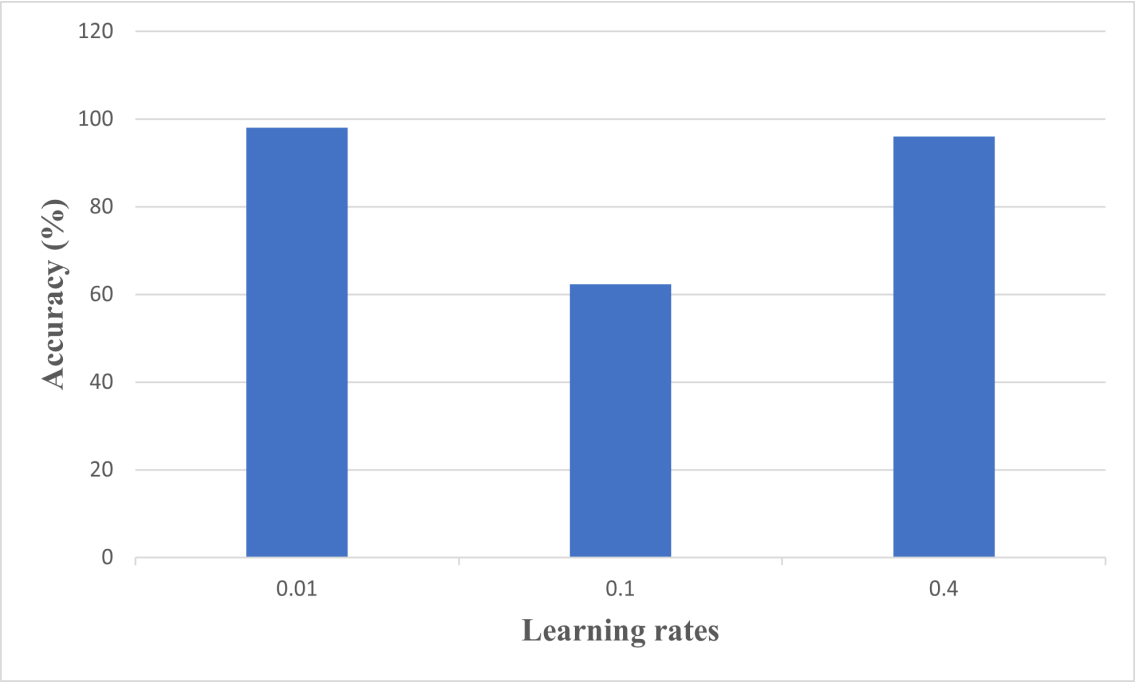

Figure 6.17: Results of the used performance metric for the used learning rates.

Chapter 7

Conclusions, Limitations, and Future Work

This chapter summarises the conclusions and limitations of studies done in this thesis. Finally, open research challenges recommended from this thesis to be further investigated are also discussed.

7.1 Conclusions

In this section, we summarize the obtained results and observations for the performance of LoRaWAN propagation models in an urban environment, LoRaWAN scalability for IoT RHM in dense urban areas, and the developed RNN-based IoT models.

7.1.1 Performance of LoRaWAN Propagation Models

In chapter 4, ATDI ICS Telecom simulator is used to evaluate and analyse LoRaWAN radio coverage at 868MHz. Four propagation models are used in Glasgow city center: Okumura-Hata, COST 231 Hata, Extended Hata, and ITU R 1225. Comparisons are made between real-world test measurements made with a LoRa transceiver while moving at a brisk pace and the simulation outputs of four distinct propagation models. While ITU R 1225 and the Extended Hata models have overestimated the real-world measured signal power, COST-231 Hata and the Okumura-Hata models have underestimated the received signal strength values. The highest accurate propagation model

is ITU R 1225 with a minimum MAE of 1.13 dBm and a S of 5.49 dBm; the minimum diversion from the real-world measured received signal strength data. The Extended Hata model has the most significant deviation from the real-world data among the four analysed models, with a MAE of 1.82 dBm and a S of 9.19 dBm; hence, the least accurate propagation model. Our findings also show that the Okumura-Hata and COST-231 Hata models' performance is similar for LoRaWAN networks in Glasgow city. Our findings offer important new information about the accuracy and performance of the four LoRaWAN propagation models, which should be considered before any LoRaWAN IoT end device deployment in any urban environment.

7.1.2 LoRaWAN Scalability Analysis

In chapter 5, we investigate LoRaWAN network scalability in terms of ATD of three gateways due to uplink interference as the number of end nodes increased. We develop a detailed network simulation model for fixed and mobile end nodes using blood pressure remote health traffic requirements in ICS Telecom simulator for the urban area of 3.5 km^2 of Glasgow city. The obtained simulation results confirm the increase of average TD for three gateways to be higher with an increasing number of mobile end nodes than with fixed end nodes. Similarly, the average TD increase of three gateways with a rising number of mobile end nodes varies with time due to the mobility effect of the end nodes. These results establish a primary study for the uplink connectivity analysis of the end nodes to any of the three gateways. Also, our results shed light on LoRaWAN scalability potentials and planning of LoRaWAN deployments with sufficient fade margins to support the obtained TD values and avoid network outage for remote healthcare applications in an urban scenario.

7.1.3 LoRa RSSI based Outdoor Node Localization System

In chapter 6, we first develop an outdoor localization system based on LoRa RSSI using Random Neural Networks. The performance of our localization model is assessed using data collected in Glasgow city's urban area using three RNN architectures with 0.01, 0.1, and 0.4 as learning rates; the proposed model works optimally with a minimum mean localization error of 0.39 m. Also, the examined RNN-based localization system architectures reveal

that no system improvement with increasing the number of hidden neurons except with the highest learning rate of 0.4. Our findings provide valuable information about LoRaWAN and RNN in localization systems and confirm LoRaWAN and RNN to be highly accurate for outdoor localization in urban areas.

7.1.4 Outdoor Node Localization System for Large Scale Urban IoT Networks

Secondly, we develop an RNN-based LoRa RSSI-based localization system. The proposed method evaluates the performance of the proposed RNN-LoRa RSSI-based localization system in a large dense urban of Antwerp city, Belgium, using 0.001, 0.01, 0.1 learning rates and 1000, 3000, 5000, and 10 000 data samples. The proposed localization model is trained using learning rates of 0.001, 0.01, 0.1, and 1, and data samples of 1000, 3000, 5000, 10,000, and 130,343 are used to examine the performance of our model with the minimum training time. Additionally, the proposed system is evaluated and achieves a minimum mean localization error of 0.29 m through thorough simulations and analysis.

7.1.5 LoRaWAN based Indoor Localization System

Furthermore, we propose a LoRaWAN- RNN-based localization model and analyse its performance and accuracy in an indoor environment in both LOS and NLOS. We use learning rates of 0.0002, 0.002, 0.02, 0.2, and 2 as well as 8, 16, and 20 hidden neurons. RNN network architecture with a learning rate of 0.2 and 20 hidden neurons has obtained a minimum average localization error of 0.12 m which is 99.52% accurate in LOS. Additionally, the developed model performs better than others in already published studies in the literature with the minimum average localization error in LOS. The results demonstrate that the developed LoRaWAN-based indoor localization model with RNN outperform the existing models in LOS indoor scenarios and can be used in large indoor sports halls or fields, large hospital wards, shopping malls, airports, and several other locations. In addition, a minimum localization error of 13.4 m with an accuracy of 44.24% in the NLOS is obtained. This can be used in intelligent auto parking applications in indoor car parks to ensure that any vehicle can be located or routed inside an industrial facility. Furthermore, it may be used to control and prevent theft by keeping a

fleet of vehicles within a restricted region in an NLOS interior environment by sending an alert if any vehicle is moved.

7.1.6 Heart Disease Prediction System

Finally, this study develops a novel RNN-based heart disease prediction model to predict heart disease using fourteen selected clinical attributes of the Cleveland data set. The proposed model achieved a prediction accuracy of 98.02% and outperformed heart disease prediction models in recent related works that have used the same UCI dataset.

7.2 Limitations

This section describes some of the limitations of this research study:

- Due to working in lockdown times and other unpredicted difficulties that came as a result of Covid 19 pandemic in 2020, the fieldwork data collection part was redesigned where pre-planned field test measurements using remote healthcare sensors could not be done and could have been used to develop a more informed and validated LoRaWAN based IoT RHM model using RNN. Moreover, data analysis part took longer than expected.
- A small dataset collected in indoor analysis may not have been enough to develop an accurate RNN-based indoor localization model.
- Mostly used research tools do not support the LoRaWAN protocol.
- A wider area of coverage could have been considered for LoRaWAN and RNN performance in indoor environments.
- Only fixed LoRaWAN gateways have been considered in this study.
- Only uplink connectivity analysis has been considered in this study.

7.3 Future Work

According to all the discussions in the chapters discussed before, it is evident that there are still some technical and practical issues that remain and

require further research. The following directions could be taken as future recommendations from the evaluations made; the performance of LoRaWAN propagation models, LoRaWAN scalability analysis for RHM applications, and RNN-based IoT intelligent systems:

- A study of LoRaWAN coverage with more LoRaWAN gateways and analysing the effects of various parameter settings of physical layer LoRa technology is essential to characterize the performance of LoRaWAN further. Moreover, the contributions of this thesis only considered the evaluations of the performance of four of the LoRaWAN propagation models. However, analysing other models would be a further crucial contribution. Furthermore, analysing the performance of LoRaWAN propagation models in suburban and rural environments is also a vital contribution for further understanding of LoRaWAN performance in other environments apart from urban areas.

- Analysing the impact of the average TD of the used three LoRaWAN gateways on the uplink connectivity of the end nodes to understand LoRaWAN connectivity further is essential and is proposed as a further investigation recommended in this study. Moreover, the minimum allowed threshold needs to be determined according to different IoT applications. Also, considering analysing more gateways would be necessary for more extensive networks. Again, using real-world measurements would be better for appropriate real-world estimations. Evaluations in suburban and rural environments could also lead to a further understanding of LoRaWAN scalability in different scenarios. Again, analysing LoRaWAN scalability for other IoT applications would lead to optimal exploitation of LoRaWAN potentials.

- Comparative performance analysis of the developed localization model to existing localization models found in literature is recommended for further analysis of the developed LoRa-RNN localization model in a small-scale urban environment. Moreover, this study also recommend evaluating the same model in suburban and rural environments for further exploration.

- Furthermore, we suggest adopting a different set of parameters in a future study to simulate the suggested system to achieve better NLOS performance. Additionally, we recommend comparing the developed

system's performance to other methods and assessing the impact of multi-path reflections of LoRaWAN signals in an NLOS indoor setting.

- In addition, we recommend considering using a new selection of clinical features different to what is used in this study to improve the prediction accuracy of heart disease prediction.
- Finally, we also recommend evaluations in the downlink connectivity and using gateways that are not fixed which are considered in this study.

References

[1] L. K. Ramasamy and S. Kadry, "Internet of things (IoT)," Blockchain Ind. Internet Things, no. May, 2021, doi: 10.1088/978-0-7503-3663-5ch1.

[2] K. Kaur, "A Survey on Internet of Things - Architecture, Applications, and Future Trends," ICSCCC 2018 - 1st Int. Conf. Secur. Cyber Comput. Commun., pp. 581–583, 2019.

[3] A. Rahaman, M. M. Islam, M. R. Islam, M. S. Sadi, and S. Nooruddin, "Developing iot based smart health monitoring systems: A review," Rev. d'Intelligence Artif., vol. 33, no. 6, pp. 435–440, 2019, doi: 10.18280/ria.330605.

[4] Statista Says a Five-Fold Increase in Ten years in Internet-Connected Devices by 2025 Will Significantly Increase the Internet's Promise of Making the World Connected [online] Available:https://www.statista.com/ statistics/471264/iot-number-of-connected-devices-worldwide/

[5] A. I. Ahmad, B. Ray, and M. Chowdhury, Performance evaluation of loraWAN for mission-critical IOT networks, vol. 1113 CCIS. Springer International Publishing, 2019.

[6] A. U. H. Qureshi, H. Larijani, J. Ahmad, and N. Mtetwa, "A Novel Random Neural Network Based Approach for Intrusion Detection Systems,"10th Comput. Sci. Electron. Eng. Conf. CEEC 2018 - Proc., pp. 50–55, 2019.

[7] A. HUSSAIN, "ERWPM-MANET: Evaluation of Radio Wave Propagation Models in Mobile Ad hoc Network by using Distance Scenario," Rev. Română Informatică și Autom., vol. 32, no. 2, pp. 35–50, 2022, doi: 10.33436/v32i2y202203.

[8] F. R. Links, "ECC Report 260," no. January, 2017.

[9] A. Poulose, J. Kim, and D. S. Han, "A sensor fusion framework for indoor localization using smartphone sensors and Wi-Fi RSSI measurements," Appl. Sci., vol. 9, no. 20, 2019, doi: 10.3390/app9204379.

[10] N. Hunn, Introducing Bluetooth ® LE Audio. 2022.

[11] K. Disale and I. M. Report, "Zigbee Wireless Sensor Market Overview , Definition , and Statistics 2022- 2028," no. November, 2022.

[12] J. Min Kang, T. S. Yoon, E. Kim, and J. B. Park, "Lane-level map-matching method for vehicle localization using GPS and camera on a high-definition map," Sensors (Switzerland), vol. 20, no. 8, pp. 1–22, 2020.

[13] G. G. Anagnostopoulos and A. Kalousis, "A Reproducible Comparison of RSSI Fingerprinting Localization Methods Using LoRaWAN," 2019.

[14] WHO,"Cardiovascular diseases." [Online]. Available:https://www.who.int/health-topics/cardiovascular-diseases.

[15] K. Mikhaylov, "Simulation of network-level performance for Bluetooth Low Energy," IEEE Int. Symp. Pers. Indoor Mob. Radio Commun. PIMRC, vol. 2014-June, no. July, pp. 1259–1263, 2014.

[16] V. Tsira and G. Nandi, "Bluetooth Technology: Security Issues and Its Prevention," Int. J. Comput. Appl. Technol., vol. 5, no. 5, pp. 1833–1837, 2014.

[17] A. A. A. Elsabaa, M. Ward, and W. Wu, "Hybrid localization techniques in lora-based WSN," ICAC 2019 - 2019 25th IEEE Int. Conf. Autom. Comput., no. September, pp. 1–5, 2019.

[18] D. Bankov and E. Khorov, "Performance Comparison of NB-Fi, Sigfox, and LoRaWAN," 2022.

[19] X. Xia, Q. Chen, N. Hou, and Y. Zheng, HyLink: Towards High Throughput LPWANs with LoRa Compatible Communication, vol. 1, no. 1, 2022. Association for Computing Machinery.

[20] N. C. Gaitan and F. Pitu, "The Implementation of a Solution for Low-Power Wide-Area Network using LoRaWAN," vol. 13, no. 6, pp. 443–448, 2022.

[21] I. A. Kamanga and J. M. Lyimo, "Review of LoRAWAN and the protocol suitability for low bandwidth wireless sensor networks over 5G," 2022.

[22] A. Ikpehai et al., "Low-power wide area network technologies for internet-of-things: A comparative review," IEEE Internet Things J., vol. 6, no. 2, pp. 2225–2240, 2019.

[23] K. Mekki, E. Bajic, F. Chaxel, and F. Meyer, "Overview of Cellular LPWAN Technologies for IoT Deployment: Sigfox, LoRaWAN, and NB-IoT," 2018 IEEE Int. Conf. Pervasive Comput. Commun. Work. PerCom Work. 2018, pp. 197–202, 2018.

[24] R. S. Sinha, Y. Wei, and S. H. Hwang, "A survey on LPWA technology: LoRa and NB-IoT," ICT Express, vol. 3, no. 1, pp. 14–21, 2017.

[25] SIGFOX, "The Global Communications Service Provider." [Online]. Available: https://www.sigfox.com/en.

[26] Sigfox, "Sigfox Technologies: Learn more about this IOT protocol." [Online]. Available:https://enless-wireless.com/en/sigfox-iot-network/.

[27] WEIGHTLESS, "WIGHTLESS LPWAN." [Online]. Available: https://www.weightless-alliance.org/.

[28] INGENU, "Technology-Ingenu," [Online]. Available: https://www.ingenu.com/technology/.

[29] LoRaWAN Specification v1.1. Available Online: https://lora-alliance.org/about-lorawan/

[30] H. H. R. Sherazi, G. Piro, L. A. Grieco, and G. Boggia, "When Renewable Energy Meets LoRa: A Feasibility Analysis on Cable-Less Deployments," IEEE Internet Things J., vol. 5, no. 6, pp. 5097–5108, 2018.

[31] L. C. C. By, S. Date, P. Date, C. Wu, L. L. L. M. Network, and L. E. Sensing, "A Low-Cost Low-Power LoRa Mesh Network for Large-Scale Environmental Sensing," pp. 0–15, 2022, doi: 10.36227/techrxiv.20365050.v1

[32] A. M. Yousuf, E. M. Rochester, B. Ousat, and M. Ghaderi, "Throughput, Coverage and Scalability of LoRa LPWAN for Internet of Things," IEEE/ACM Int. Symp. Qual. Serv., 2018.

[33] I. Butun, N. Pereira, and M. Gidlund, "Analysis of LoRaWAN v1.1 security," no. June, pp. 1–6, 2018.

[34] S. Robson and M. Haddad, "Robust Power Line Communication," no. Mv, pp. 1–8, 2021.

[35] W. W. Ii, "Fundamentals of spread-spectrum techniques," pp. 153–194.

[36] LoRa, "LoRa ISM Frequencies," [Online]. Available: https://lora.readthedocs.io/en/latest/.

[37] M. Šval, "Impact of Threshold Degradation on Availability of Digital Vpliv degradacije praga sprejema na razpoložljivost digitalnih fiksnih radijskih zvez," no. January 2014.

[38] ATDI ICS Telecom, available online at https://www.atdi.com, /ics-telecom.

[39] M. Prgomet et al., "Vital signs monitoring on general wards: Clinical staff perceptions of current practices and the planned introduction of continuous monitoring technology," Int. J. Qual. Heal. Care, vol. 28, no. 4, pp. 515–521, 2016.

[40] E.Gelenbe, "Random Neural Networks with Negative and Positive Signal and Product Form Solution."

[41] Cerkez, C., Aybay, I., and Halici, U. (1997). A digital neuron realization for the random neural network model. In International Conference on Neural Networks, 1997. (pp. 1000–1004). IEEE volume 2.

[42] Abdelbaki, H., Gelenbe, E., and El-Khamy, S. E. (2000). Analog hardware implementation of the random neural network model. In Proceedings of the IEEE-INNS-ENNS International Joint Conference on Neural Networks, 2000. IJCNN 2000 (pp. 197–201). IEEE volume 4.

[43] Abdelbaki, H. (1999). Random neural network simulator (rnnsim) v. 2. Free simulator available at ftp://ftp. mathworks. com/pub/contrib/ v5/nnet/rnnsimv2.

[44] Mohamed, S., and Rubino, G. (2002). A study of real-time packet video quality using random neural networks. IEEE Transactions on Circuits and Systems for Video Technology, 12, 1071–1083.

[45] J. Ahmad, H. Larijani, R. Emmanuel, M. Mannion, A. Javed, and M. Phillipson, "Energy demand prediction through novel random neural network predictor for large non-domestic buildings," 11th Annu. IEEE Int. Syst. Conf. SysCon 2017 - Proc., pp. 1–6, 2017.

[46] P. Richter and M. Toledano-Ayala, "Ubiquitous and Seamless Localization: Fusing GNSS Pseudoranges and WLAN Signal Strengths," Mob. Inf. Syst., vol. 2017, 2017.

[47] I. Daramouskas, V. Kapoulas, and T. Pegiazis, "A survey of methods for location estimation on Low Power Wide Area Networks," 10th Int. Conf. Information, Intell. Syst. Appl. IISA 2019, pp. 2019–2022, 2019.

[48] N. Podevijn et al., "TDoA-based outdoor positioning in a public LoRa network," IET Conf. Publ., vol. 2018, no. CP741, 2018.

[49] N. Podevijn et al., "TDoA-Based Outdoor Positioning with Tracking Algorithm in a Public LoRa Network," Wirel. Commun. Mob. Comput., vol. 2018, 2018.

[50] W. Choi, Y. S. Chang, Y. Jung, and J. Song, "Low-power LORa signal-based outdoor positioning using fingerprint algorithm," ISPRS Int. J. Geo-Information, vol. 7, no. 11, pp. 1–15, 2018.

[51] University of California,Irvine "UCI Machine Learning Repository." https://archive.ics.uci.edu /ml/datasets/Heart+Disease.

[52] Mollel, Michael Kisangiri, Michael."Comparison of Empirical Propagation Path Loss Models for Mobile Communication". Computer Engineering and Intelligent Systems. Vol.5.no.9, pp.1-10,2014.

[53] El Chall, Rida Lahoud, Samer El Helou, Melhem. (2019). LoRaWAN Network: Radio Propagation Models and Performance Evaluation in Various Environments in Lebanon. IEEE Internet of Things Journal. PP. 1-1. 10.1109/JIOT.2019.2906838.

[54] Souza Bezerra, Nibia Åhlund, Christer Saguna, Saguna Jr, Vicente. (2019). Propagation Model Evaluation for LoRaWAN: Planning Tool Versus Real Case Scenario. IEEE 5th World Forum on Internet of Things.10.1109/WF-IoT.2019.8767299.

[55] R. Sanchez-Iborra, J. Sanchez-Gomez, J. Ballesta-Vi˜nas, M.-D. Cano, and A. F. Skarmeta, "Performance evaluation of lora considering scenario conditions," Sensors, vol. 18, no. 3, p. 772, 2018.

[56] E.Harinda, H. Larijani, and R. Gibson, "Comparative Performance Analysis of Empirical Propagation Models for LoRaWAN 868MHz in an Urban Scenario," in IEEE 5th World Forum on Internet of Things, 2019.

[57] Augustin, J. Yi, T. Clausen, and W. M. Townsley, "A study of lora: Long range low power networks for the internet of things," Sensors, vol. 16, no. 9, p. 1466, 2016.

[58] L. Feltrin, C. Buratti, E. Vinciarelli, R. De Bonis, and R. Verdone, "Lorawan: Evaluation of link-and system-level performance," IEEE Internet of Things Journal, 2018.

[59] S. Hosseinzadeh, H. Larijani, and K. Curtis, "An enhanced modified multi wall propagation model," in Global Internet of Things Summit (GIoTS), 2017. IEEE, 2017, pp. 1–4.

[60] S. Hosseinzadeh, M. Almoathen, H. Larijani, and K. Curtis, "A neural network propagation model for lorawan and critical analysis with real-world measurements," Big Data and Cognitive Computing, vol. 1, no. 1, p. 7, 2017.

[61] U. Gogate and J. Bakal, "Healthcare Monitoring System Based on Wireless Sensor Network for Cardiac Patients," Biomed. Pharmacol. J., vol. 11, no. 3, pp. 1681–1688, 2018.

[62] J. Ma, H. Nguyen, F. Mirza, and O. Neuland, "Two Way Architecture Between Iot Sensors and Cloud Computing for Remote Health Care Monitoring Applications," Twenty-Fifth Eur. Conf. Inf. Sytem (ECIS), Guilmaraes, Port., vol. 2017, pp. 2834–2841, 2017.

[63] P.M.Reddy and N.Ome, "IoT Based Health Monitoring and Alert System using ARM7," vol. 05, no. 09, pp. 1888–1891, 2017.

[64] P.Kaviya and Antony Seba "Intelligent Healthcare Monitoring in IoT," Int. J. Adv. Eng. Manag. Sci., vol. 4, no. 6, pp. 441–445, 2018.

[65] H. Malik, M. M. Alam, Y. Le Moullec, and A. Kuusik, "NarrowBand-IoT Performance Analysis for Healthcare Applications," Procedia Comput. Sci., vol. 130, pp. 1077–1083, 2018.

[66] H. Zhang, J. Li, B. Wen, Y. Xun, and J. Liu, "Connecting intelligent things in smart hospitals using NB-IoT," IEEE Internet Things J., vol. 5, no. 3, pp. 1550–1560, 2018.

[67] F. Wu, T. Wu, and M. R. Yuce, "An internet-of-things (IoT) network system for connected safety and health monitoring applications," Sensors (Switzerland), vol. 19, no. 1, 2019.

[68] L. Wu, C. H. Chen, and Q. Zhang, "A mobile positioning method based on deep learning techniques," Electron., vol. 8, no. 1, pp. 11–15, 2019.

[69] R. K. Pathinarupothi, P. Durga, and E. S. Rangan, "IoT-based smart edge for global health: Remote monitoring with severity detection and alerts transmission," IEEE Internet Things J., vol. 6, no. 2, pp. 2449–2462, 2019.

[70] M. M. Alam, H. Malik, M. I. Khan, T. Pardy, A. Kuusik, and Y. Le Moullec, "A survey on the roles of communication technologies in IoT-Based personalized healthcare applications," IEEE Access, vol. 6, pp. 36611–36631, 2018.

[71] J. Petäjäjärvi et al., "Evaluation of LoRa LPWAN Technology for Indoor Remote Health and Wellbeing Monitoring," IJWIN, vol. 24, pp. 153–165, 2017.

[72] J. Kharel, H. T. Reda, and S. Y. Shin, "An architecture for smart health monitoring system based on fog computing," J. Commun., vol. 12, no. 4, pp. 228–233, 2017.

[73] J. Kharel, H. T. Reda, and S. Y. Shin, "Fog Computing-Based Smart Health Monitoring System Deploying LoRa Wireless Communication," IETE Tech. Rev. (Institution Electron. Telecommun. Eng. India), vol. 36, no. 1, pp. 69–82, 2019.

[74] A. Mdhaffar, T. Chaari, K. Larbi, M. Jmaiel, and B. Freisleben, "IoT-based health monitoring via LoRaWAN," 17th IEEE Int. Conf. Smart Technol. EUROCON 2017 - Conf. Proc., no. July, pp. 519–524, 2017

[75] N. Hayati and M. Suryanegara, "The IoT LoRa system design for tracking and monitoring patient with mental disorder," 2017 IEEE Int. Conf. Commun. Networks Satell. COMNETSAT 2017 - Proc., vol. 2018-Janua, no. October, pp. 135–139, 2018

[76] P. A. Catherwood, D. Steele, M. Little, S. McComb, and J. McLaughlin, "A Community-Based IoT Personalized Wireless Healthcare Solution Trial," IEEE J. Transl. Eng. Heal. Med., vol. 6, no. May, pp. 1–13, 2018.

[77] O. Georgiou and U. Raza.Low Power Wide Area Network Analysis:Can LoRa Scale, vol. 6, no. 2, pp. 162-165, 2017.

[78] K. Mikhaylov, M. Pettissalo, and J. Peta, "Performance of a low-power wide-area network based on LoRa technology: Doppler robustness , scalability , and coverage," vol. 13, no. 3, 2017.

[79] J. Haxhibeqiri, F. Van den Abeele, I. Moerman, and J. Hoebeke, "LoRa scalability: A simulation model based on interference measurements," Sensors (Switzerland), vol. 17, no. 6, 2017.

[80] F. Van Den Abeele, J. Haxhibeqiri, I. Moerman, and J. Hoebeke, "Scalability Analysis of Large-Scale LoRaWAN Networks in ns-3," vol. 4, no. 6, pp. 2186–2198, 2017.

[81] V. Popa, "Performance Evaluation of LoRaWAN Communication Scalability in Large-Scale Wireless Sensor Networks," vol. 2018, 2018.

[82] N. Varsier and J. Schwoerer, "Capacity limits of LoRaWAN technology for smart metering applications," in IEEE International Conference on Communications, 2017.

[83] J. Finnegan, S. Brown, and R. Farrell, "Evaluating the Scalability of LoRaWAN Gateways for Class B Communication in ns-3," 2018 IEEE Conf. Stand. Commun. Netw., pp. 1–6, 2018.

[84] J. Haxhibeqiri, I. Moerman, and J. Hoebeke, "Low Overhead Scheduling of LoRa Transmissions for Improved Scalability," IEEE Internet Things J., vol. 6, no. 2, pp. 3097–3109, 2019.

[85] D. Zorbas, G. Z. Papadopoulos, P. Maille, N. Montavont, and C. Douligeris, "Improving LoRa Network Capacity Using Multiple Spreading Factor Configurations."

[86] A. Mahmood, E. Sisinni, L. Guntupalli, R. Rondon, S. A. Hassan, and M. Gidlund, "Scalability Analysis of a LoRa Network under Imperfect Orthogonality," IEEE Trans. Ind. Informatics, vol. 15, no. 3, pp. 1425–1436, 2019.

[87] B. Reynders et al., "Improving Reliability and Scalability of LoRaWANs Through Lightweight Scheduling," IEEE Internet Things J., vol. 5, no. 3, pp. 1830–1842, 2018.

[88] K. Mikhaylov, J. Petäjäjärvi, and J. Janhunen, "On LoRaWAN Scalability: Empirical Evaluation of Susceptibility to Inter-Network Interference," pp. 0–5, 2017.

[89] A. Tiurlikova, N. Stepanov, and K. Mikhaylov, "Method of assigning spreading factor to improve the scalability of the LoRaWAN wide area network," 2018 10th Int. Congr. Ultra Mod. Telecommun. Control Syst. Work., pp. 1–4, 2018.

[90] J. Lee and W. Jeong, "A Scheduling Algorithm for Improving Scalability of LoRaWAN," 2018 Int. Conf. Inf. Commun. Technol. Converg., pp. 1383–1388, 2018.

[91] A. Javed, H. Larijani, A. Ahmadinia, R. Emmanuel, M. Mannion, and D. Gibson, "Design and Implementation of a Cloud Enabled Random Neural Network-Based Decentralized Smart Controller with Intelligent Sensor Nodes for HVAC," IEEE Internet Things J., vol. 4, no. 2, pp. 393–403, 2017.

[92] A. Javed, H. Larijani, A. Wixted, and R. Emmanuel, "Random neural networks based cognitive controller for HVAC in non-domestic building using LoRa," Proc. 2017 IEEE 16th Int. Conf. Cogn. Informatics Cogn. Comput. ICCI*CC 2017, pp. 220–226, 2017.

[93] A. Javed, H. Larijani, A. Ahmadinia, and D. Gibson, "Smart Random Neural Network Controller for HVAC Using Cloud Computing Technology," IEEE Trans. Ind. Informatics, vol. 13, no. 1, pp. 351–360, 2017.

[94] K. Simonyan and A. Zisserman, "Very deep convolutional networks for large-scale image recognition," 3rd Int. Conf. Learn. Represent. ICLR 2015 - Conf. Track Proc., pp. 1–14, 2015.

[95] A. U. H. Qureshi, H. Larijani, A. Javed, N. Mtetwa, and J. Ahmad, "Intrusion Detection Using Swarm Intelligence," 2019 UK/China Emerg. Technol. UCET 2019, pp. 1–5, 2019.

[96] A. U. H. Qureshi, H. Larijani, N. Mtetwa, A. Javed, and J. Ahmad, "RNN-ABC: A new swarm optimization based technique for anomaly detection," Computers, vol. 8, no. 3, 2019.

[97] Tahir, A.; Ahmad, J.; Morison, G.; Larijani, H.; Gibson, R.M.; Skelton, D.A. Hrnn4f: Hybrid deep random neural network for multi-channel fall activity detection. Probab. Eng. Inf. Sci. 2021, 35, 37–50. [CrossRef]

[98] Shah, S.Y.; Larijani, H.; Gibson, R.; Liarokapis, D. A Novel Random Neural Network-based Fall Activity Recognition. In Proceedings of the 2020 International Conference on UK-China Emerging Technologies (UCET), Glasgow, UK, 20–21 August 2020; pp. 1–4.

[99] A. Mackey and P. Spachos, "LoRa-based Localization System for Emergency Services in GPS-less Environments," INFOCOM 2019 - IEEE Conf. Comput. Commun. Work. INFOCOM WKSHPS 2019, pp. 939–944, 2019.

[100] I. Daramouskas, V. Kapoulas, and M. Paraskevas, "Using Neural Networks for RSSI Location Estimation in LoRa Networks," 10th Int. Conf. Information, Intell. Syst. Appl. IISA 2019, pp. 1–7, 2019.

[101] G. Bhatti, "Machine learning based localization in large-scale wireless sensor networks," Sensors (Switzerland), vol. 18, no. 12, 2018.

[102] G. Y. Ha, S. B. Seo, H. S. Oh, and W. S. Jeon, "LoRa ToA-Based Localization," 2019 Int. Conf. Inf. Commun. Technol. Converg., pp. 349–353, 2019.

[103] B. C. Fargas and M. N. Petersen, "GPS-free geolocation using LoRa in low-power WANs," GIoTS 2017 - Glob. Internet Things Summit, Proc., 2017.

[104] M. W. B, E. Verreyken, and J. Steckel, "on FPGA for Robotic Behaviour," vol. 1, no. November, pp. 694–703, 2020. R. Samanta, C. Kumari, N. Deb, S. Bose, A. Cortesi, and N. Chaki, "Node localization for indoor tracking using artificial neural network," 2018 3rd Int. Conf. Fog Mob. Edge Comput. FMEC 2018, no. April, pp. 229–233, 2018.

[105] T. Bhatnagar, "Application of Artificial Intelligence and Low- Power Wide-Area Network (LPWAN) in the development of Smart Cities," vol. 6, no. Ii, pp. 1386–1389, 2018.

[105] C. Gu and R. Tan, "LoRa-Based Localization: Opportunities and Challenges LoRa-Based Localization: Opportunities and Challenges," no. January, 2019.

[106] Z. Yi, J. Zhao, Z. Zhang, and M. Kong, "Neural Network Based Prediction and Analysis for NB-IoT Network Location," 2019 11th Int. Conf. Wirel. Commun. Signal Process. WCSP 2019, pp. 1–5, 2019.

[107] X. Ye, X. Yin, X. Cai, A. Perez Yuste, and H. Xu, "Neural-Network-Assisted UE Localization Using Radio-Channel Fingerprints in LTE Networks," IEEE Access, vol. 5, no. December, pp. 12071–12087, 2017.

[108] G. Bhatti, "Machine learning based localization in large-scale wireless sensor networks," Sensors (Switzerland), vol. 18, no. 12, 2018.

[109] H. Sallouha, A. Chiumento, S. Rajendran, and S. Pollin, "Localization in Ultra Narrow Band IoT Networks: Design Guidelines and Tradeoffs," IEEE Internet Things J., vol. 6, no. 6, pp. 9375–9385, 2019.

[110] A. B. Adege, H. P. Lin, G. B. Tarekegn, and S. S. Jeng, "Applying deep neural network (DNN) for robust indoor localization in multi-building environment," Appl. Sci., vol. 8, no. 7, pp. 1–14, 2018.

[111] B. Xu, X. Zhu, and H. Zhu, "An efficient indoor localization method based on the long short-term memory recurrent neuron network," IEEE Access, vol. 7, pp. 123912–123921, 2019.

[112] M. T. Hoang, B. Yuen, X. Dong, T. Lu, R. Westendorp, and K. Reddy, "Recurrent Neural Networks for Accurate RSSI Indoor Localization," IEEE Internet Things J., vol. 6, no. 6, pp. 10639–10651, 2019.

[113] N. Abdul, K. Zghair, M. S. Croock, A. Abdul, and R. Taresh, "Indoor Localization System Using Wi-Fi Technology," Iraqi J. Comput. Commun. Control Syst. Eng., no. April, pp. 69–77, 2019.

[114] N. Hernández, M. Ocaña, J. M. Alonso, and E. Kim, "Continuous space estimation: Increasingwifi-based indoor localization resolution without increasing the site-survey effort," Sensors (Switzerland), vol. 17, no. 1, 2017.

[115] T. Janssen, M. Weyn, and R. Berkvens, "Localization in low power wide area networks using wi-fi fingerprints," Appl. Sci., vol. 7, no. 9, 2017.

[116] F. Zafari, A. Gkelias, and K. K. Leung, "A Survey of Indoor Localization Systems and Technologies," IEEE Commun. Surv. Tutorials, vol. 21, no. 3, pp. 2568–2599, 2019.

[117] S. Sadowski and P. Spachos, "RSSI-Based Indoor Localization with the Internet of Things," IEEE Access, vol. 6, pp. 30149–30161, 2018, doi: 10.1109/ACCESS.2018.2843325.

[118] H. Kwasme and S. Ekin, "RSSI-Based Localization Using LoRaWAN Technology," IEEE Access, vol. 7, pp. 99856–99866, 2019.

[119] M. Anjum, M. A. Khan, S. Ali Hassan, A. Mahmood, and M. Gidlund, "Analysis of RSSI fingerprinting in LoRa networks," 2019 15th Int. Wirel. Commun. Mob. Comput. Conf. IWCMC 2019, no. June, pp. 1178–1183, 2019, doi: 10.1109/IWCMC.2019.8766468.

[120] Y. C. Lin, C. C. Sun, and K. T. Huang, "RSSI Measurement with Channel Model Estimating for IoT Wide Range Localization using LoRa Communication," Proc. - 2019 Int. Symp. Intell. Signal Process. Commun. Syst. ISPACS 2019, pp. 5–6, 2019.

[121] E. Goldoni, L. Prando, A. Vizziello, P. Savazzi, and P. Gamba, "Experimental data set analysis of RSSI-based indoor and outdoor localization in LoRa networks," Internet Technol. Lett., vol. 2, no. 1, p. e75, 2019.

[122] M. Aernouts, R. Berkvens, K. Van Vlaenderen, and M. Weyn, "Sigfox and LoRaWAN datasets for fingerprint localization in large urban and rural areas," Data, vol. 3, no. 2, pp. 1–15, 2018.

[123] K. H. Lam, C. C. Cheung, and W. C. Lee, "LoRa-based localization systems for noisy outdoor environment," Int. Conf. Wirel. Mob. Comput. Netw. Commun., vol. 2017-Octob, pp. 278–284, 2017.

[124] K. H. Lam, C. C. Cheung, and W. C. Lee, "RSSI-Based LoRa Localization Systems for Large-Scale Indoor and Outdoor Environments," IEEE Trans. Veh. Technol., vol. 68, no. 12, pp. 11778–11791, 2019.

[125] I. A. Zriqat, A. M. Altamimi, and M. Azzeh, "A Comparative Study for Predicting Heart Diseases Using Data Mining Classification Methods," vol. 14, no. 12, pp. 868–879, 2017, [Online]. Available: http://arxiv.org/abs/1704.02799.

[126] B. Fida, M. Nazir, N. Naveed, and S. Akram, "Heart disease classification ensemble optimization using Genetic algorithm," Proc. 14th IEEE Int. Multitopic Conf. 2011, INMIC 2011, pp. 19–24, 2011, doi: 10.1109/INMIC.2011.6151471.

[127] A. Pandey et al., "A Heart Disease Prediction Model using Decision Tree," IOSR J. Comput. Eng., vol. 12, no. 6, pp. 83–86, 2013, doi: 10.9790/0661-1268386.

[128] S. Mohan, C. Thirumalai, and G. Srivastava, "Effective heart disease prediction using hybrid machine learning techniques," IEEE Access, vol. 7, pp. 81542–81554, 2019, doi: 10.1109/ACCESS.2019.2923707.

[129] B. U. Rindhe and M. Studies, "Heart Disease Prediction Using Machine Learning," no. May, 2021, doi: 10.48175/IJARSCT-1131.

[130] K. Baby and S. Priya, "Identifying Significant Features for Heart Disease Prediction using Data Classification Techniques," vol. 10, no. 9, pp. 313–319, 2020.

[131] M. S. S. Abadpour, Lecture Notes"- Chapter 2: Radio Wave Propagation," 2018, [Online]. Available: https://www.ihe.kit.edu/img/studium /Wave Propagation.pdf.

[132] M. Shamaas, "Introduction to LoRa Technology," no. May, 2022.

[133] M. S. Gateways, "A Fair Channel Hopping Scheme for LoRa Networks with Multiple Single-Channel Gateways," pp. 1–19, 2022.

[134] R. T. Applications, "Reducing Operational Expenses of LoRaWAN-Based Internet of Remote Things Applications," pp. 1–18, 2022.

[135] Y. A. Al-gumaei, N. Aslam, M. Aljaidi, A. Al-saman, and A. Alsarhan, "A Novel Approach to Improve the Adaptive-Data-Rate Scheme for IoT LoRaWAN," pp. 1–12, 2022.

[136] Q. Qian, L. Shu, Y. Leng, and Z. Bao, "LoRaWAN Network Downlink Routing Control Strategy Based on the SDN Framework and Improved ARIMA Model," 2022.

[137] Z. Zhao, W. Gao, S. Member, W. Du, and G. Min, "IEEE Transactions on Mobile Computing Towards Energy-Fairness in LoRa Networks," 2022.

[138] Y. Singh, "Comparison of Okumura , Hata and COST-231 Models on the Basis of Path Loss and Signal Strength," vol. 59, no. 11, pp. 37–41, 2012.

[139] "Manual Propagation Models Extended Hata: Hata-and-HataSRD-implementation.pdf," 2013 [Online]. Available: http:// tractool.seamcat.org/wiki/Manual/PropagationModels/Extended-Hata.

[140] ITU-R M.1225, " Guide lines for Evaluation of Radio Transmission Technology for IMT-200", 1997. [Online]. Available: https://www.itu.int/rec/R-REC-M.1225/en.

[141] A. J. Wixted, P. Kinnaird, H. Larijani, A. Tait, A. Ahmadinia, and N. Strachan, "Evaluation of LoRa and LoRaWAN for wireless sensor networks," Proc. IEEE Sensors, vol. 0, pp. 5–7, 2017.

[142] L. P. Malasinghe, N. Ramzan, and K. Dahal, "Remote patient monitoring: a comprehensive study," J. Ambient Intell. Humaniz. Comput., vol. 10, no. 1, pp. 57–76, 2019.

[143] L. P. Malasinghe, N. Ramzan, and K. Dahal, "Remote patient monitoring: a comprehensive study," J. Ambient Intell. Humaniz. Comput., vol. 10, no. 1, pp. 57–76, 2019.

[144] M. Weenk, H. Van Goor, M. Van Acht, L. J. L. P. G. Engelen, T. H. Van De Belt, and S. J. H. Bredie, "A smart all-in-one device to measure vital signs in admitted patients," PLoS One, vol. 13, no. 2, pp. 1–12, 2018.

[145] D. Bissett, "Analysing tdoa localisation in LoRa networks," Delft University of Technology, 2018.

[146] J. N. Purohit and X. Wang, "LoRa based Localization using Deep Learning Techniques," p. 2019, "California State University", 2019.

[147] F. Bonafini et al., "Evaluating indoor and outdoor localization services for LoRaWAN in Smart City applications," pp. 300–305, 2019.

[148] H. Du, C. Zhang, Q. Ye, W. Xu, P. L. Kibenge, and K. Yao, "A hybrid outdoor localization scheme with high-position accuracy and low-power consumption," Eurasip J. Wirel. Commun. Netw., vol. 2018, no. 1, 2018, doi: 10.1186/s13638-017-1010-4.

[149] M. Anjum, M. A. Khan, S. A. Hassan, A. Mahmood, and H. K. Qureshi, "RSSI Fingerprinting-based Localization Using Machine Learning in LoRa Networks," June, 2020.

[150] A. Shokry, M. Torki, M. Youssef, "DeepLoc: A Ubiquitous Accurate and Low-Overhead Outdoor Cellular Localization System," 2021, pp. 27–29.

[151] T. Janssen, M. Aernouts, R. Berkvens, and M. Weyn, "Outdoor Fingerprinting Localization using Sigfox," no. September, 2018, doi: 10.1109/IPIN.2018.8533826.

[152] T. A. Nguyen, "LoRa Localisation in Cities with Neural Networks," p. 71,"Delft University of Technology", 2019.

[153] Multitech, "Portable, Handheld End-Point Device for Conducting LoRa® Site Surveys (MTDOT-BOX Series)," [Online]. Available: https://
www.multitech.com/brands/multiconnect-mdot-box.

[154] MultiTech, "MultiTech Conduit LoRa IoT Starter Kit," [Online]. Available: https://www.alliot
.co.uk/product/multitech-conduit-iot-starter-kit/.

[155] Tera Term, "Tera Term Software," [Online]. Available: https://ttssh2.osdn.jp/index.html.en.

[156] Destiny-College, "Destiny-College Building Glasgow city," [Online]. Available: https://destiny-college.com/.

[157] B. Islam, M. T. Islam, J. Kaur, and S. Nirjon, "LoRaIn: Making a Case for LoRa in Indoor Localization," 2019 IEEE Int. Conf. Pervasive Comput. Commun. Work. PerCom Work. 2019, pp. 423–426, 2019, doi: 10.1109/PERCOMW.2019.8730767.

[158] L. Han, L. Jiang, Q. Kong, J. Wang, A. Zhang, and S. Song, "Indoor localization within multi-story buildings using MAC and RSSI fingerprint vectors," Sensors (Switzerland), vol. 19, no. 11, 2019, doi: 10.3390/s19112433.

[159] K. Kim et al., "Feasibility of LoRa for smart home indoor localization," Appl. Sci., vol. 11, no. 1, pp. 1–17, 2021, doi: 10.3390/app11010415.

[160] R. Henriksson, "Indoor positioning in LoRaWAN networks," Diplom. rad, 2016.

[161] M. Anjum, M. A. Khan, S. A. Hassan, A. Mahmood, H. K. Qureshi, and M. Gidlund, "RSSI Fingerprinting-Based Localization Using Machine Learning in LoRa Networks," IEEE Internet Things Mag., vol. 3, no. 4, pp. 53–59, 2021, doi: 10.1109/iotm.0001.2000019.

[162] P. Manzoni, C. T. Calafate, J. C. Cano, and E. Hernández-Orallo, "Indoor vehicles geolocalization using LoRaWAN," Futur. Internet, vol. 11, no. 6, 2019, doi: 10.3390/fi11060124.

[163] M. Ramzan, A. Shafique, M. Kashif, and M. Umer, "Gait Identification using Neural Network," Int. J. Adv. Comput. Sci. Appl., vol. 8, no. 9, pp. 67–71, 2017, doi: 10.14569/ijacsa.2017.080909.

[164] X. Guo, N. Ansari, F. Hu, Y. Shao, N. R. Elikplim, and L. Li, "A survey on fusion-based indoor positioning," IEEE Commun. Surv. Tutorials, vol. 22, no. 1, pp. 566–594, 2020, doi: 10.1109/COMST.2019.2951036.

[165] L. Rubio, N. Cardona, S. Flores, J. Reig, and L. Juan-Llácer, "The use of semi-deterministic propagation models for the prediction of the short-term fading statistics in mobile channels," IEEE Veh. Technol. Conf., vol. 50, no. 3, pp. 1460–1464, 1999, doi: 10.1109/VETECF.1999.801504.